Paradigm Shift: Does River Metabolism Mask the Isotopic Signal of Nitrate Sources?

by

Sarah Elizabeth Sine

A thesis
presented to the University of Waterloo
in fulfillment of the
thesis requirement for the degree of
Master of Science
in
Earth Sciences (Water)

Waterloo, Ontario, Canada, 2017

AUTHOR'S DECLARATION

I hereby declare that I am the sole author of this thesis. This is a true copy of the thesis, including any required final revisions, as accepted by my examiners.

I understand that my thesis may be made electronically available to the public.

Abstract

Nitrate (NO_3^-) is the most ubiquitous contaminant in surface and groundwaters in Canada. Synthetic fertilizer application and manure production in intensive agricultural areas contribute large quantities of NO_3^- to the landscape with a proportion seasonally lost to groundwaters and streams. Elevated concentrations of NO_3^- in freshwater systems can result in problems for drinking water supplies and aquatic ecosystem health. The Grand River is the largest Canadian river draining to Lake Erie and the catchment's land-use is predominantly agricultural (~80%). It receives NO_3^- inputs from point (WWTPs) and non-point (agricultural manure and fertilizer) sources.

Isotopes of NO_3^- are commonly used in ecosystem studies to apportion sources (e.g. manure, septic systems, wastewater treatment plant effluent and synthetic fertilizers) and to determine the important NO_3^- transformation processes (nitrification and denitrification). For decades, several assumptions have governed these studies such as: 1) $\delta^{18}O\text{-}NO_3^-$ from nitrification can be predicted using the 2:1 rule (two O in NO_3^- come from H_2O and one O from O_2), 2) NO_3^- isotopes indicate denitrification in freshwater environments when elevated in a 2:1 ratio for $\delta^{15}N$: $\delta^{18}O$, and 3) The $\delta^{15}N$- and $\delta^{18}O$ and of NO_3^- are conservative in oxic environments and thus if $\delta^{18}O\text{-}NO_3^-$ is not elevated, the $\delta^{15}N\text{-}NO_3^-$ can be used for source apportionment.

This research indicates that these assumptions may not always be correct. The overall objectives of this thesis are to improve the use of NO_3^- isotopes for source apportionment in rivers and streams and if the isotopes cannot be used to separate sources then can a mechanistic model be used to estimate rates of N transformation processes that can ultimately help to determine the fate of NO_3^- in rivers.

Nitrate isotope data from the Grand River shows no clear denitrification line. A seasonal trend is only observed in $\delta^{15}N\text{-}NO_3^-$ (high in the summer, low in the spring and fall), not in $\delta^{18}O\text{-}NO_3^-$. Incubation experiments conducted using two sites on the Grand

River with different source inputs demonstrate that the $\delta^{15}N$- and $\delta^{18}O$-NO_3^- are not conservative and cannot be used to indicate denitrification or to discern source inputs of NO_3^-. The NO_3^- isotopes changed over time even when NO_3^- concentrations did not. Results from an in-river experiment were consistent with incubations and confirmed that in a highly productive river, such as the Grand River, source apportionment is difficult as internal N recycling can be rapid, and the effect on the isotopic signal of NO_3^- cannot be ignored.

Isotopic O-exchange between nitrite (NO_2^-) and water (H_2O) during nitrification is a mechanism that can alter the $\delta^{18}O$-NO_3^- signal from nitrification. This study found considerable amounts of O-exchange (40-100%) occurring at both sample sites in all incubation experiments under nitrifying conditions indicating that the $\delta^{18}O$-NO_3^- is "reset" toward the $\delta^{18}O$-H_2O value of the water medium.

The $\delta^{15}N$-NO_3^- and $\delta^{18}O$-NO_3^- cannot be used as conservative tracers in the river. However, a mechanistic model was developed using these isotopes to explain the results from incubation experiments and include the effects of O-exchange and large kinetic ^{18}O isotope effects on the $\delta^{18}O$-NO_3^- during nitrification. With this model, gross rates of the N cycling processes nitrification, denitrification, mineralization and uptake were obtained in order to describe the biogeochemical cycling of N in the Grand River. This model helps to determine the variability in N cycling between sites and at different times of the year.

Acknowledgements

I would first like to thank my supervisor, Dr. Sherry Schiff for providing me with the opportunity to work on this project. She has given me constant support and understanding (for all the times I have ended up concussed throughout this degree) as well as excellent feedback to get my research to where it is now. Thank you for also challenging me to think on my feet, think outside of the box and get out of my comfort zone to learn about the world of isotopes and geochemistry.

I would like to thank my other committee members Dr. Jason Venkiteswaran, Dr. Bill Taylor and Dr. Hans Dürr for their comments and suggestions. Thank you to Dr. Jason Venkiteswaran for going on long trail runs with me to teach me the ins and outs of isotopic modeling and rate constants, for allowing me to constantly pester him with questions and for sending all sorts of informative wiki pages that range anywhere from the history of a font to combatting shin splints to isotopic fractionation.

This thesis would not be possible without the help of Richard Elgood who continually provides support, understanding, wisdom and employment. Thank you for dealing with many thesis and life 'freak-outs' and always finding a solution.

Thank you to the many employees and graduate students of the Environmental Geochemistry Lab and Environmental Isotope lab at the University of Waterloo: Justin Harbin, Janessa Zhang, Fraser Cummings, Jennifer Mead, Pieter Aukes, Amanda Bichel, Amy Morrison and Madeline Rosamond to name a few.

I thank the incredibly strong women in my life, my Mom, Aunt Col and Grandma who provide so much love, instill positivity in the toughest times and are my constant inspiration. I would like to also thank another strong woman, my late Nana who always believed in me and was full of wisdom, love, and support.

A HUGE thank you to my Dad who is my rock in life and who I could not have done this without. His positive demeanor is contagious and he always makes me want to be the best version of myself. Thank you and Heather for the constant love, support and opportunities.

Thank you to my amazing sister Christina who makes me so happy and proud everyday and to my little brother JT for all the hugs and your keen interest in science.

Thank you to the rest of my family and my *unbelievable* network of friends for the love and support. Fab 4, Lolo, JD, Chanelly, Langerak clan you know who you are - thank you a million times.

Lastly, thank you to my other half, Ethan for the love, support and laughter you provide daily.

Table of Contents

List of Figures

List of Tables

Chapter 1 - Introduction

1.1 Introduction

Nitrogen (N) is naturally abundant on Earth's surface and vital for living organisms. However, few organisms (e.g. N fixing bacteria) can fix inert N_2 into forms of N such as ammonium (NH_4^+), nitrite (NO_2^-) and nitrate (NO_3^-) that can be utilized by other organisms. Prior to human alteration of biogeochemical cycles, biological N_2 fixation (110 Tg N per year) served as the primary source of terrestrial reactive N (NO_3^-, NO_x, NH_4^+, N_2O). It was not until the intensification of human activities in the 20th century that energy production and intensive agriculture resulted in the fixation of an additional ~150 Tg N per year by 1990 (Galloway & Cowling, 2002). The introduction of synthetic N fertilizers has supported population growth and the associated food demand; however, doubling the N loading globally has come at a cost to the environment and to human health (Galloway, 1998; Gruber & Galloway, 2008). Excess N not utilized by crops or microorganisms enters the environment in various forms. In aquatic ecosystems, it enters mainly in the highly mobile form, NO_3^- (DeSimone & Howes, 1998). Anthropogenic N loading from the post-WWII industrialization of agriculture is thought to be the major cause of NO_3^- pollution (Galloway, 1998; Novotny, 1999). NO_3^- is now a ubiquitous contaminant in soil, surface water and groundwater globally and is a concern for drinking water quality and aquatic health especially in agriculture-dominated watersheds (Almasri, 2007; Power & Schepers, 1989).

Prolific inorganic N fertilizer and manure application in agricultural landscapes has led to large contributions of NO_3^- as a non-point source contaminant into aquatic ecosystems (Charbonneau & Kondolf, 1993; Hill, 1983; Kato et al. 2009). The portion that does not run-off into receiving waters or is taken up by plant biota will leach through the soil into groundwater (Lang et al. 2013; Liu et al. 2005; Vitousek et al. 1997) or be retained as part of the residual soil nitrogen (RSN) (Janzen et al., 2003). The RSN can produce a legacy

N effect and a time lag of many decades before it enters the groundwater system and is eventually discharged to surface water (Schlesinger, 2009; Sebilo et al. 2013; Worrall et al. 2015). Van Meter & Basu (2015) recently produced a watershed model that quantifies catchment-scale time estimates of this time lag N based on soil nutrient accumulations and groundwater travel time distributions. Although this model will be an important contribution to future watershed management, the legacy effect remains a direct risk to groundwater quality, aquatic health and human health. Also of concern is point source NO_3^- which enters aquatic environments via wastewater treatment plants (WWTPs) in urban centers (MacQuarrie et al. 2001).

The Ontario Safe Drinking Water Act, (O. Reg. 169/03, Sched. 2; O. Reg. 268/03, s. 1; O. Reg. 248/06, s. 2; O. Reg. 242/07, s. 1.) has set the maximum acceptable concentration of NO_3^- as 10 mg N/L as concentrations exceeding this limit may result in harmful health effects to humans (Knobeloch et al. 2000; Townsend et al. 2003). NO_3^- has been linked with methemoglobinemia, more commonly referred to as "blue-baby syndrome" in infants. This disease can result when NO_2^- (a precursor of NO_3^-) oxidizes the ferrous iron in the hemoglobin of an infant's red blood cell into the ferric form to produce methemoglobin (Fan et al. 1987; Fewtrell, 2004). Methemoglobin is unable to transport oxygen leading to a blue-grey colour in the infant's skin and can lead to death. NO_3^- has also been implicated in other health outcomes such as digestive cancers, hypertension and reproductive problems (De Roos et al. 2003); however, the results have not been very conclusive (Powlson et al. 2008). Elevated NO_3^- can also be toxic to aquatic organisms (Camargo & Alonso, 2006) and the Canadian Council of Ministers of the Environment has set a guideline of 3.0 mg N/L for the protection of aquatic life (CCME, 2012). Source water protection and aquatic ecosystem monitoring are both needed to minimize NO_3^- concentrations in order to ensure a potable water supply and healthy aquatic ecosystems.

1.2 Eutrophication

Eutrophication is the greatest water quality concern for aquatic ecosystems in the world (Smith & Schindler, 2009; Smith, 2003). The results of excessive nutrient inputs of phosphorus (P) and/or N, eutrophication can lead to the growth of large, potentially toxic algae blooms in aquatic ecosystems (Schindler, 2006; Smith et al. 2006). Eutrophication has unfavorable and potentially detrimental effects that include: depletion of dissolved oxygen (DO) and the formation of harmful algal blooms (HABs). HABs may produce toxins that have adverse health effects, and also decrease aesthetic value of the water bodies and produce undesirable odours (Smith et al. 1998).

Many studies have concluded that P is the limiting nutrient in all but a few freshwater bodies and that the control of P inputs will reduce algal blooms and improve water quality (Schindler, 2012; Schindler et al. 2008; Schindler & Fee, 1974). In some cases, maintaining water quality and healthy ecosystems in coastal environments has been found to be dependent on managing nitrogen inputs (Howarth & Marino, 2006; Ryther & Dunstan, 1971); however, this issue is still up for debate and continues to be the focus of much research (Schindler et al. 2008; Smith & Schindler, 2009).

Agriculture is a major non-point source of N and P to aquatic environments and it is important that fertilizer and manure application is well understood and adequately managed to avoid eutrophication in both freshwater and marine environments. Cyanobacteria sometimes called blue-green algae are frequently found in eutrophic freshwater systems. These organisms can potentially produce the harmful toxins and some are capable of fixing N.

1.3 The Nitrogen Cycle

Inert nitrogen (N_2) in the atmosphere must be *fixed* to reactive N (NO_y, NH_x, organic N) before it is available to organisms. N_2 comprises 80% of Earth's atmosphere but is only biologically available to N_2-fixing bacteria and archaea that reduce it to NH_4^+ and incorporate it into biomass (Thamdrup, 2012). Other means of N-fixation include fixation by lightning and human activities (energy production, fertilizer production, etc.). Most prokaryotes and all eukaryotes require fixed N to live. *Uptake* is the incorporation (uptake) of NH_4^+, NO_2^- or NO_3^- into organisms. NO_3^- and NO_2^- are initially reduced by nitrite and nitrate reductases into NH_4^+ and then assimilated into organic matter. During decomposition, soil organic N is mineralized into NH_4^+ and NH_4^+ can be *volatilized* to the atmosphere or assimilated.

The transformation of NO_3^- in the environment is broadly governed by two biological reactions: *nitrification* and *denitrification* (Figure 1.1). Nitrification produces NO_3^- through the oxidation of ammonium (NH_4^+), while denitrification removes NO_3^- by reduction.

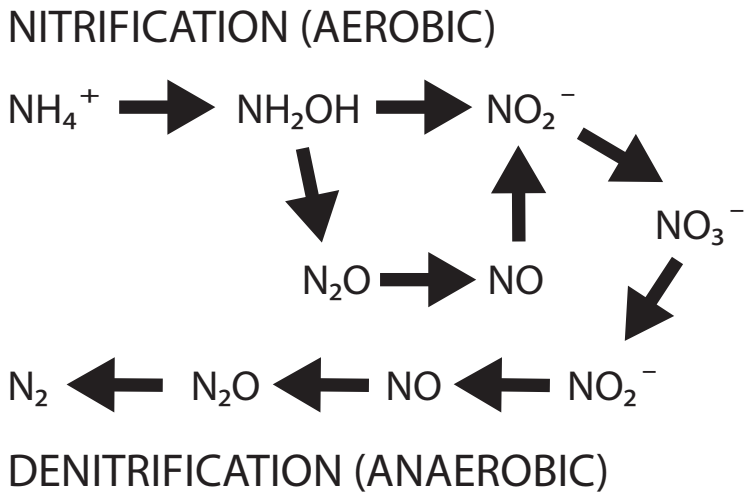

Figure 1.1: Nitrification and denitrification in the nitrogen cycle.

1.3.1 Nitrification

Nitrification is a two-step biologically mediated reaction where NH_4^+ is aerobically oxidized into NO_3^-. The microorganisms responsible for the conversion of NH_4^+ into NO_3^- are chemolithoautotrophic bacteria and archaea. In the first step of NH_4^+ oxidation an intermediate hydroxylamine (NH_2OH) is produced. A small fraction of NH_2OH is converted directly to N_2O and the rest into NO_2^-(Stein & Yung, 2003). Classically, the genera responsible for this conversion are the ammonium oxidizing bacteria (AOB), *Nitrosomonas, Nitrosospira* and *Nitrosococcus*. Resent research has found that in some soils (mainly acidic) and rivers ammonium oxidizing archaea (AOA) of the phylum Crenatchaeota were the dominant nitrifying organisms present (Gubry-Rangin et al. 2010; Leininger et al. 2006; Sonthiphand et al., 2013; Treusch et al. 2005). Nitrite oxidizing bacteria in the genera *Nitrobacter* or *Nitrospira* are responsible for the second oxidation step of NO_2^- into NO_3^- (Bartosch et al. 2002). Evidence from anoxic oceanic waters and deep sediments has shown NH_4^+ can be oxidized anaerobically to N_2 in the presence of nitrate and nitrite, a process termed anammox (Thamdrup, 2012). Recently, complete nitrification by a bacterium of the genus *Nitrospira* has been identified: this has been termed comammox (Daims et al., 2015).

Environmental controls on rates of nitrification include oxygen availability, pH and temperature. NH_4^+ will be rapidly nitrified into NO_3^- in soils, river sediments or biofilm with sufficient amounts of NH_3/NH_4^+, CO_2 and O_2. The optimal pH conditions for nitrifying bacteria has been found to be neutral to slightly alkaline; however, nitrification has been confirmed at pH extremes of 3 (De Boer & Kowalchuk, 2001) and 10 (Sorokin et al. 2001). Temperatures are environment specific but are generally between 25 and 30°C (Norton, 2008). Savard et al. (2007) conducted a groundwater study in an agricultural region and found evidence of nitrification in the winter where average temperatures were as low as -7.9°C. Depending on environmental controls and substrate availability, NO_3^- may accumulate to high concentrations in the soils or groundwater or be discharged to streams (Norton, 2008). NO_2^- has also been found to accumulate under low oxygen conditions (≤1.5

mg/L), a pH between 8-9 and temperature of approximately 30°C (Bae et al. 2001; Ruiz et al. 2003).

1.3.2 Denitrification

Denitrification is the sequential dissimilatory reduction of NO_3^- and NO_2^- into inert nitrogen (N_2) with gaseous oxides (NO, N_2O) as intermediates (Figure 1.1). The microbes that mediate this process are mostly heterotrophic facultative anaerobic bacteria from the genus *Pseudomonas* but also include: *Achromobacter*, *Bacillus*, *Micrococcus* and some fungi (Knowles, 1982; Thamdrup, 2012). Under anaerobic conditions denitrifying microbes use NO_2^- and NO_3^- as the terminal electron acceptor in the oxidation of a variety of compounds from organic carbon and Fe(II) to sulfur (Batchelor & Lawrence, 1978; Stein et al. 2003; Straub et al. 1996). Denitrification is temperature dependent and occurs optimally at temperatures between 25 to 30°C (Dawson & Murphy, 1972; Saad & Conrad, 1993).

The various oxidation and reduction reactions that drive the N cycle are performed by a diverse suite of microbial species and interactions (Falkowski, Fenchel, & Delong, 2008). Nitrification and denitrification are very closely linked in agricultural soils and aquatic environments. While nitrification provides a readily available source of NO_3^-, denitrification is responsible for the loss of fixed N to the atmosphere. Rates of N processes are important for mitigating N pollution in drinking water and aquatic ecosystem health.

1.4 Sources and Fate of Nitrogen in the Environment

There are three main sources of NO_3^- to agriculture-dominated catchments; the atmosphere, nitrified inorganic fertilizer and nitrified manure/sewage. Lightning and biological fixation from bacteria and archaea are natural processes that derive reactive N from the atmosphere. Vehicle emissions and industrial sources have increased atmospheric NO_3^- input globally (Elliot et al. 2007; Galloway & Cowling, 2002).

In aquatic ecosystems, N fertilizer and wastewater from farms, livestock facilities and septic systems/WWTPs are major non-point and point sources. Inorganic N fertilizer is produced using the Haber-Bosch process in which N from the air is combined with hydrogen gas to synthesize NH_4^+. This process was developed in 1909 and revolutionized the agricultural industry doubling fertilizer production every 8 years from 1950 to 1973 (Erisman et al. 2008; Galloway, 1998).

Organic fertilizer, such as manure and effluent discharge from septic systems/WWTPs, provides an organic source of N that can be mineralized to NH_4^+. Manure holdings must be emptied at least once a year and land applications in Ontario are regulated under the Nutrient Management Act and O. Reg. 267. Maximum application rate is calculated based on soil N concentrations. The time of year fertilizers are applied, crop demand, and climate conditions (dry versus wet year) determine the amount of NO_3^- that enters groundwater or surface water.

1.5 Stable Isotopes of Nitrate and the Nitrogen Cycle

The stable isotopes of NO_3^- can be useful for tracing the sources of NO_3^- in an aquatic system and help us better understand N-cycling processes (Figure 1.2). The dual isotope approach to NO_3^- studies uses the stable isotopes of both nitrogen ($^{15}N/^{14}N$) and oxygen ($^{18}O/^{16}O$) atoms in NO_3^-. Stable isotope ratios are typically reported as a delta (δ) with units in per mil (‰) in accordance to (Equation 1.1).

$$\delta = \left(\frac{R_{Sample}}{R_{Standard}} - 1\right) \times 1000$$

Equation 1.1

Where R_{Sample} is the isotopic ratio of the sample and $R_{Standard}$ is the isotopic ratio of the standard. The isotopic standard for nitrogen is N_2 in atmospheric air ($^{15}N/^{14}N = 0.0036765$) and the isotopic standard for oxygen is the Vienna Standard Mean Ocean Water (VSMOW) ($^{18}O/^{16}O = 0.0020052$).

Isotopes of NO_3^- have slightly different chemical and physical properties due to their difference in mass. Those differences are large enough for biological and chemical processes or reactions to fractionate (Kendall 1998). Fractionation is when the relative proportions of the isotopes in a reaction change because one isotope reacts faster than another (Kendall 1998; Peterson & Fry, 1987). Typically the lighter isotope reacts faster and is incorporated into the product faster than the heavier isotope which accumulates in the residual reactants (Kendall 1998; Kendall & Aravena, 2000). These reactions are viewed as either reversible equilibrium reactions or irreversible unidirectional kinetic reactions. Fractionation factors associated with biological or chemical reactions are necessary to trace sources of NO_3^-. In kinetic reactions, isotope fractionation factors (α) can be defined as:

$$\alpha_{p-s} = {}^{R_p}\!/_{R_s}$$

Equation 1.2

Where R_p and R_s are the ratios of the heavy isotope relative to the light isotope in the product and substrate (reactant). An isotope enrichment factor, ε can be defined as:

$$\varepsilon_{p-s} = (\alpha - 1)$$

Equation 1.3

Biological reactions such as nitrification and denitrification are unidirectional and there is potential for fractionation at every step (Kendall 1998). The step in the reaction where most of the fractionation occurs is the rate-determining or slowest step. The rate-limiting step involves a large pool of substrate where the amount of material used is small in comparison to the total pool (Kendall 1998). Estimation of fractionation factors in natural systems can be very complex because the overall fractionation of the reaction is dependent on many environmental conditions (number and type of intermediate steps, species of organism, pH, etc.).

1.5.1 Nitrogen Fixation

Nitrogen fixation is defined as the process that converts inert N_2 from the atmosphere into reactive N species (NO_y, NH_x, organic N). $\delta^{15}N$ of N_2 in the atmosphere is used as the standard and is 0‰. For that reason, the $\delta^{15}N$ of N produced by N-fixers like blue-green algae or bacteria associated with legumes is very low (-3-0‰) (Fogel & Cifuentes, 1993; Gu & Alexander, 1993) (Figure 1.2). When looking at aquatic systems, low $\delta^{15}N$ can be an indicator of N-fixing cyanobacteria responsible for some HABs around the world (Anderson et al., 2002; Kendall, 1998).

1.5.2 Uptake

Uptake is the incorporation of NH_4^+, NO_3^- and NO_2^- into organisms. N isotopic fractionations during uptake depend on the organism involved and the environmental conditions (Kendall, 1998). Assimilation of NH_4^+ or NO_3^- exhibits fractionations of N within the range of -1.6 to 1‰ for microorganisms in soil and a range of -2.2 to 0.5‰ for vascular plants (Kendall, 1998) (Figure 1.2). A larger range in fractionation factors exist in aquatic environments mainly because of the potential for more isotopic effects (Kendall, 1998). In addition, it can also be the result of greater variability of NH_4^+ and NO_3^- concentrations and lower growth rates (Fogel & Cifuentes, 1993; Kendall, 1998). Fogel & Cifuentes (1993) compiled measured values from field and laboratory studies of aquatic algae and found the range in fractionation to be -27 to 0‰ for the incorporation of NH_4^+ and NO_3^-. From cultures of marine phytoplankton, Granger et al. (2010) found the O isotope effect associated with NO_3^- uptake by marine phytoplankton was very similar to the N isotope effects such that N and O isotopes of NO_3^- fractionated to the same extent (1:1), with values ranging between -8‰ and -5‰.

1.5.3 Mineralization

In the context of the N cycle, mineralization is the conversion of organic N into NH_4^+ during decomposition of plants and animals. This process causes only a small fractionation in $\delta^{15}N$ (±1‰) between soil organic matter and soil ammonium (Kendall, 1998; Kendall & Aravena, 2000) (Figure 1.2). Production of NO_3^- can be an indicator of mineralization when NH_4^+ is subsequently nitrified.

1.5.4 Nitrification

Nitrification is the oxidation of NH_4^+ into NO_3^- by chemolithoautotrophic bacteria and archaea (Figure 1.2). Two oxidation steps characterize this process: the oxidation of NH_4^+ and the oxidation of NO_2^-. NH_4^+ is oxidized into NH_2OH and the source of this oxygen molecule is from O_2 (Equation 1.4) (Hollocher et al., 1981). An oxygen molecule from H_2O contributes next to the oxidation of NH_2OH into NO_2^- (Equation 1.5) with the potential for further oxygen exchange between NO_2^- and H_2O (Andersson & Hooper, 1983; Casciotti, 2015; Casciotti et al., 2010; Hollocher et al., 1981). Lastly, NO_2^- is oxidized into NO_3^- in the final step and it is a second water molecule that supplies an oxygen atom (Hollocher, 1984) (Equation 1.6).

$$NH_4^+ + O_2 \rightarrow NH_2OH$$

Equation 1.4

$$NH_2OH + H_2O \rightarrow NO_2^- \leftrightarrow H_2O$$

Equation 1.5

$$NO_2^- + H_2O \rightarrow NO_3^-$$

Equation 1.6

The fractionations in $\delta^{15}N$ that result from this process depend on the rate-limiting step. This is most often the slow oxidation of NH_4^+ by *Nitrosmonas* in soils (Equation 1.4) because the second oxidation step (NO_2^- to NO_3^-) has been found to be rapid in the environment

(Kendall, 1998). The amount of substrate present dictates the extent of the fractionation and systems that are N-limited have low fractionations. The total isotope effect has been found to range between -12‰ and -29‰ in soils (Shearer & Kohl, 1992).

Casciotti et al. (2010) estimated the fractionation of $\delta^{18}O$ in nitrification with cultures of marine bacteria where the combined isotope effect for O_2 and H_2O in the first oxidation step of NH_4^+ into NO_3^- was found to range between -38‰ to -18‰. The isotope effect of the final oxidation step of NO_2^- into NO_3^- was found to range between -25‰ to -9‰ (Buchwald & Casciotti, 2010). Prior to these studies, nitrification fractionations of $\delta^{18}O$ were not taken into account and values of $\delta^{18}O$-NO_3^- were calculated based on the 2:1 model (Equation 1.7) (Snider et al., 2010).

$$\delta^{18}O - NO_{3(rel.VSMOW)}^{-} = \left[\left({}^{1}/_{3}\, R_{O_2} + {}^{2}/_{3}\, R_{H_2O}\right) \div R_{VSMOW}\right] - 1$$

Equation 1.7

In aquatic systems microbial nitrification is an important NO_3^- production process. Knowing the stable isotope fractionations has been useful for understanding the transformations of NO_3^- and has often been used to determine the sources of NO_3^- in impacted aquatic ecosystems (Anisfeld et al., 2007; Mayer et al., 2002).

1.5.5 Volatilization

In the N cycle, volatilization refers to the loss of NH_3 gas to the atmosphere. Increase in temperature and/or soil pH has been found to increase volatilization when there is adequate soil moisture (Ernst & Massey, 1960). In agricultural areas most manure N used as fertilizer is in the form of urea, which is hydrolyzed to NH_4^+. This increases the pH and favours the loss of NH_3 gas via volatilization. The NH_3 gas produced has a $\delta^{15}N$ lower than the remaining NH_4^+ because the lighter isotopes react faster (Kendall, 1998). Under optimal conditions this process may also occur in streams where there are large N inputs from runoff or wastewater treatment plant effluent (Cejudo et al., 2014; Hood et al., 2013). The

actual fractionation of $\delta^{15}N$ for volatilization is dependent on temperature and other factors. Residual $\delta^{15}N\text{-}NH_4^+$ has been found to have values >20‰ after volatilization (Kendall, 1998) (Figure 1.2).

1.5.6 Denitrification

Denitrification is the reduction of NO_3^- under low oxygen conditions to N_2 with obligate intermediates N_2O and NO (Figure 1.2). Redox conditions establish the availability of oxidized material that organisms use as electron acceptors in the order of O_2, NO_3^- and SO_4^- (Kendall, 1998). When conditions are favourable, denitrification will occur in soil, groundwater and streams. It is a very important process for mitigating levels of N in impacted aquatic systems. The $\delta^{15}N$ of the residual nitrate increases exponentially as the reaction proceeds and NO_3^- concentrations decrease. Based on experiments conducted with pure cultures of denitrifying bacteria and other soil studies, the fractionations that have been recorded for $\delta^{15}N$ range from -40‰ to -5‰ (Kendall, 1998; Snider et al., 2009). As the reaction proceeds there will also be an increase in $\delta^{18}O\text{-}NO_3^-$. In marine environments a relationship of 1:1 for $\delta^{18}O$: $\delta^{15}N$ has been observed (Granger et al., 2004; D. M. Sigman et al., 2003). Granger et al. (2008) found the combined isotope effects of N and O among four facultative anaerobic denitrifiers to range between -5‰ to -25‰. In freshwater environments, an approximate 1:2 relationship has been observed reliably in groundwater studies (Aravena et al., 1998; Cey et al., 1999; Mengis et al., 1999). Using the coupled isotope effects of both $\delta^{15}N$ and $\delta^{18}O$ has thus become a commonly used tool for identifying denitrification and isolating other biogeochemical processes (Kendall et al., 2007a); however there is still much to learn as recent studies have found that O-exchange between NO_2 and H_2O may indirectly affect or in-part, control the final isotopic effect on $\delta^{18}O\text{-}NO_3^-$ during denitrification (Knöller et al., 2011; Snider et al., 2009; Snider et al., 2013).

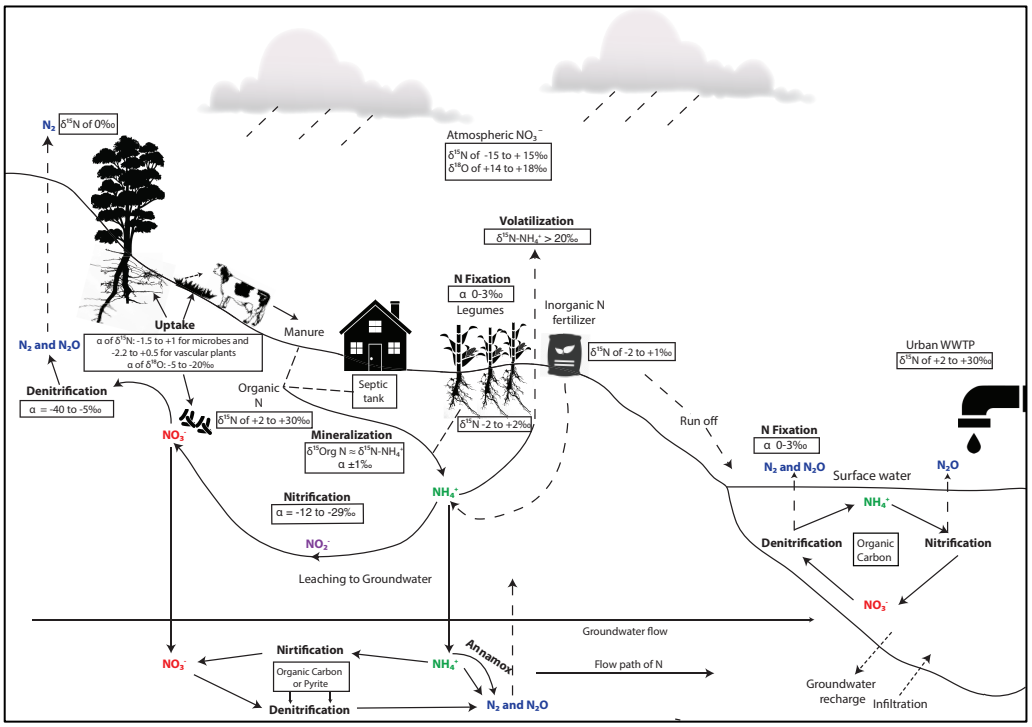

Figure 1.2: The main N transformation processes in soil, freshwater and groundwater and potential isotopic values and fractionations for NO_3^- sources and N processes (Kendall et al., 2007b) modified from (Xu et al. 2015).

1.6 Nitrate Source Determination: Current Paradigms

Dual isotopes of NO_3^-($\delta^{15}N$- and $\delta^{18}O$-NO_3^-) have been widely used to apportion sources of NO_3^- in surface water (Anisfeld et al. 2007; Lee et al. 2008; Li et al. 2010; Mayer et al. 2002) and groundwater studies (Aravena et al., 1993; Aravena & Robertson, 1998; Cey et al., 1999; Mengis et al., 1999; Wassenaar, 1995). For the past 20-25 years researchers have used the dual isotope plot (Figure 1.3) where sources of NO_3^- reside within constrained boxes. Values that fall outside the boxes are then thought to result from denitrification and would plot along a 1:1 (Granger et al., 2004; Sigman et al., 2003; Sigman et al., 2005) or 1:2 (Amberger & Schmidt, 1987; Böttcher et al., 1990; Mengis et al., 1999) line for $\delta^{18}O/\delta^{15}N$ in marine and freshwater environments, respectively.

Sources of NO_3^- have wide ranges in values of $\delta^{18}O$ and $\delta^{15}N$. Atmospheric NO_3^- has become a more important source of acidic deposition since stricter regulations on SO_x emissions were introduced (Kendall et al., 2007a). Generally, the $\delta^{15}N$-NO_3^- from wet atmospheric deposition ranges between -15‰ to +15‰ (Kendall et al., 2007a). Less is known about the $\delta^{18}O$ and large variability exists in literature values (Kendall, 1998; Kendall et al., 2007a). Compiled values from various studies have been found to range between +25‰ to +115‰ (Kendall, 1998; Michalski et al., 2012). However, values are generally constrained between +40‰ and +80‰ (Figure 1.3) (Kendall, 1998).

Many different N fertilizers, with widely varying compositions are used in agriculture and differentiating between them is important depending on whether they are naturally, synthetically or microbially derived (nitrification). The $\delta^{15}N$ of synthetic fertilizer reflects the signal of N_2 in the atmosphere and usually resides around 0‰ but can be in the range of -4‰ to +4‰ (Kendall et al., 2007a). Similarly the $\delta^{18}O$ reflects atmospheric O_2 (+23.5‰) and typically ranges between +17‰ to +25‰ (Kendall & Aravena, 2000; Kendall et al., 2007a; Wassenaar, 1995). Organic fertilizers that include plant composts and liquid and solid animal waste can have $\delta^{15}N$ values that range between +2‰ to +30‰, the wide range reflecting the different origins (Kendall et al., 2007a; Wassenaar et al., 2006). Septic waste or N manure held in holding tanks can have even higher values of $\delta^{15}N$ due to volatilization of NH_4^+ and subsequent oxidation of the residual into NO_3^-. The $\delta^{15}N$ of microbially derived NO_3^- depends on the pool of NH_4^+ available and which step in the process is rate limiting and therefore produces a very wide range of values from -8‰ to +30‰ (Kendall et al., 2007a).

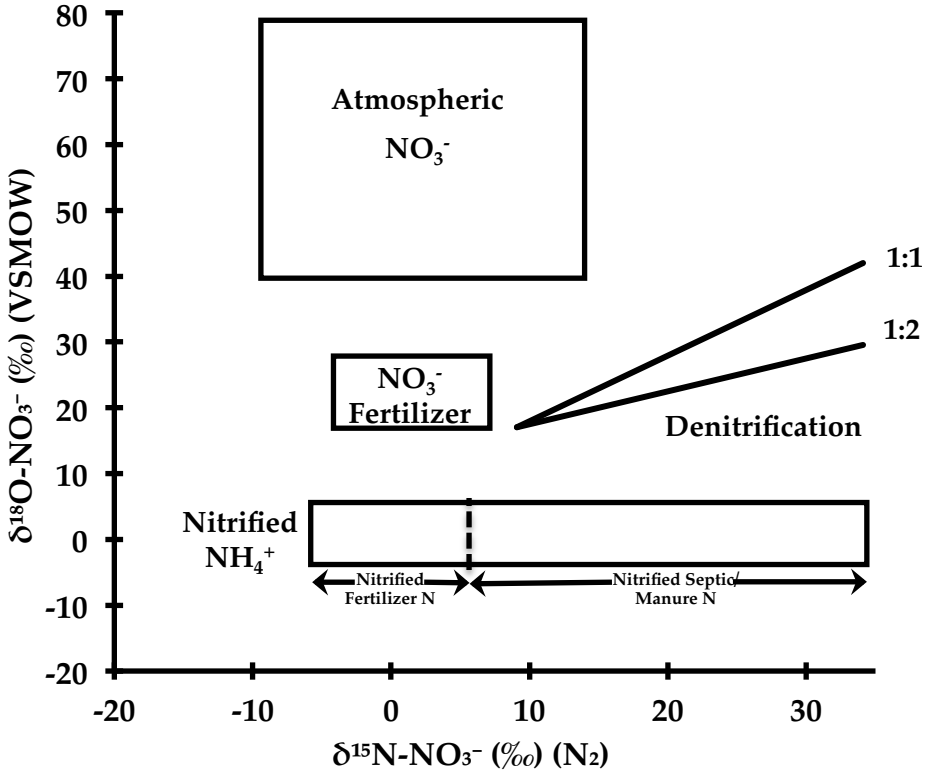

Figure 1.3*:* Values typical of $\delta^{18}O$- and $\delta^{15}N$-NO_3^- originating or nitrified from various N sources. Atmospheric and fertilizer sources are constrained to the boxes labeled "Atmospheric NO_3^-" and "NO_3^- fertilizer", respectively (Kendall & Aravena, 2000; Kendall et al., 2007b; Wassenaar, 1995). The solid lines represent denitrification and the typical slopes resulting in a marine environment (1:1) or freshwater (1:2) with initial $\delta^{15}N$ = +9‰ and $\delta^{18}O$ = +17‰. Values produced from nitrification of NH_4^+ and organic mater will reside in the box labeled "Nitrified NH_4^+" (Kendall et al., 2007b; Wassenaar et al., 2006). Make note that denitrification lines are for illustrative purposes (to show slopes) and are not reflective of source values.

There are several assumptions associated with the source plot (Figure 1.3):

1) *$\delta^{18}O\text{-}NO_3^-$ from nitrification can be predicted using the 2:1 rule (two O in NO_3^- come from H_2O and one O from O_2)*

The first oxygen molecule in the oxidation of NH_4^+ comes from O_2 and H_2O contributes the second and third oxygen molecules to produce NO_2^- and NO_3^- (Andersson & Hooper, 1983; Hollocher et al., 1981; Hollocher, 1984). Based on the initial isotopic value of NO_3^- sources, expected ranges in isotopic values of NO_3^- have been determined for microbial nitrification based on their origin i.e. fertilizer or manure/septic waste. Historically, very few studies measure the actual value of $\delta^{18}O\text{-}NO_3^-$ and rather determine this value using this 2:1 model (Equation 1.7) (Snider et al., 2010).

2)

a. *Expected $\delta^{18}O\text{-}NO_3^-/\delta^{15}N\text{-}NO_3^-$ from denitrification is 1:2 for freshwater and 1:1 for marine environments.*

For decades it has been known that denitrification causes a predictable increase in the $\delta^{18}O$ and $\delta^{15}N$ of the residual NO_3^- (Amberger & Schmidt, 1987). Data collected largely from groundwater studies has consistently shown increases of $\delta^{18}O$ and $\delta^{15}N$ to be in an approximately 1:2 ratio (Aravena et al., 1993; Aravena & Robertson, 1998; Cey et al., 1999; Lehmann et al., 2003; Mengis et al., 1999). It has therefore been generally accepted that natural freshwater data plotting along a slope of 0.5 for $\delta^{18}O$ and $\delta^{15}N$ indicates denitrification. Findings from culture experiments with marine denitrifiers show a 1:1 relationship of $\delta^{18}O$ and $\delta^{15}N$ for denitrification (Granger et al., 2004; D. M. Sigman et al., 2003).

b.

i. $\delta^{18}O\text{-}NO_3^-$ *elevated beyond expected ranges of sources at a particular site indicates denitrification.*

ii. $\delta^{18}O\text{-}NO_3^-$ *is conservative, and thus if* $\delta^{18}O\text{-}NO_3^-$ *is not elevated, then* $\delta^{15}N\text{-}NO_3^-$ *can be used for source apportionment*

$\delta^{15}N\text{-}NO_3^-$ is very well understood and a greater abundance of source data exists relative to that for $\delta^{18}O\text{-}NO_3^-$ (Kendall et al., 2007b); however, when dealing with complex N pools and processes $\delta^{18}O\text{-}NO_3^-$ isotopes are more indicative of NO_3^- source (Amberger & Schmidt, 1987). This is because NO_3^- produced from an inorganic fertilizer should exclusively reflect $\delta^{18}O\text{-}O_2$ (+23.5‰) and NO_3^- from nitrification should contain $\delta^{18}O\text{-}H_2O$ (-8 to -10‰) (Amberger & Schmidt, 1987). $\delta^{18}O\text{-}NO_3^-$ isotopes are therefore conservative and if elevated beyond expected ranges of source values (in conjunction with $\delta^{15}N\text{-}NO_3^-$) will indicate denitrification. However, if not elevated then $\delta^{15}N\text{-}NO_3^-$ can be used independently for source apportionment.

1.7 Nitrate Source Determination: Challenging Paradigms

Recent research has found greater complexity in the N cycle than previously thought (Thamdrup, 2012) and discovery of new N processing mechanisms (Casciotti, 2015; Casciotti et al. 2010; Snider et al. 2010; Wunderlich et al. 2013), suggest that the previously listed assumptions may not always hold true. It can be shown that $\delta^{18}O\text{-}NO_3^-$ is not conservative and is influenced by a number of factors, including rapid abiotic O-exchange and large kinetic isotope effects, varying microbial community composition and changes to diel cycling of dissolved O_2 on a temporal or spatial scale.

O-exchange has been found to occur between nitrite (NO_2^-) and water (H_2O) during nitrification (Andersson et al. 1982). Depending on the relative amount and rate of O-exchange that occurs, the original $\delta^{18}O\text{-}O_2$ signal may be greatly reduced or eliminated. In

studies that have measured the actual value of $\delta^{18}O\text{-}NO_3^-$, values range between 0‰ and 16‰. These values are lower than those that would result if calculated using the 2:1 model (Equation 1.7) (Snider et al., 2010). The fraction of abiotic O-exchange (*f*abiotic) was determined for three types of soil NO_3^- by Snider et al. (2010) in a series of laboratory incubations. They found the three soil types had a different *f*abiotic from each other and from that which assumed a 2:1 incorporation of oxygen from H_2O and O_2. In addition, the $\delta^{18}O$ fractionation factors of O_2 and H_2O uptake during nitrification had never been included in the 2:1 model until Buchwald and Casciotti (2010) and Casciotti et al. (2010) estimated these factors with marine bacteria. If denitrification has occurred, the current model states that $\delta^{18}O\text{-}NO_3^-$ will be elevated beyond an expected range based on known isotope effects (Amberger & Schmidt, 1987). However, it is possible that rapid O-exchange and cycling could result in the loss of the denitrification signal all together (Wunderlich et al., 2013).

Exploring the community composition of nitrifying organisms will provide more information on their role in this complex process (Thamdrup, 2012). Ammonium oxidizing archaea (AOA) rather than ammonium oxidizing bacteria (AOB) have been found in greater abundance in soils (Gubry-Rangin et al. 2010; Leininger et al. 2006) and had the most important role in acidic soils (Zhang et al. 2012). In a freshwater study, Sonthiphand et al. (2013) explored the sediment and water column inside and outside a WWTP effluent plume in the Grand River, Ontario, and found a dominance of AOA outside the plume, AOB within and distinct in-river AOA patterns compared to those in the effluent. This study shows how multifaceted a system can be. Although there is limited literature on how much community composition influences isotopic transformations, these studies emphasize the importance of multidisciplinary research combining microbial, molecular and isotopic techniques.

Venkiteswaran et al. (2015) conducted a whole-river study on the Grand River. Nighttime $\delta^{18}O\text{-}O_2$ values were always higher than daytime values; however, nighttime values did not

always return to the atmospheric equilibrium value for $\delta^{18}O\text{-}O_2$ of +24.2‰. Diel O_2 values could change the isotopic signal of the resulting NO_3^-, however they are also unaccounted for in the 2:1 model. Current $\delta^{18}O\text{-}NO_3^-$ research, largely focused on soil, contains many gaps for highly impacted freshwater ecosystems. Years of data collected from the Grand River in southwestern Ontario, Canada, suggest that the $\delta^{18}O\text{-}NO_3^-$ signal for denitrification is lost in the river. This information in addition to the recent literature has lead to this research in which data from incubation experiments and river-chamber experiments supports literature suggesting that $\delta^{18}O\text{-}NO_3^-$ is not conservative and that other mechanisms play a role in the cycling of NO_3^- and in effect, river metabolism masks NO_3^- sources.

1.8 Objectives of this Research

The overall objective of this thesis is to improve the use of NO_3^- isotopes for apportioning sources in rivers. This research will provide a greater understanding of the complexity of within-river N cycling and processing. The study site, the Grand River watershed is dominated by agriculture and NO_3^- pollution is a widespread concern as many communities use the Grand River as their source of drinking water.

The specific objectives of Chapter 2 are to answer the question of whether of not $\delta^{18}O\text{-}NO_3^-$ is conservative and can be reliably used for source apportionment of NO_3^-. This question is addressed through the examination of historical data collected from the Grand River as well as data generated during three laboratory incubation experiments and two river-chamber experiments. Chapter 3 will examine the mechanisms responsible for changes to nitrate isotopes that contradict current isotope paradigms. A new mathematical model of nitrification and associated isotope fractionations is used to model observed data and more importantly, to determine rates of uptake, incorporation and release of NO_3^-. Chapter 4 will conclude the findings of this research and offer a prospective for future research and the use of the stable isotopes of NO_3^- in source apportionment studies.

1.9 Study Site – Grand River, Ontario

The Grand River watershed located in southern Ontario is the largest (6800km^2) Canadian river draining to Lake Erie (Figure 1.4). It is 7th order system at the mouth and flows north to south for ~300km with an average annual discharge of ~80m^3/s (Venkiteswaran et al., 2015). The land-use is predominantly agriculture (~80%) with five large urban areas (Kitchener, Waterloo, Cambridge, Guelph and Brantford) (Rosamond, 2013). There are 30 wastewater treatment plants discharging to the river and its tributaries. These treatment plants serve >75% of population (950,000) living in the watershed (Venkiteswaran et al., 2015). The geology in the upper section of the river is largely glacial till and the lower section is clay and silt (Gao et al., 2006). High nutrient loading from agriculture and wastewater treatment plants (WWTPs) is a threat to drinking water quality making the Grand River an ideal study site for this research (GRCA, 2014).

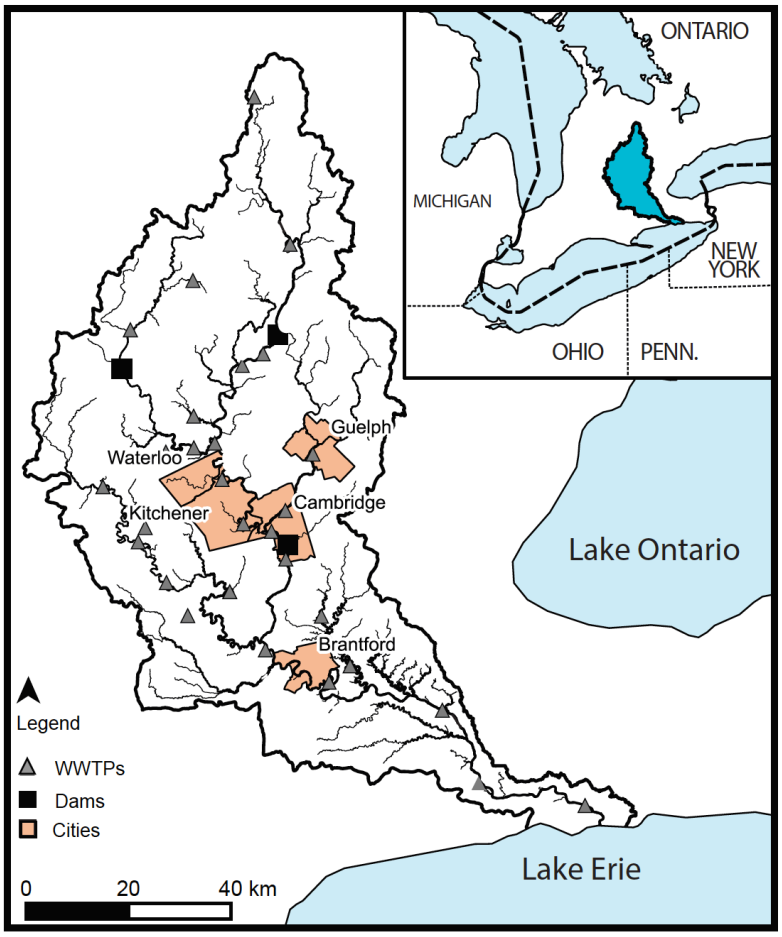

Figure 1.4: The Grand River watershed located in southwestern Ontario, Canada is the largest Canadian river discharging to Lake Erie. Urban areas are concentrated at the center of the catchment. WWPT = wastewater treatment plant. Figure modified from Venkiteswaran et al. (2015).

Chapter 2 – Challenging Paradigms: NO_3^- Isotopes in the Grand River are not Conservative

2.1 Introduction

Nitrate (NO_3^-) is one of the most pervasive contaminants in surface and groundwaters in Canada (Power & Schepers, 1989; Ritter et al., 2002) and worldwide. Since the intensification of agricultural practices during the 20th century, synthetic fertilizer application and manure production contribute large quantities of NO_3^- to the landscape with a proportion lost to groundwaters and streams depending on season (Galloway & Cowling, 2002). Elevated NO_3^- in freshwater systems can result in problems for drinking water supplies and aquatic ecosystem health. Determining the sources of NO_3^- to the environment is important for managing impacted systems like the Grand River in southwestern Ontario that, at times, approaches the drinking water limit of 10 mg N/L (Figure 2.1). Concentrations exceeding this limit are most harmful to infants (Fan et al., 1987).

The Grand River supplies drinking water to approximately 650 000 people across Brantford, Waterloo Region, Guelph and Six Nations Territory (GRCA, 2014) and dilutes water from a total of 30 wastewater treatment plants (WWTPs), 6 of which are above Waterloo region and 15 above Brantford. Two of these major WWTPs are located in Kitchener and Waterloo. The Kitchener WWTP underwent system upgrades in 2010 to modify the system in order to nitrify (NH_4^+ into NO_3^-) the wastewater before release. Prior to these modifications wastewater was released primarily as NH_4^+. The combination of point and non-point sources of NO_3^- from WWTPs and agricultural runoff from intensive agricultural practices in the area pose many risks to water quality for municipalities that draw water directly from the river. In order to implement best management practices to protect the aquatic system and keep drinking water NO_3^- levels to a minimum, it is important for watershed managers to understand whether NO_3^- is coming from point or non-point sources.

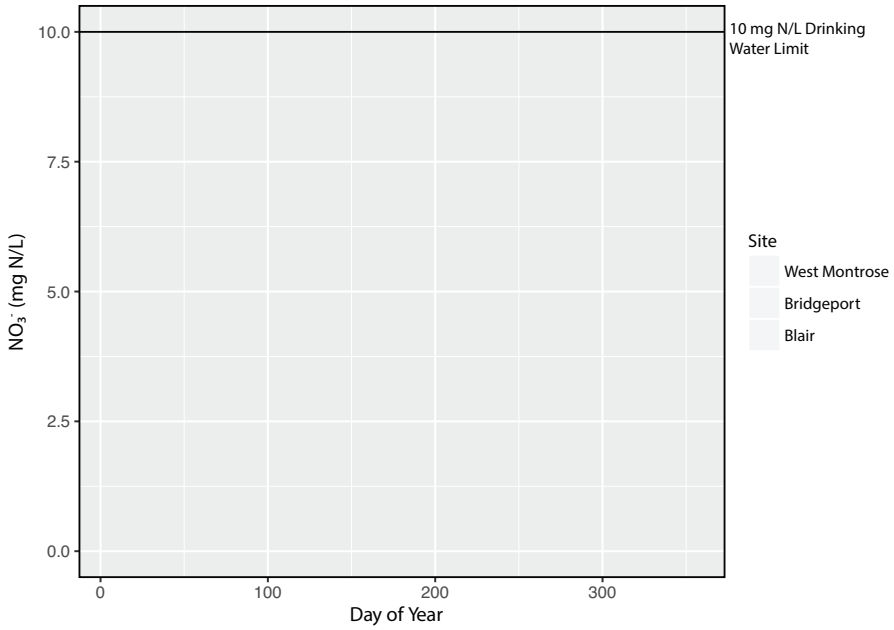

Figure 2.1: Nitrate in the Grand River from 2005-2013 for three sites: West Montrose, Bridgeport and Blair that are 98km, 119km and 145km from the headwaters, respectively. Blair is downstream from the WWTP outlets of the two largest cities in the watershed, Waterloo and Kitchener. The solid black line represents the 10 mg N/L drinking water limit set by The Ontario Safe Drinking Water Act, (O. Reg. 169/03, Sched. 2; O. Reg. 268/03, s. 1; O. Reg. 248/06, s. 2; O. Reg. 242/07, s. 1.).

Dual isotopes of NO_3^- are commonly used in ecosystem studies to apportion sources, e.g., manure, septic systems and synthetic fertilizers (Anisfeld et al., 2007; Aravena et al., 1993; Burns & Kendall, 2002; Cey et al., 1999; Kendall, 1998; Lee et al., 2008; Li et al., 2010; Mayer et al., 2002; Mengis et al., 1999; Pardo et al., 2004; Spoelstra et al., 2001; Xu et al., 2015). For decades, several assumptions have governed these studies, including: 1) $\delta^{18}O$-NO_3^- from nitrification can be predicted using the "1:2 rule" (oxygen incorporation of one O atom from $\delta^{18}O$-O_2 and two O atoms from $\delta^{18}O$-H_2O, respectively), 2) $\delta^{18}O$-NO_3^- elevated beyond expected ranges of sources indicate denitrification, 3) both $\delta^{15}N$-NO_3^- and $\delta^{18}O$-NO_3^- are conservative, and thus if $\delta^{18}O$-NO_3^- is not elevated, then $\delta^{15}N$-NO_3^- can be used for

source apportionment, 4) manure/septic and soil sources of NO_3^- are sufficiently separated in $\delta^{15}N$ and 5) that biological assimilation of NO_3^- imparts no isotopic fractionation. However, recent research in agricultural catchments suggests that these assumptions may not always be correct (Casciotti et al., 2010; Snider et al., 2010; Wunderlich et al., 2013).

In the past, $\delta^{18}O\text{-}NO_3^-$ has been used to provide information on NO_3^- sources, based on the fact that industrially produced NO_3^- will have a $\delta^{18}O$ signal close to that of atmospheric O_2 while nitrified NO_3^- will be much lower due to the much lower value of $\delta^{18}O$ of H_2O. Snider et al. (2010) assembled field and incubation data of $\delta^{18}O\text{-}NO_3^-$ produced from nitrification in groundwater, surface water and various soil types. They found that <10% of the assembled $\delta^{18}O\text{-}NO_3^-$ data fit theoretical values based on the "1:2 rule" for oxygen incorporation during nitrification. Using the "1:2 rule" to calculate $\delta^{18}O\text{-}NO_3^-$ values is problematic, as it does not take into account potentially large isotope effects or rapid oxygen exchange between $\delta^{18}O\text{-}H_2O$ and $\delta^{18}O\text{-}NO_2^-$ or changes in the $\delta^{18}O\text{-}O_2$ during nitrification (Snider et al., 2010; Venkiteswaran et al., 2007). It was not until Casciotti et al. (2010) estimated the combined effect for O_2 and H_2O incorporation in the initial oxidation steps of nitrification and Buchwald & Casciotti (2010) calculated the isotope effect for the incorporation of H_2O in the final oxidation step that kinetic isotope effects could be considered. Researchers have documented O-exchange between H_2O and NO_2^- (Andersson & Hooper, 1983; K. Casciotti, 2015; K. L. Casciotti et al., 2010; Martin & Casciotti, 2016; Nishizawa et al., 2016) however the amount or fraction of O-exchange is not well known, especially in aquatic systems. Isotopic exchange causes $\delta^{18}O\text{-}NO_3^-$ values to be "reset" toward the $\delta^{18}O\text{-}H_2O$ of the medium and this could alter the signal of nitrified sources and mask the denitrification signal.

The $\delta^{18}O\text{-}O_2$ should also be considered as diel changes in the isotope signal on both a temporal and spatial scale have been reported (Venkiteswaran et al., 2015, Venkiteswaran et al., 2007; Wassenaar et al., 2010). Bacterial biofilms in streams and rivers have been found to play a large role in the function and metabolism of many aquatic ecosystems (Battin et al.,

2016; Findlay, 2010) and understanding the diversity of microorganisms may also influence the nitrification signal.

High abundances of ammonia oxidizing archaea (AOA) rather than ammonia oxidizing bacteria (AOB) have been discovered in some soils (Gubry-Rangin et al., 2010; Jia & Conrad, 2009; Leininger et al., 2006), although it is unknown how the microbial community composition may influence the isotopic signal of NO_3^- in the river. In a microbial characterization freshwater study, Sonthiphand et al. (2013) explored the sediment and water column inside and outside a WWTP effluent plume in the Grand River, Ontario. Diverse assemblages of AOA and AOB on a spatial scale were found. AOA and AOB have potentially different ammonia-oxidation pathways (Stahl & de la Torre, 2012; Walker et al., 2010) and this could mean the end-member isotopic signal of NO_3^- is different between microbial groups. Research conducted by Nishizawa et al. (2016) found no apparent difference in the isotopic fractionation between AOA and AOB. However, the N and O isotope effects determined for AOA are limited compared to what has been obtained for AOB (Buchwald & Casciotti, 2010; Casciotti et al., 2010). Given that recently discovered comammox bacteria oxidize NH_4^+ all the way through to NO_3^-, this further complicates the situation as the final isotopic composition of NO_3^- could potentially be altered by these bacteria (Laura Sauder, personal communication April 2017).

Furthermore, recent research identifies the significance of including large isotope effects, rapid O-exchange, variations in microbial community composition and diel $\delta^{18}O\text{-}O_2$ changes when looking at N transformation processes in order to confidently use $\delta^{18}O\text{-}NO_3^-$ isotopes to identify nitrified sources or denitrification.

The objectives of this chapter are to (1) determine if the ($\delta^{15}N$) ^{15}N- and ($\delta^{18}O$) ^{18}O-NO_3^- are conservative in surface waters unless altered by denitrification, (2) if determined to be conservative, can the isotopes be used to indicate denitrification and sources of NO_3^- to aquatic surface water ecosystems and (3) is the interpretation of the isotopic systematics and

N cycling processes consistent for either non-point agriculture and point WWTP input. This study uses $\delta^{18}O$-H_2O and $\delta^{18}O$- and $\delta^{15}N$-NO_3^- labeled water in laboratory incubation experiments and in-river chamber experiments to observe changes to $\delta^{18}O$-NO_3^- and $\delta^{15}N$-NO_3^- isotopes with N cycling processes. The goal of the laboratory incubations was to quantify the influence of rock biofilm on NO_3^- isotopes and concentrations over time and to ultimately determine the fraction of O-exchange occurring between NO_2^- and H_2O during nitrification.

2.2 Study Sites

The Grand River watershed is the study site for this research. Land use in the Grand River watershed is largely agricultural (~80%) with five urban cities located centrally in the watershed (70% of the population) (Figure 2.2) (Rosamond, 2013; Venkiteswaran et al., 2015). The treatment plants serving the five major cities (Brantford, Cambridge, Guelph, Kitchener and Waterloo) handle ~90% of the wastewater for the entire watershed (GRCA, 2014). The sample sites for this study, West Montrose and Blair (Figure 2.2) encompass a ~100km stretch of the Grand River's 300km length. Depending on river flow, it takes two to three days for water to travel this distance between sample sites (Mark Anderson, personal communication). Diffuse agricultural NO_3^- sources enter the river upstream of West Montrose and mainly point source NO_3^- from the Kitchener and Waterloo WWTP enters upstream of Blair. Elevated NO_3^- concentrations that result from increased loading tend not to decrease between these sites (Venkiteswaran et al., 2015). The surficial geology in these areas is largely glacial till and gravel (Gao et al., 2006). River flow in the Grand varies seasonally with high flow in the spring and fall and low-flow summer conditions of 5 m^3/s and 11 m^3/s for West Montrose and Blair, respectively (GRCA, 2014).

The sampling sites are located in the Huron Slopes climate zone that receives moisture picked up by winds over Lake Huron (Brown et al., 1980; GRCA, 2014). The moisture condenses and creates a "snow belt" with higher than average rainfall or snow

accumulation in some regions, depending on the year (Brown et al., 1980). Annual precipitation for Waterloo Region typically ranges between 900-920mm (University of Waterloo Weather Station). The Region of Waterloo has experienced both "wet" (defined as above average precipitation) and "dry" (defined as below average precipitation) years over the last decade. The amount of precipitation has a profound effect on nutrient loading to the river and nutrient dynamics such as N transformations (nitrification, denitrification, uptake, volatilization and mineralization) within the river (Cummings, 2015). This study took place in the summer (June-August) and fall months (September-November) of 2014 and 2015. In 2014, according to the University of Waterloo weather station, total precipitation was 949.6mm, ~45mm more than what was estimated for that year (904mm). The average temperature was 24.5°C during the summer (June, July and August) of 2014 and 12.7°C in the fall (September, October, November) of 2014. Total precipitation in 2015 was 814.2mm, ~100mm less than what was estimated for that year (916.3mm). The average temperature was 24.7°C in the summer and 16.4°C in the fall of that year.

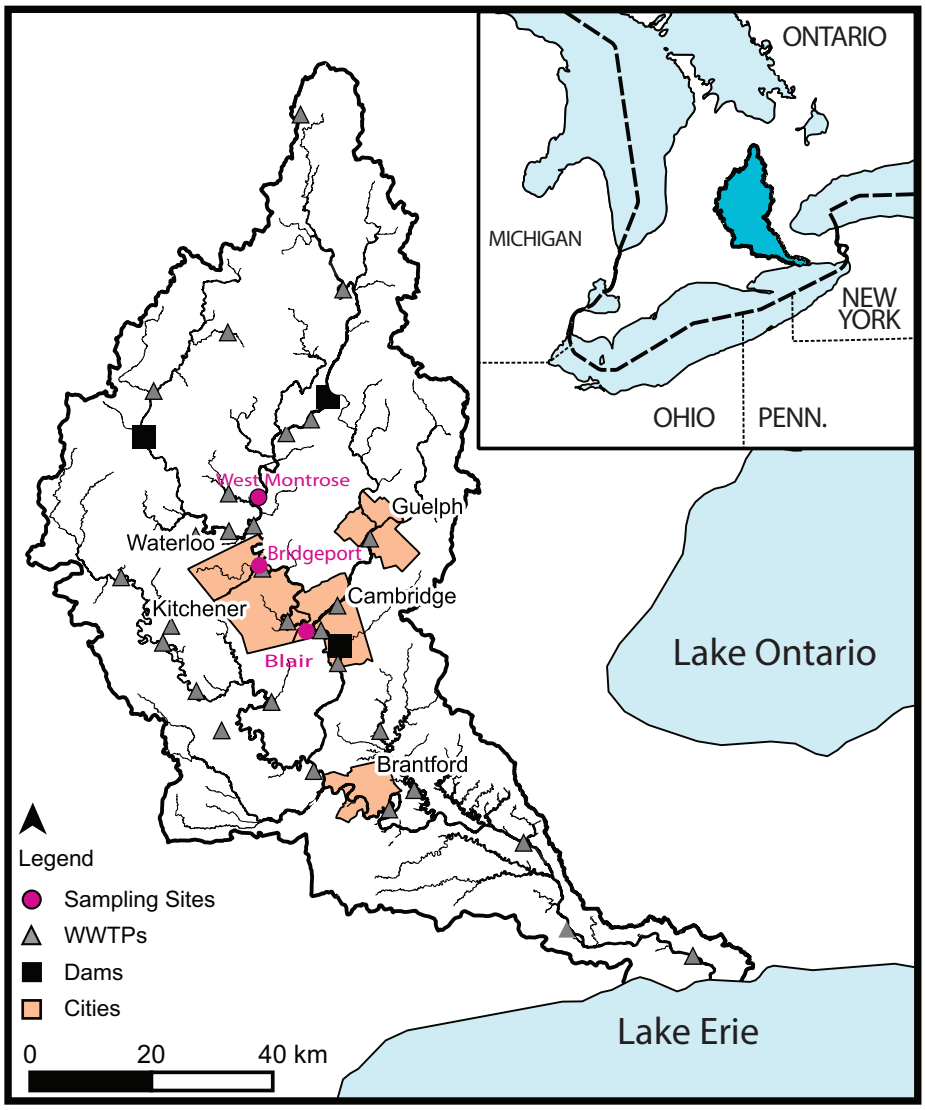

Figure 2.2: West Montrose and Blair sampling sites. Modified from Venkiteswaran et al. (2015).

2.3 Methods

2.3.1 Laboratory Incubation Experiments

To conduct the laboratory incubation experiments, one biofilm-covered rock was placed in each of six 2L beakers (Figure 2.3). Beakers contained river water that was spiked with a solution of KNO_3 (USGS 32) with known isotopic values for $\delta^{18}O\text{-}NO_3^-$ (+25.7‰) and $\delta^{15}N\text{-}NO_3^-$ (+180‰). Prior to field sampling, an isotopic mass balance (Equation 2.1) was used to determine the amount of KNO_3^- solution needed to alter the NO_3^- isotopes in the river water to provide the necessary sensitivity to observe isotopic changes over time.

$$\boldsymbol{\delta_f = \frac{NO_{3(River)} \times \delta_{(River)} + NO_{3(Standard)} \times \delta_{(Standard)}}{NO_{3(River)} + NO_{3(Standard)}}}$$

Equation 2.1

Where δ_f is the value of either $\delta^{18}O\text{-}NO_3^-$ or $\delta^{15}N\text{-}NO_3^-$ after mixing. $\delta_{(River)}$ and $\delta_{(Standard)}$ represent the approximate value of either $\delta^{18}O\text{-}NO_3^-$ or $\delta^{15}N\text{-}NO_3^-$ at the study site (based on average NO_3^- isotope values for this time of year) and the known isotope values of the KNO_3^- standard. The concentration of the standard was made to be approximately the same as the river concentration at each site, determined by field measurements from routine field sampling and continuous data provided from a SUNA NO_3^- sonde located at Bridgeport, just downstream of West Montrose. $NO_{3(River)}$ and $NO_{3(Standard)}$ was the mass of NO_3^- calculated using the concentrations and volumes of water that would be used in the experiment. The target values after mixing were determined to be approximately +6‰ and +48‰ for $\delta^{18}O\text{-}NO_3^-$ or $\delta^{15}N\text{-}NO_3^-$, respectively.

The water was also labeled in four of the six beakers with a distinct water isotope ($\delta^{18}O\text{-}H_2O$) value. Incubations were run in duplicate (Beaker A and B) and designated as a "level" of $\delta^{18}O\text{-}H_2O$: low, medium and high. The low beakers had no spike and therefore had a $\delta^{18}O\text{-}H_2O$ typical of the central Grand River, ranging between -9‰ and -11‰ relative to VSMOW (Venkiteswaran et al., 2015). The $\delta^{18}O\text{-}H_2O$ spike for medium and high beakers

was prepared by diluting a 97-atom % ^{18}O-H_2O standard to a 10-atom % solution. A second isotope mass balance was conducted to determine the correct volume of 10-atom % to add to the beakers to reach target values of +50‰ and +90‰ for medium and high, respectively.

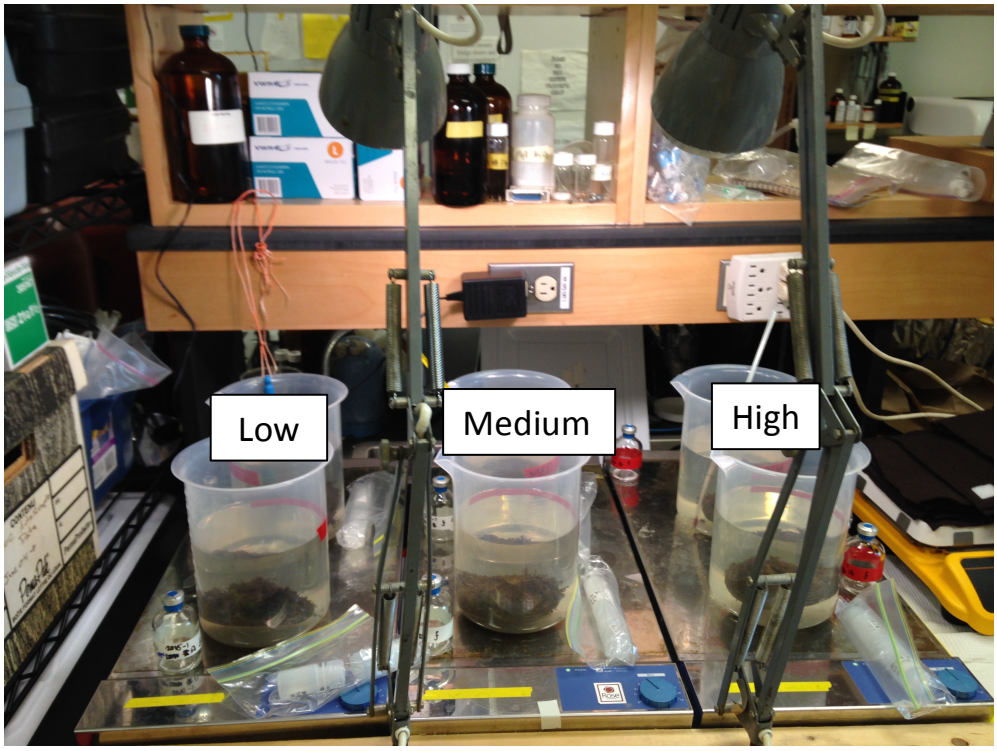

Figure 2.3: Laboratory incubation experiment set-up. Six 2L beakers are shown, each containing one biofilm-covered rock and 1.4L of river water spiked with KNO_3 of known isotopic value for $\delta^{18}O$-NO_3^- (+25.7‰) and $\delta^{15}N$-NO_3^- (+180‰). Duplicate beakers were labeled according to the $\delta^{18}O$-H_2O value of -8‰, +50‰ and +90‰ for Low, Medium and High beakers, respectively.

Two laboratory incubations were initiated on July 7, 2015 and September 2, 2015 with water and biofilm covered rocks from West Montrose. These incubations lasted for 60 and 72 hours, respectively. A third incubation, using water from Blair began on July 29, 2015 and ran for 60 hours. Field sampling took place the morning of each incubation experiment. River temperature and dissolved oxygen (DO) concentration were measured at the site using a handheld HACH 40Qd field meter, and 10L of water was retrieved for the

incubations in plastic carboys. Additional small volume samples were collected for total nitrogen (TN), inorganic N species (NH_4^+, NO_3^- and NO_2^-) and NO_3^- isotopes. Samples for chemical analysis were syringe filtered (0.45μm) into 30 mL HDPE bottles in the field. Filtered samples were also collected for $\delta^{18}O\text{-}H_2O$ in 1mL chromatography vials in the field. Six biofilm-covered rocks were collected and stored in plastic containers for transport back to the laboratory. Upon return to the laboratory, samples for chemical analysis were frozen and $\delta^{18}O\text{-}H_2O$ samples were stored at room temperature until analysis.

Based on previous calculations, 0.5L of the enriched KNO_3 solution was added to 0.9L of river water yielding a total of 1.4L in each beaker. All three pairs of beakers rested on magnetic stir plates and contained a magnetic stir bar. The purpose of the magnetic stir plates was to simulate river flow and also keep the system well oxygenated. A rock was placed into each beaker, and was positioned against the beaker wall so that flow simulated by the stir bar would create a current above the biomass, similar to that in the river. Following NO_3^- isotope enrichment, river $^{18}O\text{-}H_2O$ was enriched by adding 1.5mL and 2.85mL of 10-atom % $^{18}O\text{-}H_2O$ into the medium and high beakers, respectively. Two lamps with 630 lumens incandescent bulbs were utilized to simulate daytime light conditions. At sundown, the beakers were wrapped with dark brown felt ("beaker cozies") that loosely covered the tops to mimic nighttime conditions and were removed at sunrise the following morning (Figure 2.4).

Figure 2.4: Laboratory incubation experiment set-up with six 2L beakers. At sundown "beaker cozies" shown as the brown fabric were used to cover the beakers mimic nighttime conditions.

Beakers were sampled immediately after sufficient time (~2 minutes) was allowed for the sample and spike to mix completely (time 0 [T0]). Subsequent samples were taken at time T0.1, T0.5, T1, T2, T4, T8, T12, T24, T36, T48, T60, and T72 hours (West Montrose September 2015 only). Each time the beakers were sampled, temperature and DO were also measured with the same handheld HACH meter used in the field. To prevent cross-contamination between beakers, two 300mL beakers were filled with excess river water and after rinsing probes with DI were used to rinse the probe between sampling events. Beakers used for rinsing the probe were rinsed and refilled with new water after every sampling event. Temperature and DO were consistent for all experiments and over the course of each experiment, temperatures fluctuated between 22°C (night) and 24°C (daytime) and the DO between 5mg/L and 8mg/L, sufficient for nitrification. At each time point samples were

taken from each beaker using a 60mL syringe and filtered to 0.45μm. Two 30mL HDPE bottles were filled at each time point for TN, NO_3^-, NH_4^+, and NO_2^- analysis. Two 1mL chromatography vials were filled at time points T0.1 and T60 or T72 (West Montrose September 2015) for $\delta^{18}O$-H_2O and an additional 30mL HDPE bottle was taken for NO_3^- isotopes analysis at times: T0.1, T4, T12, T24, T48 and T60 or T72 (West Montrose September 2015) hours. Following sampling at each time point, 30mL samples for chemical analysis were immediately frozen and 1mL vials stored at room temperature until analysis. All samples, including those from initial field sampling were analyzed as soon as possible following the incubations.

Rock samples from the July West Montrose experiment and the July Blair experiment were scraped with a stainless steel spatula followed by a soft brush. Biofilm surface area was determined using a standard weight relationship in which the scraped area was estimated by covering it with aluminum foil that was then weighed. The samples were rinsed with nanofiltered water and poured into 90mL Starplex containers where they were frozen and subsequently then freeze-dried. Sub-samples were taken for isotopic and nutrient analyses.

2.3.2 In-River Chamber experiments

The purpose of the in-river chamber experiments was to observe how river metabolism alters NO_3^- isotopes and concentrations over time and to provide *in-situ* results under conditions comparable to those created in the laboratory incubations. In-river chamber experiments run in duplicate (Chamber A and Chamber B) were initiated at West Montrose on September 27, 2015 (CHWM1) for 24 hours. Prior to the experiment, a KNO_3 solution of known isotope values ($\delta^{18}O$ = +25.7‰ and ^{15}N = +180‰) was prepared (Equation 2.1) to sufficiently enrich the NO_3^- isotopes in the chambers. Target isotope values were calculated to be approximately +12‰ and +65‰ for $\delta^{18}O$ and $\delta^{15}N$, respectively.

Recirculating chambers as described by Bott et al. (1997) were used to allow containment of the spiked sample and five biofilm-covered rocks (Figure 2.5). The circulation of the 7L sample simulated river flow conditions. Before the chambers were deployed, water samples were collected and filtered to 0.45µm for TN, NO_3^-, NO_2^-, NH_4^+ and NO_3^- isotope ($\delta^{18}O$- and $\delta^{15}N$-NO_3^-) and $\delta^{18}O$-H_2O analysis. Samples for N species and N isotopes were placed on ice in a cooler until they could be taken back to the laboratory and frozen. Temperature and DO were measured in the river with a handheld HACH meter.

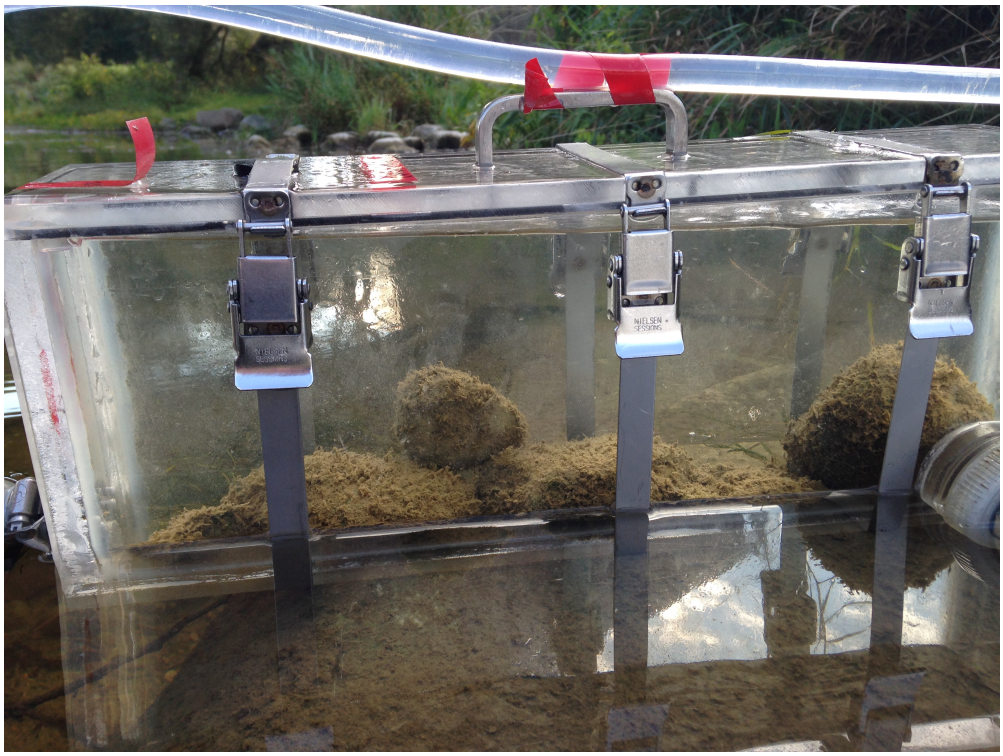

Figure 2.5: In-river chamber experiment set-up. Two 7L chambers contained seven biofilm covered rocks and river water spiked with KNO_3^- ($\delta^{18}O$ = +25.7‰ and ^{15}N = +180‰). A pump circulated the water in the chambers to simulate river flow. At sampling time points, the chamber was removed from the water and opened at the top to collect samples.

Five rocks selected from the river bottom were placed in the duplicate chambers along with 2L of KNO_3 solution and approximately 5L of river water to fill the chamber. After the pumps were started and the water sufficiently mixed, the first sample (T0) was taken using a 60mL syringe. Both chambers were then sealed and submerged in the river to maintain constant temperature until the next sampling time point. Samples for TN, NO_3^-, NO_2^-, NH_4^+ and NO_3^- isotope (^{18}O- and ^{15}N-NO_3^-) were collected and filtered to 0.45μm at time points: T0, T8, T18, T22, T24 hours. Water isotopes were sampled only at time T0 and T24 hours. Samples were returned to the Environmental Geochemistry Laboratory and frozen immediately. Batteries were checked and/or changed every four hours to ensure continuous flow in the chambers. As a result, DO levels closely reflected the DO in the river, with concentrations ranging between a high of 14 mg/L during the day to a low of 5mg/L at night. This range is typical of diel O_2 fluctuations previously observed at the study location (Venkiteswaran et al., 2007).

The Environmental Geochemistry Lab at the University of Waterloo conducted routine field sampling every two weeks for seven main channel sites on the Grand River (including West Montrose and Blair) that supplemented concentration and isotopic data for this study.

2.3.3 Analytical Methods

Nitrate Concentration

A Dionex ICS-2100 ion chromatograph, with an IonPac AS18 analytical and guard column and AS40 automated sampler was used to analyze water samples for NO_3^- concentrations. Samples were corrected to a calibration curve, created by standards run at the same time. The minimum detection limit (MDL) for this analysis was 0.02 mg N/L with a precision of 0.07 mg N/L.

Nitrite Concentration

A Unity Scientific SmartChem 200 (Discrete Analyzer) was used to analyze NO_2^- concentrations in water samples based on the method outlined by the USEPA EPA 353.2 Revision 2.0 (1993). NO_2^- concentration is measured by diazotizing the sample with sulphanilamide followed by coupling with N-(1-naphthyl)-ethylenediamine dihydrochloride to form a highly coloured azo dye which is measured colorimetrically at 550 or 529nm. The MDL for this method is 0.01 mg NO_2^- N/L with a precision of 5%.

Ammonium Concentration

Total ammonia N ($NH_4^+ + NH_3$) concentrations from water samples were analyzed using a Unity Scientific SmartChem 200 (Discrete Analyzer) using the method outlined by the USEPA EPA 350.1 Revision 2.0 (1993). The sample is buffered at a pH of 9.5 with a borate buffer and then distilled into a 2% solution of boric acid. Ammonia reacts with alkaline phenol and hypochlorite to form indophenol blue and the colour is intensified through the addition of sodium nitroprusside and measured colorimetrically at 630nm. The MDL using this method for this method is 0.01 mg NH_4-N/L with a precision of 5%.

Nitrate Isotopes: $\delta^{18}O\text{-}NO_3^-$ and $\delta^{15}N\text{-}NO_3^-$

Stable isotopes analysis of NO_3^- was conducted in the Environmental Isotope Laboratory (UWEIL) at the University of Waterloo, using the chemical denitrification method (conversion of NO_3^- to N_2O) as described by Mcllvin and Altabet (2005). All samples were kept frozen prior to analysis. Analysis of $\delta^{18}O\text{-}N_2O$ and $\delta^{15}N\text{-}N_2O$ was conducted using a Trace Gas – Isoprime, Continuous Flow Stable Isotope Ratio Mass Spectrometer (Thermo Finnigan/Bremen-Germany). The isotopic composition of the original NO_3^- is ultimately determined by creating a correction equation using the NO_3^- standards (EGC 17, USGS 34 and USGS 35) prepared and analyzed with each sample run. Stable isotope ratios are expressed as delta (δ) and expressed in per mil (‰). The precision for this analysis is ±0.3‰ for $\delta^{15}N$ and ±0.8‰ for $\delta^{18}O$.

$\delta^{15}N$ of Rock Biofilm

All dry samples for $\delta^{15}N$ were analyzed on a Delta Plus, Continuous Flow Stable Isotope Ratio Mass Spectrometer (Thermo Finnigan Bremen-Germany) coupled to a Carlo Erba Elemental Analyzer (CHNS-O EA1108 – Italy) in the Environmental Isotope Laboratory (UWEIL) at the University of Waterloo. Stable isotope ratios are measured relative to atmospheric air for nitrogen and Peedee Belemnite for carbon. The isotope ratios are expressed as delta values. Carlo Erba Elemental Standards B2005, B2035, and B2036 standards were used to calculate percentage compositions of nitrogen with a precision of +/- 1%.

2.4 Results

2.4.1 Temporal and Spatial Trends of NO_3^- isotopes in the Grand River

Throughout the year, samples from three sites (West Montrose, Bridgeport and Blair) in the main channel of the Grand River consistently plot in the nitrified septic/manure N box of the "Kendall plot" with values between +5‰ and +15‰ for $\delta^{15}N$ and values between -0.1‰ and +2‰ for $\delta^{18}O$ (Figure 2.6). Considering previous research, this plot would be enough to confirm that the main source of NO_3^- to the river is nitrified NH_4^+ originating from an allochthonous septic/manure source. However, it is unlikely that the soil N signal is not observed for any of these sites, particularly in the agricultural headwaters where animal population is lower (Figure 2.7). Visually, a denitrification trend could be observed in this dual isotope plot, however, few of these data actually follow the 0.5 slope that is diagnostic of denitrification (Figure 2.8). Slopes of the best-fit linear model II regression for West Montrose, Bridgeport and Blair are all greater than 0.5 (Figure 2.8). This would typically indicate that no denitrification had occurred and therefore $\delta^{15}N\text{-}NO_3^-$ could be used for source apportionment.

Seasonal trends in $\delta^{15}N$ values (lowest in the spring and fall and highest in the summer) exist for these sites on the Grand River but there is no apparent seasonal trend in $\delta^{18}O$ values (Figure 2.9). Some of the highest $\delta^{15}N$ values (> +10‰) are accompanied by the lowest NO_3^- concentrations (0-2mg N/L) suggestive of denitrification (Figure 2.10). However, the $\delta^{18}O$ values observed at these times are among the lowest (-2‰ to +2‰). Almost all the samples at the Blair site have NO_3^- concentrations greater than 2 mg N/L because of the upstream nutrients inputs from two major WWTPs. These data makes source apportionment difficult using the dual isotope plot (Figure 2.6) and therefore a better explanation for these $\delta^{18}O$-NO_3^- values must be developed.

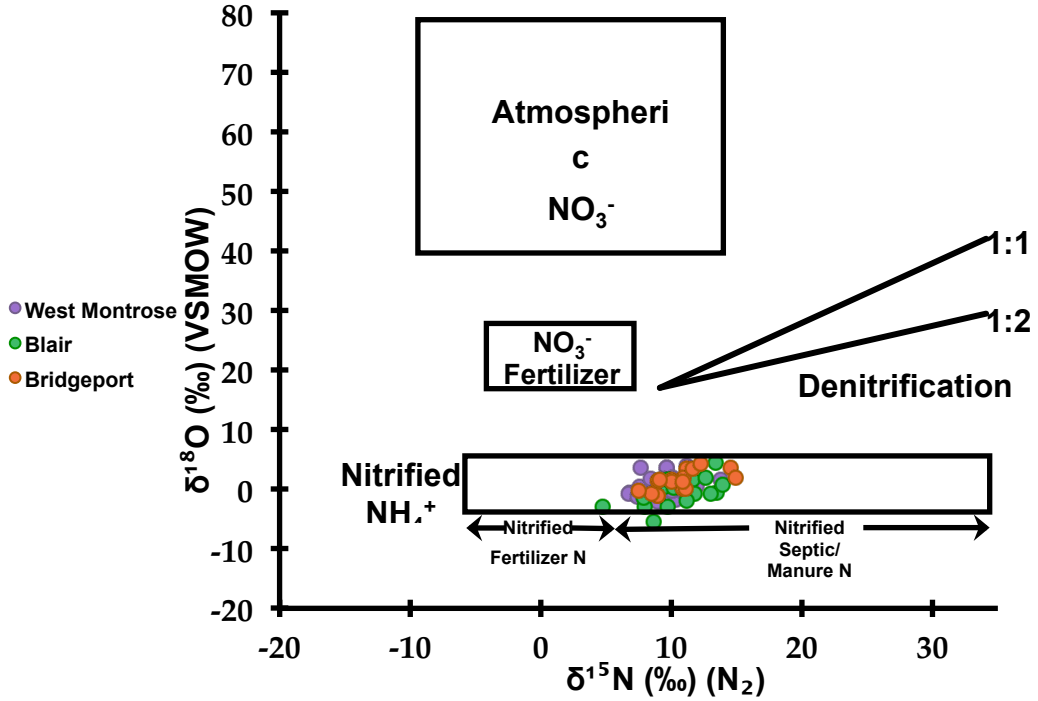

Figure 2.6: Kendall (2007b) source plot of $\delta^{15}N$-NO_3^- vs. $\delta^{18}O$-NO_3^- with data from three sites on the Grand River: West Montrose 21km and 47.7km upstream of Bridgeport and Blair, respectively. All data plot on the low end of the nitrified septic/manure N box with a range between +5‰ and +15‰ for $\delta^{15}N$ and the majority of the $\delta^{18}O$ between -0.1‰ and +2‰.

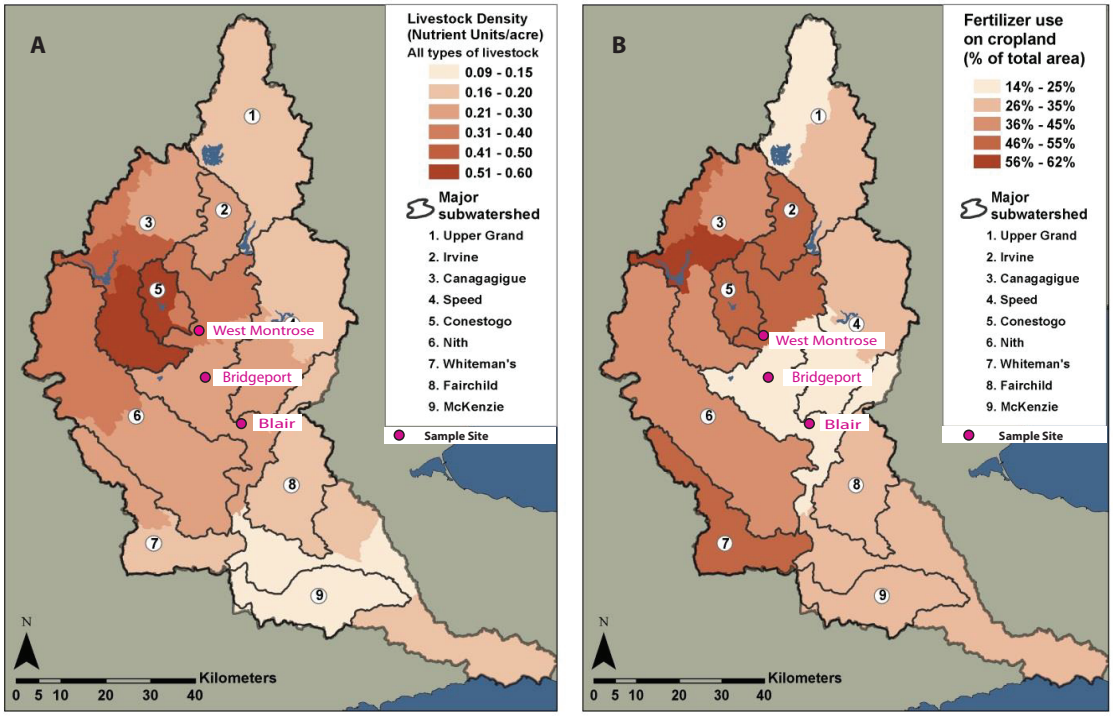

Figure 2.7: Density of nutrient production from all livestock types (A) and proportion of sub watershed area where there is use of agricultural fertilizer (B) (GRCA, 2013). Data from 2006 Census of Agriculture.

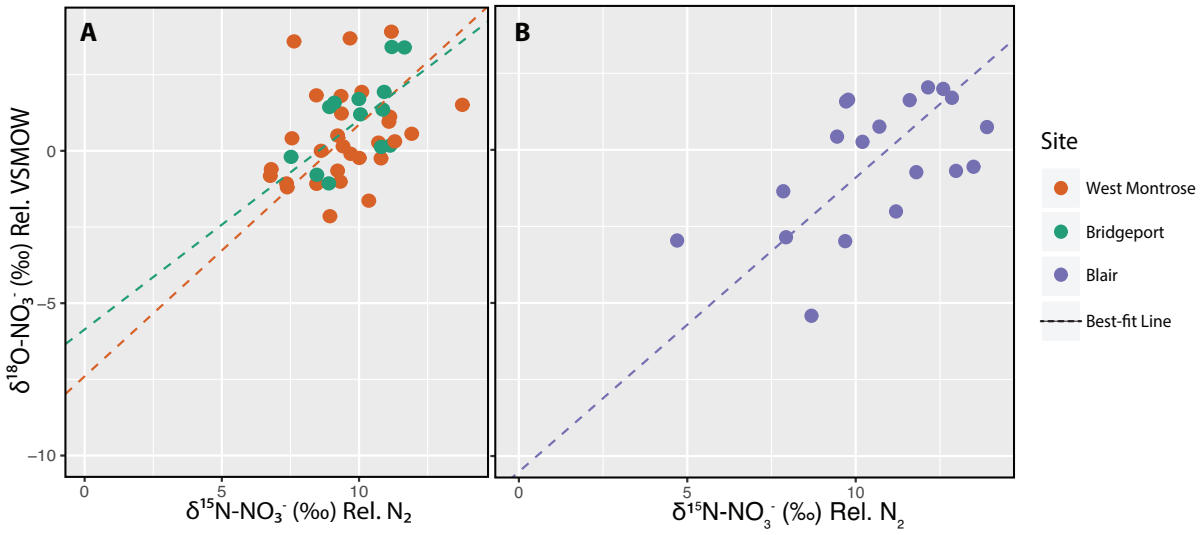

Figure 2.8: NO_3^- isotope data from three sites on the Grand River: West Montrose 21km and 47.7km upstream of Bridgeport (A) and Blair (B). The dashed line represents the best-fit model II regression lines for these sites with slopes of 0.83, 0.69 and 1.09 and r^2 of 0.079, 0.41 and 0.37 for West Montrose, Bridgeport and Blair, respectively.

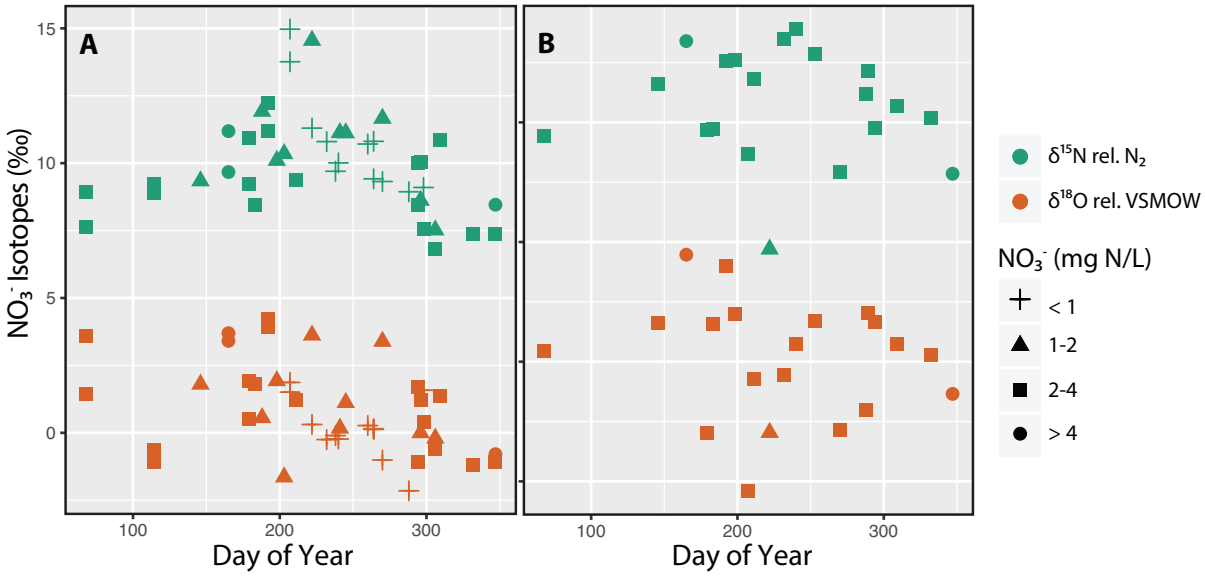

Figure 2.9: Seasonal variation in the $\delta^{18}O$- and $\delta^{15}N$-NO_3^- for all Grand River isotope data collected at West Montrose and Bridgeport (A) and Blair (B) from 2007-2015. Ranges in concentration as mg N/L (<1, 1-2, 2-4, >5) are depicted by the shapes identified in the legend.

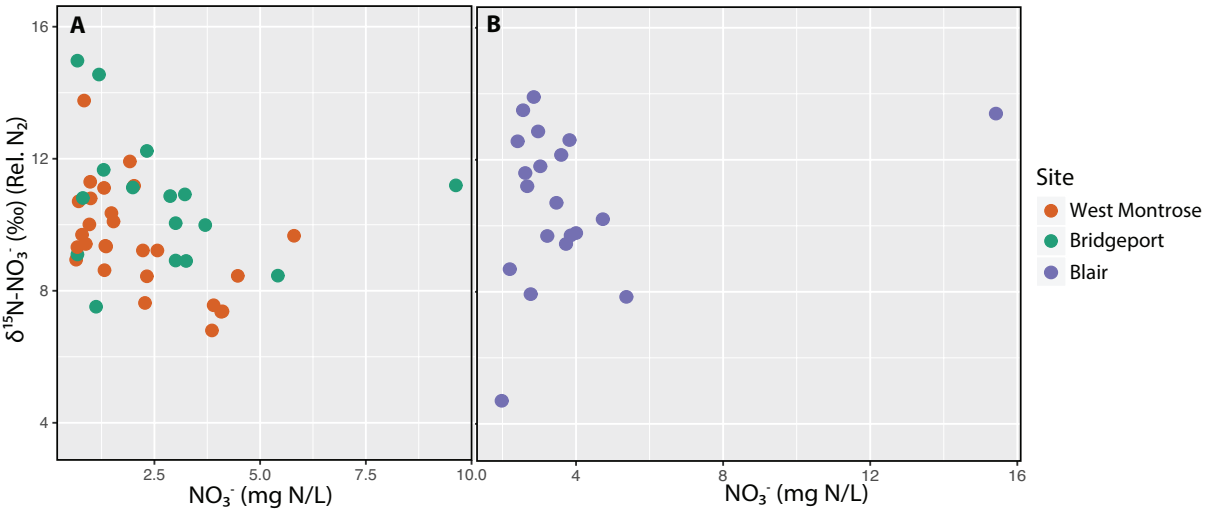

Figure 2.10: NO_3^- vs. $\delta^{15}N$-NO_3^- plots for three central Grand River sites: West Montrose and Bridgeport (A) and Blair (B). Two major WWTPs in Kitchener and Waterloo, Ontario discharge into the river between the Bridgeport and Blair sites.

2.4.2 Laboratory Incubations

In all incubations, the trends in the N concentration were different between the initial and final periods (T0-T24 hours and T24-T60).

I. West Montrose Experiment #1: July 7, 2015 (WM1)

The initial concentration of NO_3^- in the river was 1.9 mg N/L (Figure 2.11). This was reflected in the initial incubation values (T0) in all but one beaker (High B) where the initial concentration was higher. NO_3^- concentrations changed very little over the first 24 hours (T0-T24) in all beakers (Table 2.1). By the end of the incubation at T60, there was a net increase of NO_3^- in all six beakers by 1-2 mg N/L.

NO_2^- was not detected in the initial river sample and was low or undetected during the first 24 hours (Figure 2.11). The highest NO_2^- concentration was 0.5 mg N/L in Low A at T60. Accumulation of NO_2^- could be the result of slower rates of nitrification where NO_2^- has a higher residence time. Overall, NO_2^- concentrations in the Medium and High beakers remained constant and low (<0.2 mg N/l) from T24 to T60 except in Low A where concentration gradually increased over time.

NH_4^+ was not detected in the initial river sample and the concentration remained low or below the detection limit until T24 in all beakers (Figure 2.11). NH_4^+ in beaker High A changed very little from T36-T60 in the range of 0.03 to 0.06 mg N/L. The other beakers fluctuated on a 12-hour cycle as follows: NH_4^+ increased at T24 and T48 and decreased at T36 and T60 with the exception of Medium A that continued to increase after T24 to T36. At the final time point (T60) NH_4^+ was not detected in any of the six beakers.

The initial river NO_3^- isotope values obtained were typical of summer isotope values in the Grand River at West Montrose (Figure 2.9). The initial river $\delta^{15}N$-NO_3^- value was +12‰ and similar to the $\delta^{15}N$ of biomass (+8‰ to +9‰) (Gris, 2016). The initial incubation values ranged between +73‰ to +84‰ (Figure 2.11). Final $\delta^{15}N$ values ranged between +33‰ and +46‰ by the end of the experiment (T60). Values decreased by about 35‰ in all beakers

over time (Table 2.2). The $\delta^{15}N$ changed by 15‰ and 20‰ whether there was very little NO_3^- concentration change (T0-T24) or 1.1 mg N/L change (Table 2.1). Thus NO_3^- isotope values are changing even when NO_3^- concentrations are not changing. The net $\delta^{15}N$ added to the system could not be calculated for this experiment because there was not enough change in concentration relative to the shift in isotopic values.

The separation in $\delta^{18}O\text{-}NO_3^-$ between Low, Medium and High showed the incorporation of the $\delta^{18}O\text{-}H_2O$ even when NO_3^- concentrations remained constant or changed very little (Figure 2.11). The $\delta^{18}O\text{-}NO_3^-$ of the initial river sample was +0.6‰ and the initial experimental values of $\delta^{18}O\text{-}NO_3^-$ ranged between +10‰ and +13‰ for all beakers. At T24 the $\delta^{18}O\text{-}NO_3^-$ in the Low beakers had not shifted much (~1‰) from the initial values but by T60 values had decreased by 6‰ (Table 2.3). The $\delta^{18}O$ increased in the Medium and High beakers by 8‰ and 16‰ from T0 to T24 and continued to increase throughout the experiment. The $\delta^{18}O$ values changed/tended toward their $\delta^{18}O\text{-}H_2O$ values regardless of any net NO_3^- concentration change (Table 2.3).

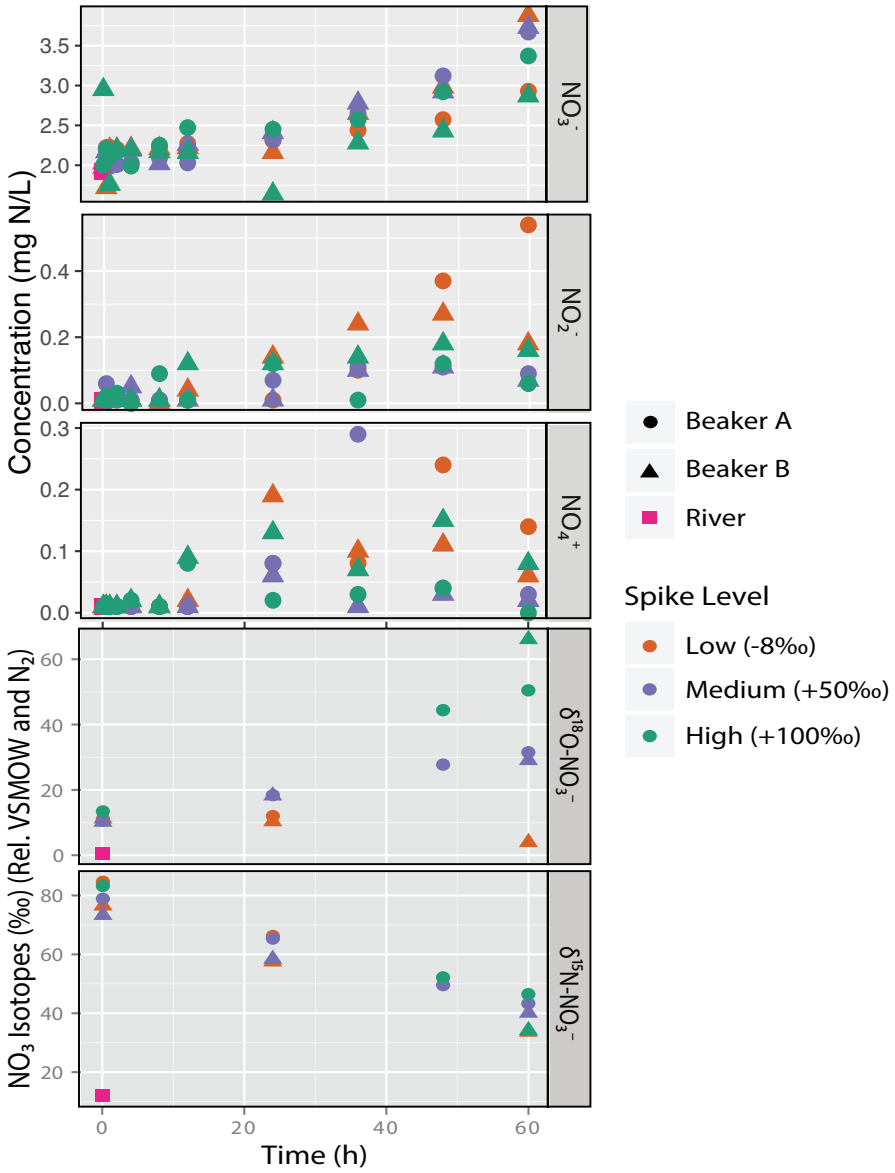

Figure 2.11: NO_3^-, NO_2^- and NH_4^+ concentration (top) and $\delta^{18}O$- and $\delta^{15}N$-NO_3^- isotope results (bottom) vs. time for the first West Montrose incubation conducted on July 7, 2015. The three pairs of beakers were labeled according to levels of $\delta^{18}O$-H_2O: Low (-9‰), medium (+62‰) and high (+100‰) and denoted by colours orange, purple and green in the figure, respectively. Each pair of beakers was labeled either 'A' or 'B' and are represented by circles and triangles in the figures, respectively. Initial river samples that were not spiked are marked by pink squares.

II. West Montrose Experiment #2: September 2, 2015 (WM2)

A second West Montrose incubation was conducted in September 2015 to confirm the results of the first experiment and to address changes over the growing season. The initial river NO_3^- concentration was 1.3 mg N/L (Figure 2.12), and similar to the river concentrations in July 2015. Initial NO_3^- concentrations in the beakers ranged between 0.9-1.0 mg NL. Similar to July WM1, NO_3^- concentration showed very little change in the first 24 hours (T24) (Table 2.1). NO_3^- increased between T24 and T72 hours by about 0.9 mg N/L in all beakers except for High A that only increased by 0.2 mg N/L. Similar to WM1 there was net NO_3^- production over the course of the incubation. However, the change in NO_3^- over the course of the experiment was smaller (~1 mg N/L) compared to the July experiment (1.3-1.7 mg N/L) (Table 2.1).

NO_2^- was not detected in the initial river sample (Figure 2.12). Similar to the July incubation NO_2^- concentrations were low (0.02 mg N/L) in the Low and Medium beakers and undetected in the High beakers. At T36 hours, NO_2^- remained in only one beaker (Medium B) and then was undetected in all beakers until T72 when it was detected at a low concentration of 0.01 mg N/L in Medium B and High A.

Similar to the July incubations, NH_4^+ was not detected in the initial river sample and NH_4^+ was low (0.02-0.04 mg N/L) in the Low and High beakers at T0 (Figure 2.12). The exception was the Medium beakers where it was undetected. NH_4^+ was not detected in any beaker until T36 when a low concentration of 0.02 mg N/L was observed in Low A. Similar to July, NH_4^+ fluctuated on a 12-hour cycle increasing between T36 and T48 hours then decreasing between T48 and T60 hours in most beakers. The highest NH_4^+ concentration of 0.07 mg N/L was observed in High A at T72. The lowest net NO_3^- production was also observed in this beaker. With the exception of High A, NH_4^+ was low (0.01-0.02 mg N/L) or undetected over the course of the incubation.

Isotopes of NO_3^- also responded similarly to the July incubations. The initial $\delta^{15}N$-NO_3^- river value was +12‰ and the $\delta^{15}N$ of the rock biofilm was +8‰. The initial $\delta^{15}N$-NO_3^- values ranged between +77‰ and +86‰ and they decreased uniformly as they did in the July experiment by close to 42‰ over the course of the incubation in most of the beakers (Table 2.2). The exception was High A where there was only an 18‰ decrease in $\delta^{15}N$ overtime. This can be attributed to low net NO_3^- production in this beaker. The NO_3^- concentration showed little change, especially in the first 24 hours, while the $\delta^{15}N$ values decreased around 17‰ and then further decreased around 25‰ from T24 to T72 in most beakers (Table 2.2). Much like the first West Montrose experiment, the net $\delta^{15}N$ added to the system could not be calculated for this experiment because there was not enough change in concentration relative to the shift in isotopic values.

The initial river value of $\delta^{18}O$-NO_3^- was +1.1‰ and the initial experiment value (T0) was +11.5‰ in all beakers (Figure 2.12). The $\delta^{18}O$-NO_3^- in the beakers with low $\delta^{18}O$-H_2O decreased by approximately 10‰ over the course of the experiment and increased in most of the Medium and High beakers by approximately 14‰ and 40‰, respectively (Table 2.3). The exception was High A that only increased by 14‰ over the course of the experiment and was the result of having the lowest net NO_3^- production (0.2 mg N/L) of all the beakers. Even though the final $\delta^{18}O$-NO_3^- value of High A closely resembled Medium A and B, the shift in $\delta^{18}O$ of 14‰ was still substantial. The $\delta^{18}O$-NO_3 isotopes shifted by ~4‰, ~8‰ and ~16‰ in the Low, Medium and High beakers, respectively in the first 24 hours despite the lowest change in NO_3^- concentration during this time period (0.1 mg N/L net production) (Table 2.3). The separation in $\delta^{18}O$-NO_3^- values was distinct for the three water labels (Low, Medium and High) and consistent with the results from the West Montrose July incubations. Overall, the results from this second experiment supported the findings from the July experiment.

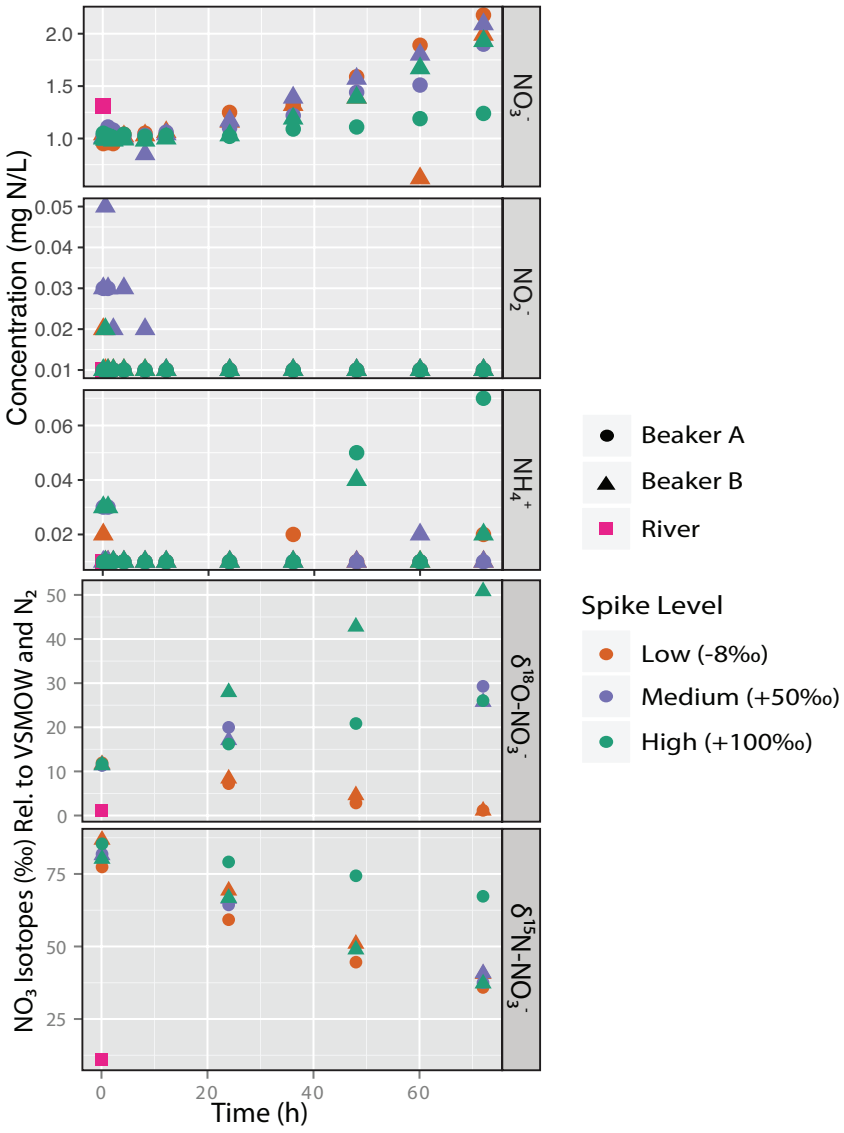

Figure 2.12: NO_3^-, NO_2^- and NH_4^+ concentration (top) and $\delta^{18}O$- and $\delta^{15}N$-NO_3^- isotope results (bottom) vs. time for the second West Montrose incubation conducted on September 2, 2015. The three pairs of beakers were labeled according to levels of $\delta^{18}O$-H_2O: Low (-9‰), medium (+62‰) and high (+100‰) and denoted by colours orange, purple and green in the figure, respectively. Each pair of beakers was labeled either 'A' or 'B' and are represented by circles and triangles in the figures, respectively. Initial river samples that were not spiked are marked by pink squares.

III. Blair: July 29, 2015

An incubation was also conducted with biofilms from the Blair site to observe if changes in concentrations and isotopes downstream of the wastewater treatment plants where concentrations of all nutrients including NO_3^- are typically higher were similar to the upstream site with lower nutrient concentrations.

The initial river NO_3^- concentration at Blair was 3.27 mg N/L (Figure 2.13). This is a typical concentration at Blair in July (Figure 2.1) and higher than the concentrations at the West Montrose site. The initial experiment NO_3^- concentration was 2.9 mg N/L in the Low beakers and ranged between 3.5-4 mg N/L in the Medium and High beakers. NO_3^- concentrations showed little change in the first 24 hours similar to the West Montrose incubations and then gradually increased over time. The NO_3^- concentration increased in the Low and Medium beakers by about 2.5 mg N/L and by about 2.0 mg N/L in the High beakers from T0 hours to T60 hours. Net production of NO_3^- in this incubation was at least 1 mg N/L greater than the net production in both West Montrose incubations (Table 2.1). Visually and texturally the rocks at West Montrose had a finer, slimy green film whereas the biomass on the Blair rocks tended to be more rough and stringy.

The initial river NO_2^- concentration was 0.40 mg N/L and the initial incubation concentrations in all six beakers were around 0.30 mg N/L (Figure 2.13), much higher than the concentrations at West Montrose. Between West Montrose and Blair there are two large WWTPs whereas upstream of West Montrose, there are mostly diffuse non-point source nutrient inputs. NO_2^- concentrations decreased over time but NO_2^- was present in almost all beakers from T0 to T48 (0.1-0.2 mg N/L). NO_2^- was mostly absent by T60 (except in Low A and Medium A at 0.02 and 0.03 mg N/L, respectively). The highest NO_2^- concentrations were consistently seen in the Medium and Low beakers.

Of the three incubations, Blair had some of the highest observed NH_4^+ concentrations initially and throughout the experiment. The initial river NH_4^+ concentration was 0.12 mg

N/L (Figure 2.13). NH_4^+ was detected in three of the six beakers at the start of the incubation (0.1 mg N/L in Low A and Medium B and 0.04 mg N/L in Low B). The highest NH_4^+ concentrations (>1.0 mg N/L) were observed in Low B and Medium B at T24 and T36, respectively. NH_4^+ concentrations were undetectable in all beakers by the end of the experiment (T60). The greatest net NO_3^- production (1.9 mg N/L) was observed following the decrease in NH_4^+ concentration in beaker Medium B.

The initial river $\delta^{15}N\text{-}NO_3^-$ value was +12‰, similar to the West Montrose site but the $\delta^{15}N$ of the rock biofilm was much higher, +14‰ to 17‰ (Gris, 2016). The initial $\delta^{15}N$ in the beakers ranged between +30‰ and +40‰. Similar to the West Montrose incubations, $\delta^{15}N\text{-}NO_3^-$ values uniformly decreased over time by approximately 8‰ in most beakers (Table 2.2). The exception was High B that had decreased by 14‰ at T60. Of the three incubations, Blair had the greatest net NO_3^- production throughout the experiment and the net $\delta^{15}N$ approached the $\delta^{15}N$ of rock biofilm in most beakers (Figure 2.14). Blair had the lowest change in $\delta^{15}N\text{-}NO_3^-$ isotopes overtime compared to the two West Montrose experiments (Table 2.1, 2.2 and 2.3). This suggests rate of processing may have been different between the two sites but the higher $\delta^{15}N$ of biomass influenced the amount of isotopic shift during the experiment. The initial river isotope value of $\delta^{18}O\text{-}NO_3^-$ was -0.73‰ (Figure 2.13), similar to that at West Montrose in July and September. Isotope values of $\delta^{18}O\text{-}NO_3^-$ at T0 of the experiment were +6‰ in Low A, +9‰ and +12‰ in Medium A and B, respectively and +7‰ in the High beakers. The $\delta^{18}O\text{-}NO_3^-$ in the low beakers decreased over time by 6‰ and the values increased in the Medium beakers by 22‰. The $\delta^{18}O\text{-}NO_3^-$ in the High beakers increased over time by about the same amount as the Medium beakers (25‰) and the final $\delta^{18}O\text{-}NO_3^-$ values in both High beakers closely resembled those of the Medium beakers that had lower $\delta^{18}O\text{-}H_2O$. However, the highest NO_2^- concentrations were observed in Medium beakers (0.22 mg N/L). Given that O-exchange has been found to occur between NO_2^- and H_2O during nitrification, slower rates of nitrification could have caused NO_2^- to accumulate and enhanced O-exchange yielding a similar final $\delta^{18}O\text{-}NO_3^-$ in the Medium and High

beakers. To account for differences in initial $\delta^{18}O\text{-}NO_3^-$ values, results of these incubations were recalculated to report isotopic ratios relative to the initial $\delta^{18}O\text{-}NO_3^-$ values (Figure 2.15). The $\delta^{18}O\text{-}NO_3^-$ values approached the $\delta^{18}O\text{-}H_2O$ of each water medium (-9‰, +52‰ and +102‰) regardless of any net NO_3^- concentration change (Table 2.3).

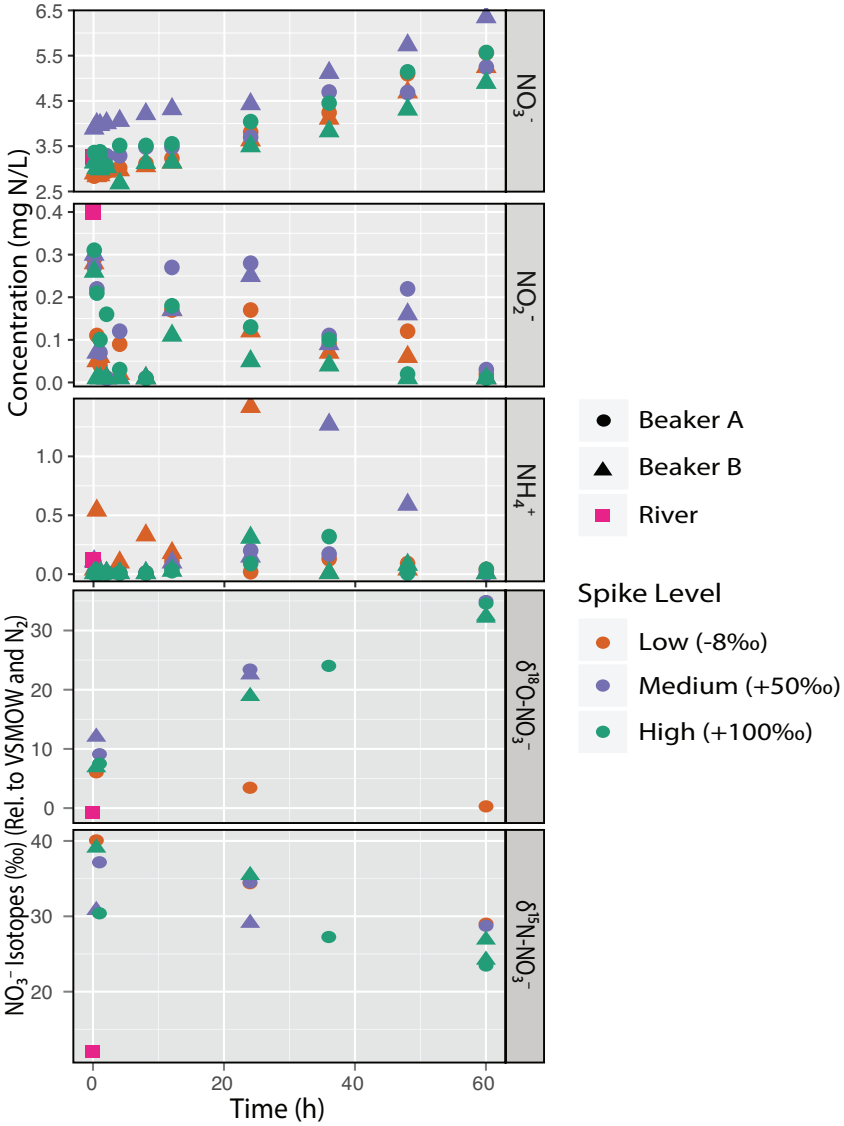

Figure 2.13: NO_3^-, NO_2^- and NH_4^+ concentration (top) and $\delta^{18}O$- and $\delta^{15}N$-NO_3^- isotope results (bottom) vs. time for the Blair incubation conducted on July 29, 2015. The three pairs of beakers were labeled according to levels of $\delta^{18}O$-H_2O: Low (-9‰), medium (+62‰) and high (+100‰) and denoted by colours orange, purple and green in the figure, respectively. Each pair of beakers was labeled either 'A' or 'B' and are represented by circles and triangles in the figures, respectively. Initial river samples that were not spiked are marked by pink squares.

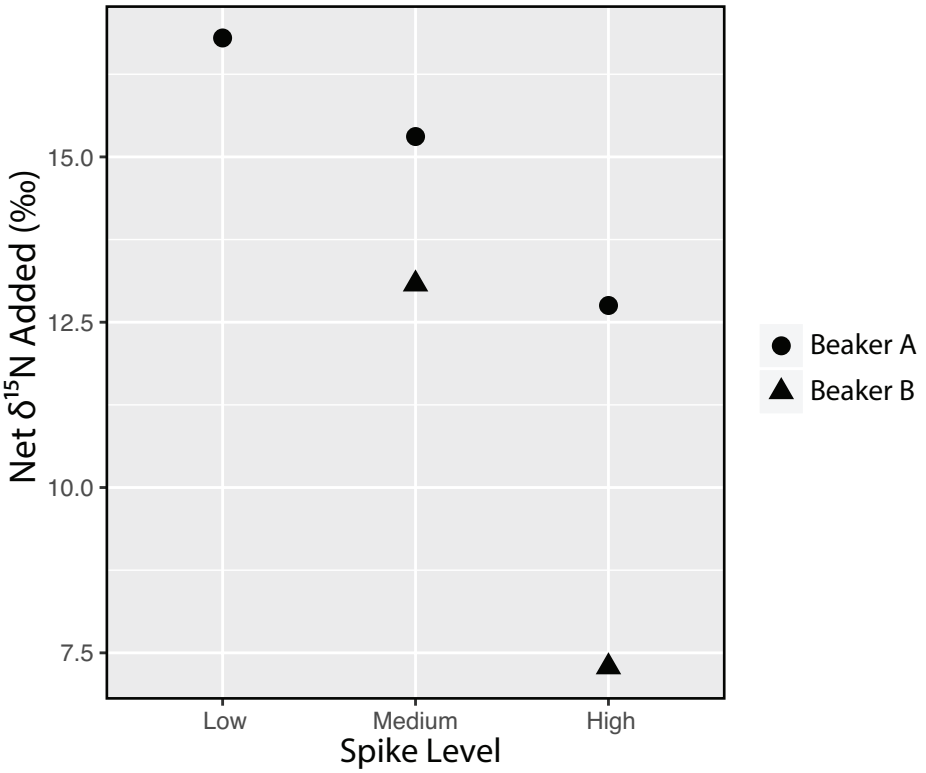

Figure 2.14: Net $\delta^{15}N$ for the Blair (July) incubation experiment. Net ^{15}N added to the system was calculated from an isotope mass balance similar to Equation 2.1. Triangles and circles represent duplicate beakers, A and B used in each experiment.

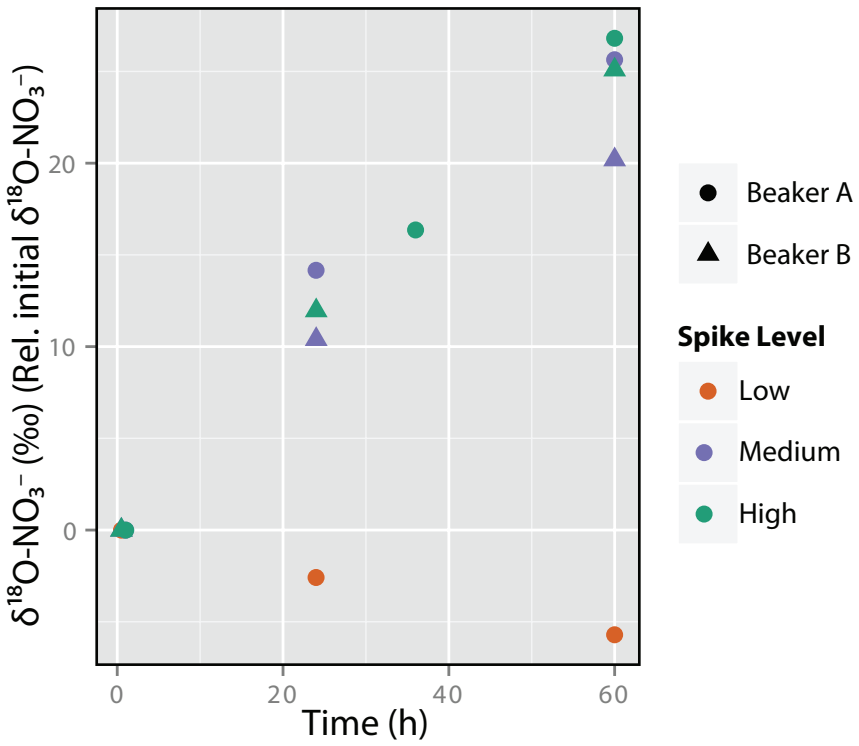

Figure 2.15: Isotope results for the Blair incubation conducted on July 29, 2015 shown relative to the initial $\delta^{18}O\text{-}NO_3^-$ in each beaker. The three pairs of beakers were labeled according to levels of $\delta^{18}O\text{-}H_2O$: low (-9‰), medium (+52‰) and high (+102‰) and denoted by colours orange, purple and green in the figure, respectively. Each pair of beakers were labeled either 'A' or 'B' and are represented by circles and triangles in the figures, respectively.

2.4.3 River Chamber Experiments

Chamber Experiment – September 17, 2015

The chamber experiment conducted in the river showed different concentration changes but isotopic effects similar to the three incubation experiments. The initial NO_3^- concentration in the river and chambers were 0.71 mg N/L and 0.99 mg N/L, respectively (Figure 2.16). Over time the NO_3^- concentration decreased by over half to 0.4 mg N/L at T24 in both chambers (Table 2.1). Net NO_3^- loss rather than net production (incubations) suggests that the environment in the beaker and chambers was different.

NO_2^- was not detected in the initial river sample or in either chamber throughout the experiment, similar to most beakers in the West Montrose incubations (Figure 2.16).

The initial concentration of NH_4^+ in the river was 0.01 mg N/L and increased to 0.03 mg N/L in both chambers at T0. NH_4^+ was not detected until T24 in both Chamber A (0.01 mg N/L) and Chamber B (0.08 mg N/L) (Figure 2.16).

The initial river $\delta^{15}N\text{-}NO_3^-$ value was 10.3‰ and the initial experiment values were +54.6‰ in Chamber A and +55.5‰ in Chamber B (Figure 2.16). The $\delta^{15}N$ values decreased continually over the 24 hours in both chambers by about 10‰ (Table 2.2).

The initial river value of $\delta^{18}O\text{-}NO_3^-$ was -1.6‰ and the initial experiment values were +14.7‰ in Chamber A and +15.3‰ in Chamber B. In 24 hours, $\delta^{18}O\text{-}NO_3^-$ values decreased by 2‰ in Chamber A and increased by 2‰ in Chamber B (Table 2.3).

Though the NO_3^- concentrations were low and decreased over time, the isotopes changed comparably to the incubation beakers as N was processed in the chambers (Table 2.2 and Table 2.3).

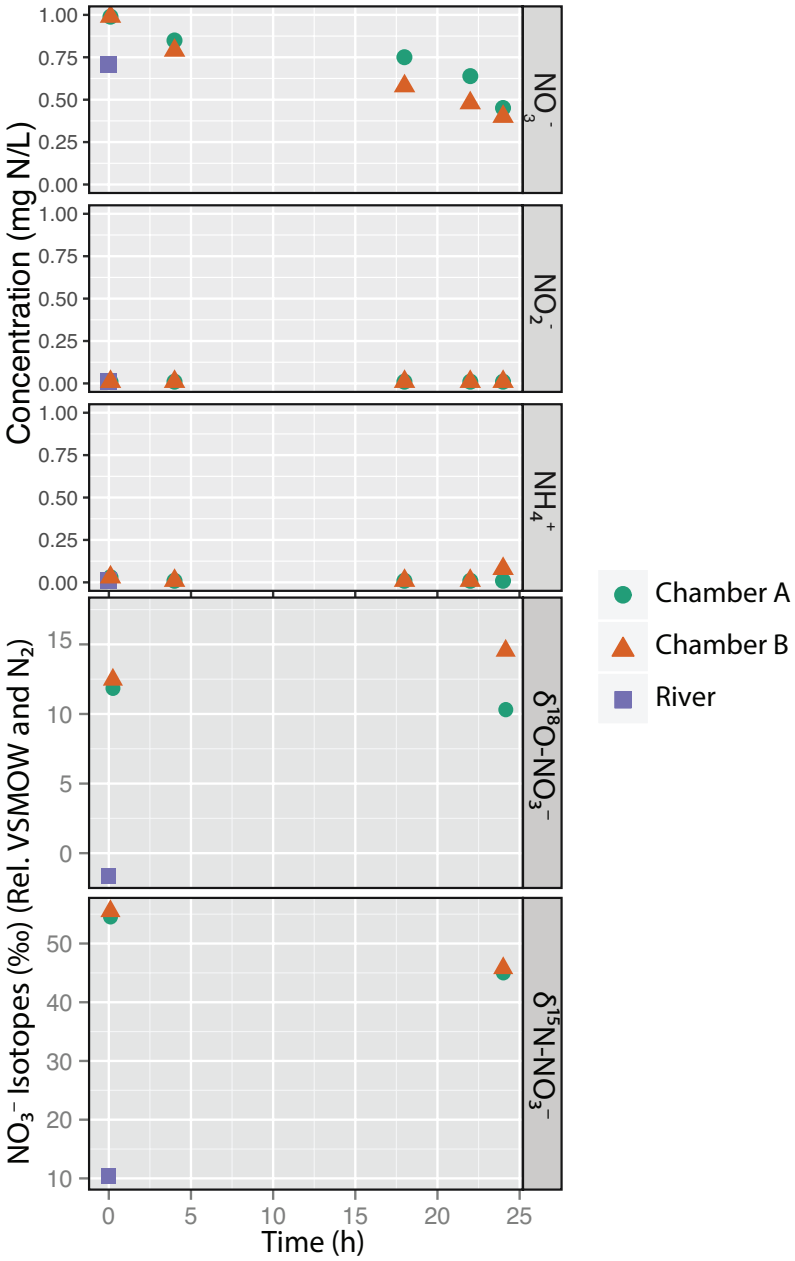

Figure 2.16: NO_3^-, NO_2^- and NH_4^+ concentration (top) and $\delta^{18}O$- and $\delta^{15}N$-NO_3^- isotope results (bottom) vs. time for the chamber experiment conducted on September 17, 2015. The two chambers were labeled 'A' or 'B' denoted as green circles and orange triangles, respectively. Initial river samples that were not spiked are denoted by purple squares.

Table 2.1: Change in NO_3^- concentration for two distinct time periods during each of three incubation experiments and one chamber experiment. Positive (+) values indicate net production of NO_3^- and negative (-) values indicate net loss. Net changes were calculated as final minus initial.

	T0-T24 hours (mg N/L)	T24-T60 or T72 Hours (mg N/L)	Total change in NO_3^- (mg N/L)
West Montrose July 2015	+0.3	+1.1	**+1.4**
West Montrose September 2015	+0.1	+0.9	**+1**
Blair July 2015	+0.6	+1.7	**+2.3**
West Montrose Chamber September 2015	-0.45	NA	**-0.45**

Table 2.2: Change in $\delta^{15}N$-NO_3^- values (in ‰) for two distinct time periods during each of three incubation experiments and one chamber experiment. Positive (+) values indicate an increase and negative (-) values indicates a decrease in isotopic values. Net changes were calculated as final minus initial and the net $\delta^{15}N$ added was calculated with an isotope mass balance.

	T0-T24 hours (‰)	T24-T60 or T72 Hours (‰)	Total change in $\delta^{15}N$ (‰)	Net $\delta^{15}N$ Added (‰)
West Montrose July 2015	-15	-20	**-35**	**NA**
West Montrose September 2015	-17	-25	**-42**	**NA**
Blair July 2015	-3	-5	**-8**	**5-17**
West Montrose Chamber September 2015	-10	NA	**-10**	**NA**

Table 2.3: Change in $\delta^{18}O\text{-}NO_3^-$ values (in ‰) for two distinct time periods during each of three incubation experiments and one chamber experiment. Positive (+) values indicate an increase and negative (-) values indicates a decrease in isotopic values. Net changes were calculated as final minus initial.

	T0-T24 hours			**T24-T60 or T72 (BL1) Hours**			**Total change in $\delta^{18}O$**		
Beaker	*Low*	*Medium*	*High*	*Low*	*Medium*	*High*	***Low***	***Medium***	***High***
West Montrose July 2015	-0.8	+8	+16	-6	+12	+20	**-6.8**	**+20**	**+36**
West Montrose September 2015	-4	+8	+16	-6.5	+8.5	+22	**-10.5**	**+16.5**	**+38**
Blair July 2015	-2	+12	+13	-3	+10	+12	**-5**	**+22**	**+15**
West Montrose Chamber September 2015	-2	NA	NA	NA	NA	NA	**-2**	**NA**	**NA**

2.5 Discussion

Without a complete understanding of the $\delta^{18}O$ values, one might disregard the role of denitrification and rapid internal N cycling in the river (Figure 2.17B). Even when NO_3^- concentrations are not changing in rivers, stable isotopes of NO_3^- can indicate the presence of NO_3^- cycling. No change in concentration means only balanced rates and not that $\delta^{15}N$- and $\delta^{18}O$-NO_3^- are conservative in the river.

2.5.1 Concentrations of N Species

Similar sized rocks were collected for the incubations but some of the variability between duplicate beakers is likely due to differences in rock surface area or biofilm biomass. Concentrations were not corrected for these two variables.

I. Role of NO_3^- in Rivers

No change in NO_3^- simply means that net rates are balanced. This was observed in most beakers during the first 24 hours of all three incubation experiments indicating balanced rates of N cycling processes (mineralization, nitrification, denitrification and uptake). Net NO_3^- production can occur but may be difficult to discern in rivers if there are additional sources of NO_3^-. Net NO_3^- production from 24-60 or 72 hours in the beakers could be due to biomass mineralizing into NH_4^+ and subsequently nitrifying into NO_3^-. Rates of nitrification would have been greater than the rate of denitrification and uptake combined (Figure 2.17). Blair had higher NO_3^- concentrations and the greatest net NO_3^- production compared to West Montrose. Blair is directly downstream from the Waterloo and Kitchener WWTPs and receives point-source nutrients while West Montrose is upstream of the WWTPs and receives mostly non-point source agricultural inputs. Nutrient concentrations are therefore higher at Blair but also the concentrations of other chemicals besides nutrients are present and thus the water quality is different than West Montrose. Rate and/or amount of nitrification were highest at the Blair site compared to the upstream West Montrose site (Table 2.4). These net rates were comparable to literature rates for watersheds with mixed

land-use (Table 2.5) similar to the Grand River watershed. The lowest NO_3^- concentrations were observed in the river chamber experiments at West Montrose. Lower and decreasing NO_3^- concentrations suggest that rates of uptake and/or denitrification were greater than nitrification in the chambers. The two scenarios from the laboratory incubation experiments: 0-24 hours (no net change in NO_3^-) and 24-60/72 hours (net NO_3^- production) allowed the opportunity to examine changes in $\delta^{15}N$- and $\delta^{18}O$-NO_3^- under both conditions over time.

II. Role of NO_2^- in Rivers

The low NO_2^- that in most beakers in the West Montrose incubations could have resulted from fast rates of nitrification compared to mineralization such that the lifetime of NO_2^- in the beakers was short. Sufficient DO, temperature and light in the beakers would have also facilitated the reaction to go to completion. High NO_2^- observed in the river at the Blair site and in the Blair incubations could have been the result of higher NO_2^- input from upstream WWTPs and/or slower rates of nitrification that allowed for the accumulation of NO_2^-. Although NO_2^- exchange with H_2O can occur without an accumulation of NO_2^-, the presence of NO_2^- indicates that the residence time of NO_2^- was likely longer at the Blair site compared to the West Montrose site. Where NO_2^- was detected in the laboratory incubations, there was a greater opportunity for O-exchange between NO_2^- and H_2O to occur which would cause a greater overall shift in $\delta^{18}O$-NO_3^- toward the $\delta^{18}O$-H_2O of the medium.

III. Role of NH_4^+ in Rivers

NH_4^+ has a short half-life in the Grand River and is usually nitrified or taken up by biota (Cejudo, 2016) but higher concentrations may arise intermittently because of upstream nutrients or rainfall events. NH_4^+ was only observed at the Blair site during initial river sampling because of nutrient inputs from WWTPs. NH_4^+ concentrations in all three incubation experiments showed small increases and subsequent decreases that fluctuated on a 12-hour cycle and sometimes corresponded inversely with NO_3^- concentrations. These

changes were likely the result of mineralization and subsequent nitrification. The $\delta^{15}N\text{-}NH_4^+$ released from mineralization should reflect that of the rock biomass (if there is little or no fractionation) and would affect the end member value of $\delta^{15}N\text{-}NO_3^-$ after nitrification.

Denitrification of NO_3^- and uptake of NH_4^+ or NO_3^- may have also altered the concentrations of these N species; however, neither were expected to be important relative to mineralization and nitrification (Battin et al., 2016; Burgin & Hamilton, 2007; Mulholland et al., 2008). Denitrification would have been unlikely in these experiments because the beakers were well oxygenated and stirred continuously. In addition, the increase in NO_3^- concentrations over time in all incubations experiments indicates the rate of mineralization and subsequent nitrification of NH_4^+ was greater than any uptake of N species. It is difficult to discern the relative amounts of uptake/denitrification versus mineralization and subsequent nitrification in rivers with concentration data alone and with unquantified inputs of NO_3^-. Isotopes are required to constrain relative rates of these processes.

2.5.2 Role of $\delta^{15}N$- and $^{18}O\text{-}NO_3^-$ in Source Apportionment of a Highly Impacted River

I. Are $\delta^{15}N$- and $^{18}O\text{-}NO_3^-$ conservative in surface waters?

Results from this study indicate that the $\delta^{15}N$- and $\delta^{18}O\text{-}NO_3^-$ are *not* conservative in the Grand River. NO_3^- isotopes changed even when NO_3^- concentrations more or less stayed the same (T0-T24 of incubations). Changes were also observed when NO_3^- concentration both increased (T24-T60 or T72 of incubations) and decreased (West Montrose chamber experiment). This contradicts the necessary assumption for source apportionment where no change in NO_3^- means conservative NO_3^- isotopes (Figure 2.17A).

Studies have found the $\delta^{15}N$ of biomass to range between +8‰ and +9‰ at the West Montrose site and from +14‰ to +17‰ at the Blair site (Gris, 2016). The high initial $\delta^{15}N\text{-}NO_3^-$ in the incubations was expected to decrease in all experiments over time as NO_3^- was cycled because any NO_3^- produced from biomass mineralization and nitrification would have a much lower $\delta^{15}N$ than the initial incubation value. The $\delta^{15}N\text{-}NO_3^-$ values decreased

uniformly in all beakers overtime in all experiments, and net $\delta^{15}N$ for the Blair site approached the $\delta^{15}N$ biomass values. The $\delta^{18}O\text{-}NO_3^-$ changed toward the $\delta^{18}O\text{-}H_2O$ value of the medium in all beakers and chambers over time even when NO_3^- did not change. Equilibrium O-exchange between NO_2^- and H_2O during nitrification thus alters end member isotope values.

II. Can $\delta^{15}N$- and $^{18}O\text{-}NO_3^-$ be used to indicate denitrification and sources to the Grand River?

In most cases, denitrification produces higher values of $\delta^{15}N$ and $\delta^{18}O$ and nitrification produces lower values of $\delta^{15}N$ and $\delta^{18}O$ (Figure 2.17A). However, these isotopes are not conservative and values of $\delta^{18}O\text{-}NO_3^-$ are variable making it difficult to predict end member values. Therefore $\delta^{15}N$- and $\delta^{18}O\text{-}NO_3^-$ cannot be used to indicate denitrification in the Grand River. River metabolism influences rapid isotopic changes and masks the original source and denitrification signal even where and when we know denitrification is occurring (Rosamond, 2013).

III. Is the interpretation of isotopic systematics consistent between two sample sites: West Montrose and Blair?

Differences were observed between the two study sites, adding to the complexity of riverine NO_3^- cycling and the use of NO_3^- isotopes for source apportionment. These differences were evident in the concentrations of nutrients, the net production of NO_3^- and the value of the $\delta^{15}N$ of biomass (all greatest at the Blair site). These differences can be attributed to the input of the additional nutrients from the WWTPs upstream of the Blair site compared to the West Montrose site.

In addition, rates of incorporation of the three $\delta^{18}O\text{-}H_2O$ labels into NO_3^- and the uptake and release of NO_3^- were not the same over time (between beakers and sites) and therefore, relative rates of N transformation processes should be considered as well as the mechanism(s) for the "reset" of $\delta^{18}O\text{-}NO_3^-$ toward the $\delta^{18}O\text{-}H_2O$ (Chapter 3).

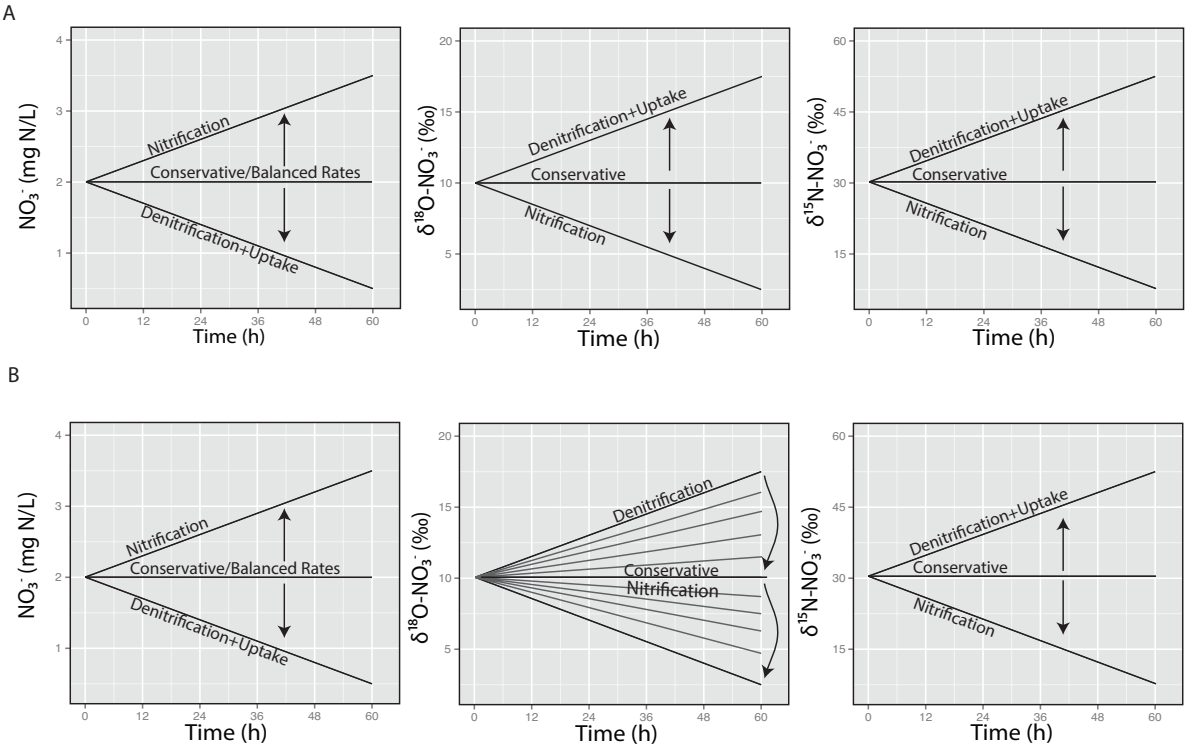

Figure 2.17: Schematic representation of NO_3^- transformation processes and the expected trends for NO_3^- concentration and NO_3^- isotopes. The top figure (A) indicates what would be expected if the $\delta^{18}O$- and $\delta^{15}N$-NO_3^- were conservative in the river and B represents potential trends in values if the $\delta^{18}O$- and $\delta^{15}N$-NO_3^- were not conservative.

Table 2.4: Net rates of NO_3^- production for two distinct time periods (0-24 hours and 24-60 hours) for each incubation experiment, two at West Montrose in July and September and one at Blair and one chamber experiment. Positive (+) values indicate net release and negative (-) values indicate net consumption. Areal biomass corrections were made for the West Montrose and Blair incubations in July.

Experiment	0-24 Hours ($\mu g\ N\ L^{-1}\ h^{-1}$)	0-24 Hours ($\mu g\ N\ cm^{-2}\ h^{-1}$)	24-60 Hours ($\mu g\ N\ L^{-1}\ h^{-1}$)	24-60 Hours ($\mu g\ N\ cm^{-2}\ h^{-1}$)
West Montrose July 2015	15.5	0.11	36.8	0.26
West Montrose September 2015	4.51	NA	21.3	NA
Blair 2015	26.0	0.17	45.2	0.30
West Montrose Chamber September 2015	-23.5	NA	NA	NA

Table 2.5: Net rates of NO_3^- production found in literature across different stream and watershed characteristics.

Rate ($\mu g\ N\ cm^{-2}\ h^{-1}$)	Source	Stream/Watershed Characteristics
0.77	(Dodds et al., 2000)	Upland prairie stream
0.65	(Grimm et al., 1991)	Intermittent desert stream
0.48	(Starry et al., 2005)	Appalachian headwater stream
0.26	(Starry et al., 2005)	Appalachian headwater stream
0.45	(Strauss & Lamberti, 2000)	3rd-order stream; watershed of mixed land use

2.6 Summary and Implications

The objectives of this chapter were to determine if the $\delta^{18}O\text{-}NO_3^-$ and the $\delta^{15}N\text{-}NO_3^-$ are conservative and, if so, can those isotopes be used as an indicator of denitrification and source in the Grand River at differences sites.

Isotope data from routinely sampled sites on the Grand River showed seasonal patterns in the NO_3^- concentrations and $\delta^{15}N\text{-}NO_3^-$ but no clear trend in $\delta^{18}O\text{-}NO_3^-$ values. A "Kendall source plot" illustrated that all Grand River isotope data was in the nitrified manure source box and that denitrification does not affect the isotopes at any of these sites. It is unlikely that the seasonal shift in $\delta^{15}N$ is caused by a change in N from fertilizer to manure within the same season because of the lower livestock density in the agricultural headwaters.

To examine the use of NO_3^- isotopes for source apportionment and identification of denitrification in rivers, three laboratory incubation experiments and one in-river chamber experiment were conducted. The first two incubation experiments were conducted with river water and biofilm covered rocks from West Montrose in July and September. The third laboratory incubation conducted in July used river water and rocks from Blair, downstream of West Montrose and inputs to the river from the Waterloo and Kitchener WWTPs.

The highest concentrations of NO_3^-, NO_2^- and NH_4^+ and the highest net NO_3^- production were observed at Blair (Figure 2.13). In all incubations from both sites NO_3^- concentration changed very little in the first 24 hours (T0-T24) and then steadily increased from T24-T60 or T72 (Table 2.1). The production of NO_3^- was due to mineralization and subsequent nitrification, as NH_4^+ did not increase. The $\delta^{15}N\text{-}NO_3^-$ values decreased by approximately the same amount in each incubation experiment regardless of any change in N concentrations (Table 2.2). The $\delta^{18}O\text{-}NO_3^-$ changed during the experiment toward the $\delta^{18}O\text{-}H_2O$ of the medium even when NO_3^- concentrations did not change or changed very little (Table 2.3). All three incubations showed a separation in $\delta^{18}O\text{-}NO_3^-$ corresponding to

each of the distinct isotopic water labels indicating that water exchange was the involved mechanism that altered the $\delta^{18}O\text{-}NO_3^-$ (Low, Medium and High). This is consistent with the effect of O-exchange between NO_2^- and H_2O which is known to be rapid.

A submerged chamber experiment that ran for 24 hours at West Montrose was conducted to compare *in-situ* river conditions with the laboratory beaker incubations. The NO_3^- concentration decreased over time because rates of uptake and or/denitrification were greater than nitrification. The data from the chamber experiment and the laboratory incubations was comparable because the NO_3^- isotope values in the chambers shifted approximately the same amount as they did within the first 24 hours in the Low beakers of the incubation experiments (Table 2.2 and Table 2.3).

The $\delta^{18}O\text{-}NO_3^-$ values changed relative to the $\delta^{18}O\text{-}H_2O$ in the beakers while $\delta^{15}N\text{-}NO_3^-$ decreased over time and net $\delta^{15}N$ of biomass at the Blair site resembled the $\delta^{15}N$ of rock biomass. This trend was observed in every experiment and provided evidence that both the $\delta^{15}N$ and $\delta^{18}O$ of NO_3^- are not conservative and therefore cannot be used as an indicator of source and denitrification in the Grand River. As N was transformed in the beakers and the chambers, NO_3^- isotopes were rapidly cycled even when net NO_3^- production was low (Table 2.1). This study has shown that the biofilm that covers the rocks and the river bottom has a profound effect on river metabolism and N cycling processes in the Grand River. The use of isotopes for source apportionment of NO_3^- in rivers needs to be revised for highly impacted systems like the Grand River. This information is valuable to those concerned with the fate of elevated NO_3^- and who have used NO_3^- isotopes for source determination in the past. Managers should be cautious before isotopes are used to determine source and first understand the complexity of N cycling and NO_3^- isotopes.

In order to improve the use of NO_3^- isotopes as a tool for source apportionment in rivers, the possible mechanisms responsible for altering the $\delta^{18}O\text{-}NO_3^-$ should be examined. Abiotic O-exchange that occurs between NO_2^- and H_2O is one such mechanism. Research

has found that the amount of abiotic O-exchange that occurs between NO_2^- and H_2O (*f*abiotic) can influence the $\delta^{18}O\text{-}NO_3^-$ (Snider et al., 2010). The "1:2 rule" for oxygen incorporation assumes that during nitrification, the fraction of abiotic O-exchange is 0 (Snider et al., 2010). The *f*abiotic in the Grand River can be calculated from the $\delta^{18}O\text{-}NO_3^-$ results of these incubation experiments. If the fraction of abiotic exchange could be placed on a scale of 0 to 1, rates of N cycling in the Grand River could potentially be characterized. This could be a useful tool for managers in conjunction with the NO_3^- isotopes to understand the fate of NO_3^- in the river and improve water quality. For instance, *f*abiotic of 0 and no O-exchange could mean low or high rates of N transformations processes. NO_3^- would be conservative in the river and persist. A *f*abiotic value of 1 and equilibration of H_2O and NO_2^- would mean high rates of N processing: greater nitrification, denitrification and potentially more transient incorporation of NO_3^- into biomass. A model must be created next to elucidate the rates of N transformation processes (mineralization, uptake, nitrification and denitrification) in the Grand River. Chapter 3 will use incubation data to examine the potential mechanisms responsible for altered riverine $\delta^{18}O\text{-}NO_3^-$ and use a mathematical model to look at the rates of N transformation processes.

Chapter 3 – Improving NO_3^- Isotope Tools in Productive Rivers

3.1 Introduction

In-river productivity can have a profound impact on N cycling and the resulting NO_3^- isotope values. Field and experimental data (Chapter 2) indicate that the $\delta^{15}N$- and $\delta^{18}O$-NO_3^- in the Grand River are not conservative. In-river metabolism alters the isotopic signal such that it cannot be used to indicate denitrification or sources of NO_3^- to an impacted river.

Nitrification is the oxidation of NH_4^+ to NO_2^- and then NO_3^- and involves the incorporation of three oxygen molecules: one from O_2 and two from H_2O. The O_2 is the first to be incorporated to form NH_2OH, followed by one water-oxygen to form NO_2^- and then another water-oxygen to form NO_3^- (Figure 3.1). Studies have documented further O-exchange between H_2O and NO_2^- during NH_4^+ oxidation (Andersson et al., 1982; Casciotti et al., 2010; DiSpirito & Hooper, 1986; Snider et al., 2010). The kinetic ^{18}O isotope fractionations that result from the incorporation of O_2 ($^{18}\varepsilon_{O2}$) and H_2O ($^{18}\varepsilon_{H2O,1}$ and $^{18}\varepsilon_{H2O,2}$) in nitrification are large and were first estimated by Casciotti et al. (2010) and Buchwald & Casciotti (2010) (Figure 3.1). The combined isotope fractionations for O_2 and H_2O incorporation ($^{18}\varepsilon_{O2}$ + $^{18}\varepsilon_{H2O,1}$) in the initial oxidation stages was found to range between -38‰ and -18‰ for four marine ammonia-oxidizing bacteria (AOB) and the isotope effect for H_2O incorporation ($^{18}\varepsilon_{H2O,2}$) in the final oxidation step ranged between -25‰ and -9‰ for three marine nitrite-oxidizing bacteria. Casciotti et al. (2010) also found that the percentage of isotopic O-exchange between NO_2^- and H_2O during NH_4^+ oxidation among four species of marine nitrifying bacteria varied between 1% and 25% among species. The results of this study on O-exchange between NO_2^- and H_2O can likely be explained by the abiotic equilibrium isotope effect (ε_{eq}) (Casciotti et al., 2007). At equilibrium, this effect will cause the $\delta^{18}O$-NO_2^- to be ~14‰ higher than the $\delta^{18}O$-H_2O with which it is in equilibrium. Contrary to the

findings from Casciotti et al. (2010), other studies (Buchwald & Casciotti, 2010; DiSpirito & Hooper, 1986; Hollocher et al., 1981) found very little isotopic exchange between NO_2^- and H_2O (0-3%).

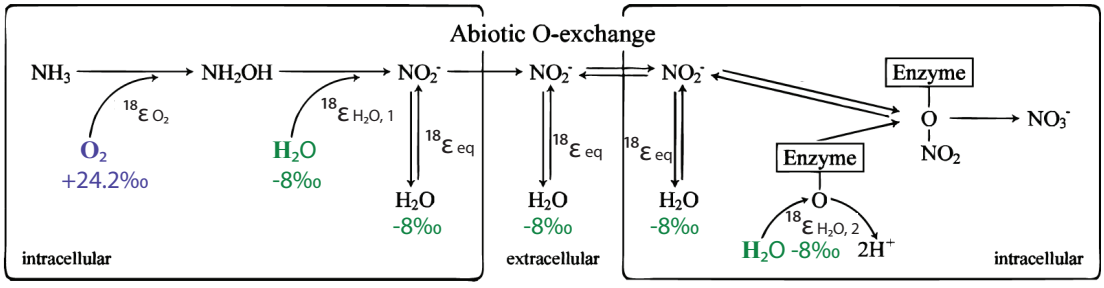

Figure 3.1: Bacterial nitrification schematic modified from Snider et al. (2010). NH_3 is oxidized to NO_3^- and one O from O_2 molecule (purple) and two O from H_2O molecules (green). The ^{18}O effects for nitrification are shown as $^{18}\varepsilon O_2$, $^{18}\varepsilon H_2O,1$, $^{18}\varepsilon eq$, and $^{18}\varepsilon H_2O,2$, respectively. The $\delta^{18}O$ value of O_2 is +24.2 assuming river water had fully equilibrated with atmospheric air and -8‰ for $\delta^{18}O$-H_2O a typical value at the study site.

Isotopic O-exchange between H_2O and NO_2^- during denitrification has also been documented (Kool et al., 2007). Denitrification is the reduction of NO_3^- into N_2O and N_2. If high amounts of O-exchange occur during nitrification or denitrification, the $\delta^{18}O$ signal of NO_3^- will be altered and will vary unpredictably depending on the amount of exchange that occurs (Figure 3.2). As O molecules between H_2O and NO_2^- are exchanged and begin to equilibrate during nitrification (Figure 3.1), the final microbial end-member value of $\delta^{18}O$-NO_3^- will approach the $\delta^{18}O$-H_2O of the medium and may eliminate the initial $\delta^{18}O$-O_2 signal.

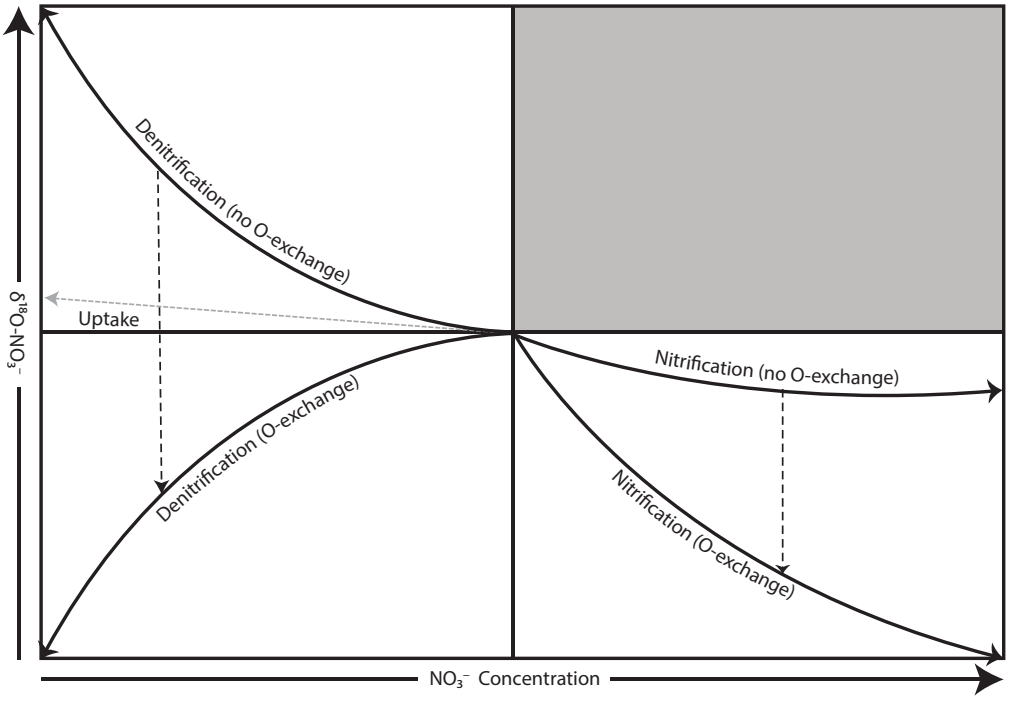

Figure 3.2: Schematic representation of the variability in $\delta^{18}O\text{-}NO_3^-$ with different amounts of abiotic O-exchange between NO_2^- and H_2O during nitrification and denitrification. This schematic is assuming internal sources of NO_3^- only (no additional NO_3^- sources entering from the environment). Solid lines represent a hypothetical trajectory of values for $\delta^{18}O\text{-}NO_3^-$ as NO_3^- concentration increases or decreases and no O-exchange has occurred. Dashed lines represent varying amounts of O-exchange. The grey box is a region where $\delta^{18}O\text{-}NO_3^-$ values are not likely to occur. The grey dashed arrow indicates NO_3^- uptake, which was not expected to influence NO_3^- production or NO_3^- isotope values.

Prior to research on the equilibrium isotope effect and estimates of the O isotope effects for nitrification, neither large kinetic ^{18}O fractionations nor the effect of isotopic equilibrium with water were considered in NO_3^- isotope research. Instead, the $\delta^{18}O\text{-}NO_3^-$ values that were used were estimated from the "1:2 rule" for oxygen incorporation (Snider et al., 2010) rather than actual calculated values (Equation 3.1).

$$\delta^{18}O - NO_{3(rel.VSMOW)}^- = \left[\left({}^1/_3\, R_{O_2} + {}^2/_3\, R_{H_2O}\right) \div R_{VSMOW}\right] - 1$$

Equation 3.1

Where R is the $^{18}O/^{16}O$ ratio of O_2, H_2O or VSMOW (Snider et al., 2010). Fewer than 10% of the values of $\delta^{18}O\text{-}NO_3^-$ produced from nitrification in groundwater, surface water and soils collected from field data fit theoretical values for $\delta^{18}O\text{-}NO_3^-$ formed from nitrification using the "1:2 rule"(Snider et al., 2010). They showed that using this model to estimate $\delta^{18}O\text{-}NO_3^-$ values is problematic and does not work in many systems.

Recent literature has enhanced our understanding of kinetic isotope effects and O-exchange during nitrification and denitrification. Snider et al. (2010) were the first to consider the large kinetic effects, the equilibrium isotope effect and the fraction of O-exchange (*f*abiotic) in the formation of $\delta^{18}O\text{-}NO_3^-$ during nitrification in soils (Equation 3.2). Their study highlighted the importance of oxygen isotope effects and the variability in O-exchange during nitrification to alter the final $\delta^{18}O\text{-}NO_3^-$ value. Snider et al. (2010) conducted incubation experiments with three levels of ^{18}O enriched water and three soil types. They calculated the *f*abiotic for the different soil types and found that it differed among the soils types and differed from the *f*abiotic that was calculated based on the 1:2 model for O-incorporation.

$$\delta^{18}O - NO_3^- = {}^1/_3\,(2 + f_{ABIOTIC})\delta^{18}O - H_2O \; + \; {}^1/_3\,[f_{ABIOTIC}(2^{18}\varepsilon_{eq} - \delta^{18}O - O_2 - {}^{18}\varepsilon_{O2} - {}^{18}\varepsilon_{H2O,1}) + \delta^{18}O - O_2 + {}^{18}\varepsilon_{O2} + {}^{18}\varepsilon_{H2O,1} + {}^{18}\varepsilon_{H2O,2}]$$

Equation 3.2

Although the $\delta^{18}O\text{-}NO_3^-$ cannot be used to indicate that denitrification has altered the isotopic values in productive rivers like the Grand River, it may be possible that NO_3^- isotopes can be used to obtain the relative rates of NO_3^- transformation processes (nitrification and denitrification). Calculating the *f*abiotic can provide insight into how much O-exchange has occurred relative to what is expected with the 1:2 "rule" for O incorporation (Equation 3.3 and Equation 3.4).

When no abiotic O-exchange has occurred between NO_2^- and H_2O such that *f*abiotic = 0 then:

$$\delta^{18}O - NO_3^- = \frac{2}{3}(\delta^{18}O - H_2O) + \frac{1}{3}\left(\delta^{18}O - O_2 + {}^{18}\varepsilon_{O2} + {}^{18}\varepsilon_{H2O,1} + {}^{18}\varepsilon_{H2O,2}\right)$$

Equation 3.3

When O-exchange has occurred and NO_2^- and H_2O have fully equilibrated such that *f*abiotic = 1 then:

$$\delta^{18}O - NO_3^- = \delta^{18}O - H_2O + \frac{2^{18}\varepsilon_{eq} + {}^{18}\varepsilon_{H2O,2}}{3}$$

Equation 3.4

This research focuses on how abiotic O-exchange and large isotope effects can alter the isotopic values of riverine NO_3^-. However, it is important to also understand the two other potential mechanisms that could alter the $\delta^{18}O\text{-}NO_3^-$ and result in varying end-member NO_3^- isotopic values: diel changes in $\delta^{18}O\text{-}O_2$ and different nitrifying organisms.

Temporal and spatial changes of $\delta^{18}O\text{-}O_2$ have been identified in several Canadian streams and reservoirs (Venkiteswaran et al., 2015; Venkiteswaran et al., 2008; Venkiteswaran et al., 2007; Wassenaar et al., 2010). Reported diel values of $\delta^{18}O\text{-}O_2$ in the Grand River range between +6‰ and +29‰ with the lowest $\delta^{18}O$ values observed in the central part of the river where O_2 saturation is the highest (Venkiteswaran et al., 2015). Dynamics of O_2 should be considered because a value greater than or less than the atmospheric $\delta^{18}O\text{-}O_2$ constant of +24.2‰ can drastically alter the end member nitrification values of $\delta^{18}O\text{-}NO_3^-$ especially in a productive system.

River biofilms are composed of complex assemblages of microorganisms. Isotopic effects of nitrifying bacteria (AOB) have been extensively studied (Buchwald & Casciotti, 2010; Casciotti et al., 2010; Kool et al., 2007). However, isotopic effects of ammonia oxidizing

archaea (AOA) have not. Several studies document a substantial presence of AOA (Gubry-Rangin et al., 2010; Leininger et al., 2006; Sonthiphand et al., 2013) compared to ammonia oxidizing bacteria (AOB). This presents another mechanism with which the end member $\delta^{18}O\text{-}NO_3^-$ nitrification signal could be altered as AOA and AOB have potentially different ammonia-oxidation pathways (Stahl & de la Torre, 2012; Walker et al., 2010). There have been several proposed AOA oxidation pathways (Stahl & de la Torre, 2012), however most of these have recently been disproved (Kozlowski et al., 2016) and still very little is known. There have been no definitive results that suggest different isotopic fractionations between the two groups (Nishizawa et al., 2016), however this research is very limited. Comammox bacteria, which oxidize NH_4^+ all the way to NO_3^- could also have the potential to alter the $\delta^{18}O\text{-}NO_3^-$ during nitrification, however the comammox pathway has yet to be studied but may resemble a combination of AOB and NOB (nitrite oxidizing bacteria) pathways (Laura Sauder, personal communication April 2017).

Biofilm covers the river bottom and submerged rocks and vegetation in the Grand River. This biofilm has been shown to influence river metabolism and rapid in-river N cycling is evident in the isotopic values (Chapter 2). Two contrasting productivity scenarios could exist with regard to O-exchange: 1) A productive river with rapidly cycling N will afford a greater opportunity for O-exchange to occur; or 2) A productive river with rapidly cycling N will have less O-exchange because the half-life of NO_2^- is short. It is possible for both these scenarios to be occurring in the river but it is difficult to discern without further isotopic analysis.

The amount of O-exchange (*f*abiotic) can be used in conjunction with the ^{18}O isotope effects during nitrification (Figure 3.1) in a model to obtain rates of processes. The $\delta^{15}N\text{-}NO_3^-$ is equally important in the model to further constrain rates of N cycling processes and further provide a look at turnover in the NO_3^- pool. Based on the findings from Chapter 2, the $\delta^{15}N$ should show predictable changes over time in the model and the $\delta^{18}O$ should vary with respect to the $\delta^{18}O\text{-}H_2O$ of the medium when rates (and concentrations) are held

constant. If NO_3^- isotopes can be used to estimate rates of processes then the fate of NO_3^- and how it is cycled in the river can be understood.

The objectives of this chapter are to: (1) Observe any large isotopic effects and calculate the amount of O-exchange between NO_2^- and H_2O that alters the observed/measured $\delta^{18}O$ values in the Grand River, (2) develop and apply a mechanistic model that can be used to explain the variation in observed $\delta^{18}O$-NO_3^- values in incubation experiments and in the Grand River and (3) determine gross rates of NO_3^- cycling in the Grand River and incubation experiments to understand the fate of NO_3^- using the mechanistic model.

3.2 Methods

Incubations of river water from West Montrose and Blair on the Grand River (described in Chapter 2) were used to calculate the fraction of abiotic O-exchange (*f*abiotic) during nitrification and without denitrification at these sites. The *f*abiotic for each incubation (West Montrose July 2015, West Montrose September 2015 and Blair July 2015) was calculated in a similar manner to Snider et al. (2010) using the slopes from the model II regression of the $\delta^{18}O$-NO_3^- values at T60 hours (T72 hours for the West Montrose September incubation) for each of the Low, Medium and High $\delta^{18}O$-H_2O treated beakers. The model II regressions were completed in R with the lmodel 2 package (Appendix A) (Legendre, 2014). To correct for differing NO_3^- production rates, final $\delta^{18}O$-NO_3^- values were normalized for NO_3^- production using an isotope mass balance (Equation 3.5).

$$\delta^{18}O - NO_{3(N)}^- = \frac{(\delta^{18}O_{(f)} \cdot NO_{3(f)}^-) - (\delta^{18}O_{(i)} \cdot NO_{3(i)}^-)}{NO_{3(f)}^- - NO_{3(i)}^-}$$

Equation 3.5

Where $\delta^{18}O - NO_{3(N)}^-$ represents the NO_3^- normalized $\delta^{18}O$ value used in the model II regression to calculate the *f*abiotic. $\delta^{18}O_{(f)}$ and $NO_{3(f)}^-$ are the $\delta^{18}O$-NO_3^- value and the NO_3^- concentration at the final time point of the incubation experiments. While $\delta^{18}O_{(i)}$ and $NO_{3(i)}^-$

are the $\delta^{18}O$- NO_3^- value and the NO_3^- concentration at the start of the incubations (Snider et al., 2010).

The *f*abiotic expected if the $\delta^{18}O$-NO_3^- derived from nitrification were formed by only one $\delta^{18}O$-O_2 and two $\delta^{18}O$-H_2O was calculated using the 1:2 "rule" for O-incorporation (Equation 3.6). The *f*abiotic value formed from the 1:2 "rule" for O-incorporation during nitrification and without denitrification was used to compare the *f*abiotic from the incubation experiments. The $\frac{2}{3}$ represents the two $\delta^{18}O$-H_2O and the $\frac{1}{3}$ represents the one $\delta^{18}O$-O_2 that are incorporated during nitrification. The +24.2‰ is the atmospheric $\delta^{18}O$-O_2 constant for O_2 dissolved in water and is used in this calculation assuming river water had fully equilibrated with atmospheric air and no respiratory O_2 consumption took place. This value was also assumed to be constant throughout the duration of the incubation experiments:

$$y = \frac{2}{3}x + \frac{1}{3}(24.2)$$

Equation 3.6

3.2.1 NO_3^- Isotope Model

To examine the rates of N cycling processes in the incubation experiments (Chapter 2) a box model was created using Stella version 10.0.1, http://www.iseesystems.com/(Appendix A). The model had three stocks: NO_3^-, ^{18}O-NO_3^- and ^{15}N-NO_3^- (Figure 3.3) and included rates as well as isotope effects for nitrification, denitrification, mineralization and uptake (Table 3.1). The model produced transient curves of NO_3^- concentration and NO_3^- isotopes that were compared with data from the incubations experiments. Data was modeled for two different time periods for each incubation experiment: Time 0-24 and Time 24-60. The model assumed that O-exchange only occurred in nitrification and the amount of O-exchange that occurred was constant. It also assumed that the $\delta^{18}O$-O_2 and $\delta^{18}O$-H_2O was constant throughout the experiment and in the river and first order rates (nitrification, denitrification and uptake) were constant over time and assumed constant production (zero order kinetics)

of NH_4^+ over time. This model was based on a closed system meaning no new N inputs from upstream environments or the atmosphere was added. The ranges in isotope values (Table 3.1) were considered in this model and median values were used where necessary ($^{18}\varepsilon$ Uptake and $^{18}\varepsilon$ Denitrification). The intercept value and *f*abiotic calculated (Figure 3.4) were used in **Error! Reference source not found.** to obtain the value for $^{18}\varepsilon$ Nitrification in the odel (Appendix A) to encompass any large variation in isotope effects ($^{18}\varepsilon_{O_2}$, $^{18}\varepsilon_{H_2O,1}$ and $^{18}\varepsilon_{H_2O,2}$). Model curves were obtained through inverse modelling. Observed incubation values for NO_3^- concentration and NO_3^- isotopes as well as calculated values like the *f*abiotic were input and gross rates were determined based on the fit of the model output values to the observed incubation values.

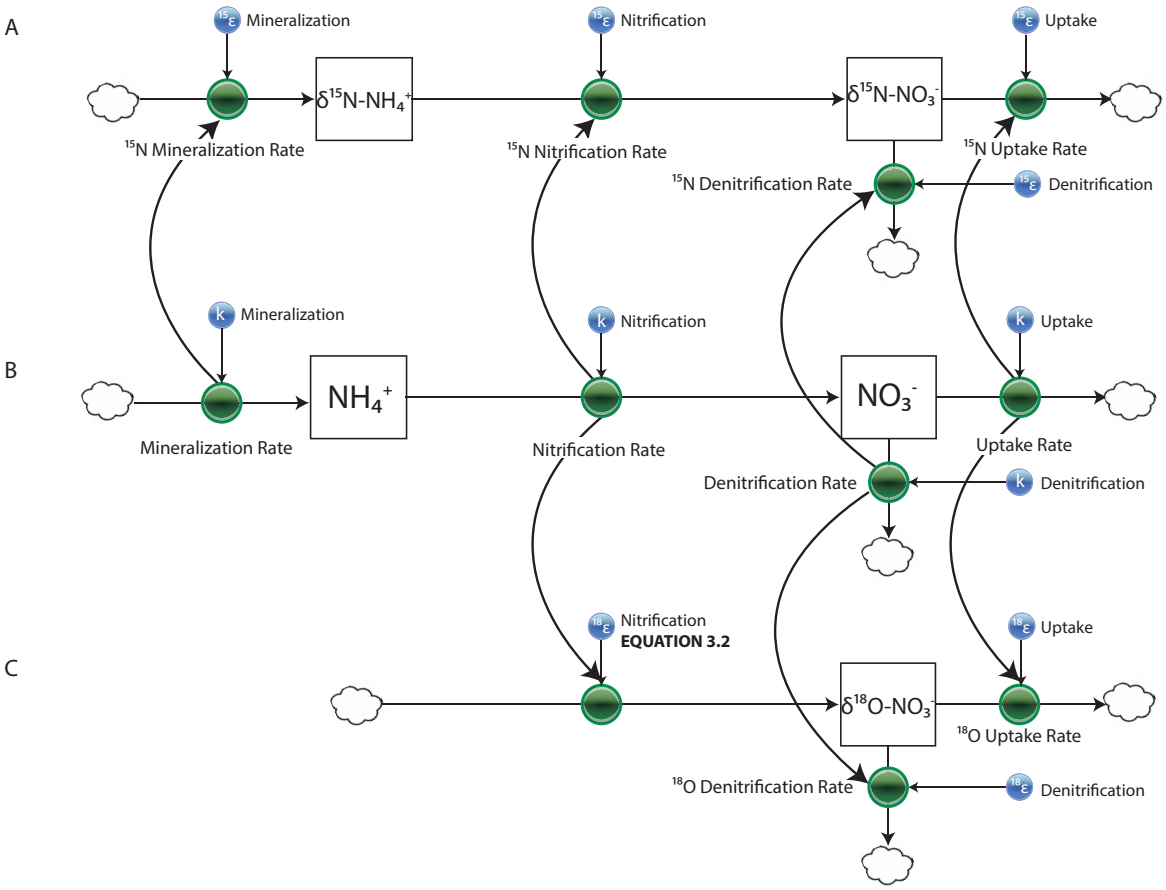

Figure 3.3: Simplified schematic representation of the box model for estimating rates of N cycling processes: nitrification, denitrification, mineralization and uptake for three stocks $^{15}N\text{-}NO_3^-$ (A), NO_3^- (B) and $^{18}O\text{-}NO_3^-$ (C). Arrows represent connecting links between the three stocks.

Table 3.1: Ranges of literature values for the fractionation factors used in the model.

Parameter	Value Ranges (‰)	Source
$^{15}\varepsilon$ Mineralization	+1	(Kendall, 1998)
$^{15}\varepsilon$ Nitrification	-29 to -12	(Shearer & Kohl, 1988)
$^{15}\varepsilon$ Uptake	-8 to -5	(Granger et al., 2010)
$^{15}\varepsilon$ Denitrification	-40 to -12	(Kendall, 1998)
δ^{15}N Biomass	+11	Measured, N=6 (Schiff, unpublished data)
$^{18}\varepsilon$ Nitrification (Equation 3.2): $\delta^{18}O - NO_3^- added = {}^1/_3(2 + f_{ABIOTIC})\delta^{18}O - H_2O + {}^1/_3[f_{ABIOTIC}(2^{18}\varepsilon_{eq} - \delta^{18}O - O_2 - {}^{18}\varepsilon_{O2} - {}^{18}\varepsilon_{H2O,1}) + \delta^{18}O - O_2 + {}^{18}\varepsilon_{O2} + {}^{18}\varepsilon_{H2O,1} + {}^{18}\varepsilon_{H2O,2}]$ (Snider et al., 2010)		
$^{18}\varepsilon O_2 + {}^{18}\varepsilon H_2O$,1	-38 to -18	(K. L. Casciotti et al., 2010)
$^{18}\varepsilon H_2O$,2	-25 to -9	(Buchwald & Casciotti, 2010)
ε_{eq}	+14	(Casciotti et al., 2007)
$^{18}\varepsilon$ Uptake	-8 to -5	(Granger et al., 2010)
$^{18}\varepsilon$ Denitrification	-23 to -5	(Granger et al., 2008)

3.3 Results

3.3.1 Abiotic O-Exchange and Equilibrium Isotope Effects

The $\delta^{18}O\text{-}NO_3^-$ in each of the beakers from the three incubations were strongly correlated with the $\delta^{18}O\text{-}H_2O$ values in the medium with r^2 values for Time 0-24 hours of 0.98 and 0.99 for West Montrose July 2015 and Blair July 2014, respectively and r^2 values for Time 24-60 of 0.98, 0.99 and 0.99 for West Montrose July 2015, West Montrose September 2015 and Blair July 2015, respectively (Figure 3.4). The slopes of the lines of each incubation experiment for both time periods were different than the slope calculated from the "1:2" rule of 0.67.

The *f*abiotic calculated for each incubation experiment and both time periods were all greater and statistically significant than the *f*abiotic from the "1:2" rule of 0 (Table 3.2). The *f*abiotic was always higher in the first 24 hours and corresponded to some of the greatest changes in $\delta^{18}O\text{-}NO_3^-$ when NO_3^- changed the least (Table 2.1 and Table 2.3). The slope of 0.90 for the West Montrose July 2015 incubation during the time period of 24-60 hours was not statistically significantly different from the slope of 0.92 for the West Montrose September 2015 incubation but was different from a slope of 0.80 for the Blair 2015 incubation (Appendix A). The calculated y-intercept for each experiment ranged between 3.5‰ to 9‰ in the first 24 hours and -1.75‰ to 2.8‰ in the second time period (24-60 or 72 hours). These experimental intercepts were almost all different from the intercept of 8.06‰ calculated with the "1:2" rule.

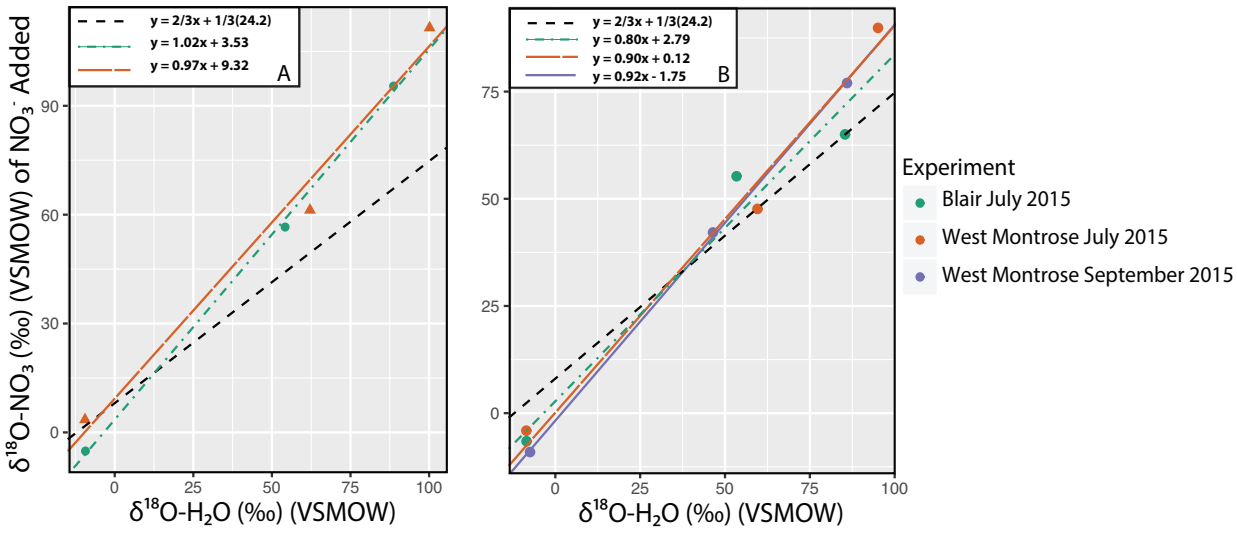

Figure 3.4: $\delta^{18}O\text{-}NO_3^-$ values of NO_3^- added from nitrification vs. $\delta^{18}O\text{-}H_2O$. Three regression lines were drawn from the results of the model II regression for two time periods: 0-24 hours (A) and 24-60 hours (B). West Montrose July 2015 is in orange and the shapes represent the actual incubation data values. The second West Montrose experiment in September 2015 is shown in purple and the Blair July 2015 experiment is in green. The black dashed line represents the fourth regression drawn from the "1:2" rule for oxygen incorporation during nitrification. The second West Montrose incubation (September) could not be represented in the first 24 hours because the change in concentration was so small that net $\delta^{18}O$ of NO_3^- added could not be calculated.

Table 3.2: The fraction of abiotic O-exchange between H_2O and NO_2^- during nitrification was calculated the same as in Snider et al. (2010) using the slopes from Figure 3.4 and Equation 3.2. Slopes, *f*abiotic and y-intercepts were found for each incubation experiment and the two different time periods.

Experiment	Time Period (Hours)	Slope	*f*abiotic	y-Intercept
"1:2" Rule (Snider et al., 2010)	-	0.67	0	8.06
West Montrose July 2015	0-24	0.97	0.88	9.32
West Montrose July 2015	24-60	0.90	0.70	0.12
West Montrose September 2015	0-24	-	0.88*	-1.75*
West Montrose September 2015	24-60	0.92	0.77	-1.75
Blair July 2015	0-24	1.02	1.06	3.53
Blair July 2015	24-60	0.80	0.43	2.79

**f*abiotic/intercept was approximated because concentration change between T0-T24 was so small that net $\delta^{18}O$ added could not be calculated

3.3.2 NO_3^- Isotope Best-fit Model

Small changes in model parameters were found to generate predictable and important changes in the model output (Figure 3.5). Four biogeochemical rate constants and three levels of enriched $\delta^{18}O$-H_2O clearly produced different results in the model output patterns for concentrations and NO_3^- isotope values of two distinct time periods (0-24 hours and 24-60 or 72 hours). The model results for all three experiments: West Montrose July 2015 (Figure 3.6), West Montrose September 2015 (Figure 3.7) and Blair July 2015 (Figure 3.8) had strong correlations with the actual incubation data for all concentrations and NO_3^- isotopes (Table 3.3, Table 3.4 and Table 3.5). This model could almost entirely explain the variability in the NO_3^- concentrations, $\delta^{18}O$-NO_3^- and $\delta^{15}N$-NO_3^- from the incubation data sets (Table 3.3, Table 3.4 and Table 3.5). The NO_3^- concentrations were almost always within measurement error (<0.05 mg N/L) as were the NO_3^- isotope values (<1‰).

Gross rates of uptake were held constant at 0.010 μg N L^{-1} h^{-1} for both time periods and all three experiments because uptake was not expected to change t (Table 3.6). Rates of nitrification and mineralization were almost always the lowest in the first 24 hours (44-67 μg N L^{-1} h^{-1}) where *f*abiotic was the highest and NO_3^- concentrations changed the least (Table 2.1) during all three experiments. Higher rates of nitrification and mineralization (40 to 122 μg N L^{-1} h^{-1}) were observed during 24-60 hours for the first West Montrose (July 2015) and Blair incubations when increase in NO_3^- concentration was the greatest. The nitrification and mineralization rates for the second West Montrose experiment (September 2015) had the lowest rates of the three incubation experiments and changed little between the two time periods. This experiment overall had the smallest change in NO_3^- concentration in both 0-24 hours and 24-60 hours time periods. The greatest overall gross rates of nitrification and mineralization were observed in the Blair experiment where the greatest changes in NO_3^- concentrations and NO_3^- isotopes were observed (Table 2.1, Table 2.2 and Table 2.3).

Rates of denitrification were expected to be less than the rates of nitrification and mineralization because the experimental system was well oxygenated, stirred and the biofilm layer was thin. Gross rates were low and ranged between 0.10 to 4.0 μg N L^{-1} h^{-1} depending on the incubation beaker. There was no distinctive trend between the two time periods and were very similar across all three experiments.

Literature values reported for gross NO_3^- consumption (denitrification + uptake) ranged between 0.044 to 0.084 μg N cm^{-2} h^{-1} (Table 3.7) and average incubation rates corrected for biomass area ranged between 0.025 to 0.031 μg N cm^{-2} h^{-1} (Table 3.6). Gross rates are similar to literature values. In general, gross rates are not often reported because they more difficult to obtain than net rates so there was not much to compare in terms of catchment characteristics, etc. No literature rates were found for gross NO_3^- release (mineralization and nitrification).

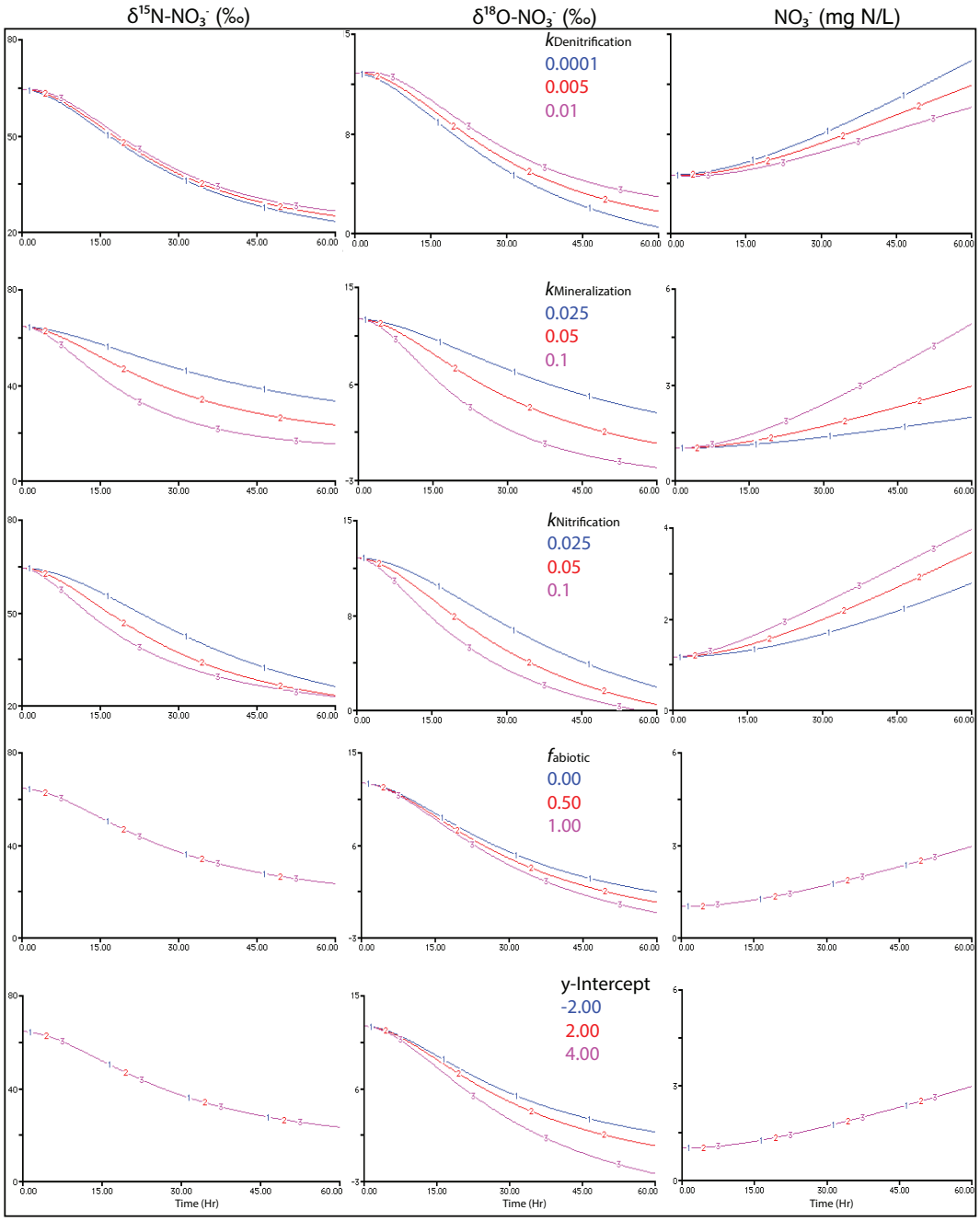

Figure 3.5: Model sensitivity analysis for five model parameters: three first order rate constants ($k_{Denitrification}$, $k_{Mineralization}$ and $k_{Nitification}$), the $f_{abiotic}$ and the y-intercept of Equation 3.2. Three outcomes are shown for $\delta^{15}N\text{-}NO_3^-$, $\delta^{18}O\text{-}NO_3^-$ and NO_3^- concentration.

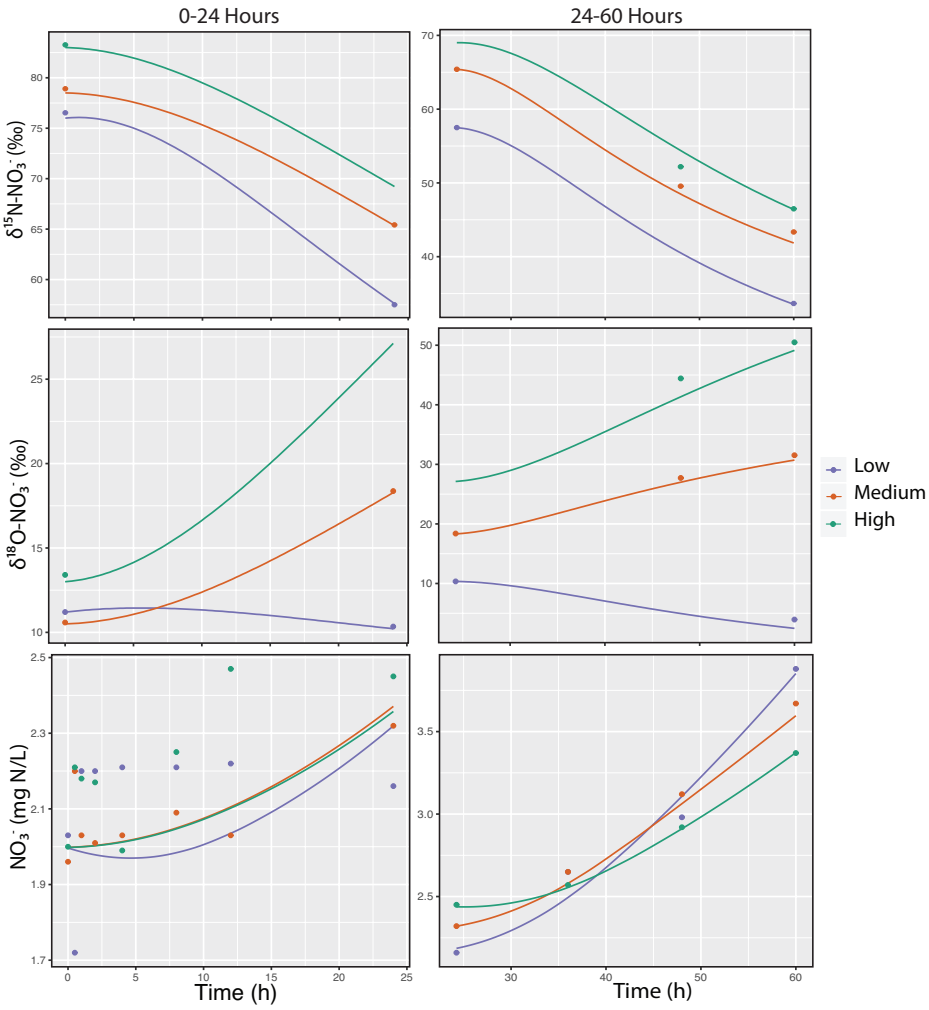

Figure 3.6: Modeled results of the first incubation experiment at the West Montrose site conducted on July 7, 2015. The modeled output values are depicted as the solid lines and the observed incubation values are the dots. $\delta^{15}N\text{-}NO_3^-$ (top), $\delta^{18}O\text{-}NO_3^-$(middle) and NO_3^- concentration (bottom) were the parameters modeled vs. time. The model used a calculated fabiotic (Figure 3.4) of 0.88 and 0.70 (for 0-24 hours and 24-60 hours, respectively), fractionation factors for N cycling processes (Appendix A), and incubation data (Figure 2.11) to look at the rates of N cycling processes. Incubation water that was not spiked with enriched $\delta^{18}O\text{-}H_2O$ (Low) is shown in purple. The incubation water that was spiked with enriched $\delta^{18}O\text{-}H_2O$ was shown as orange (Medium = +50‰) and green (High = +90‰).

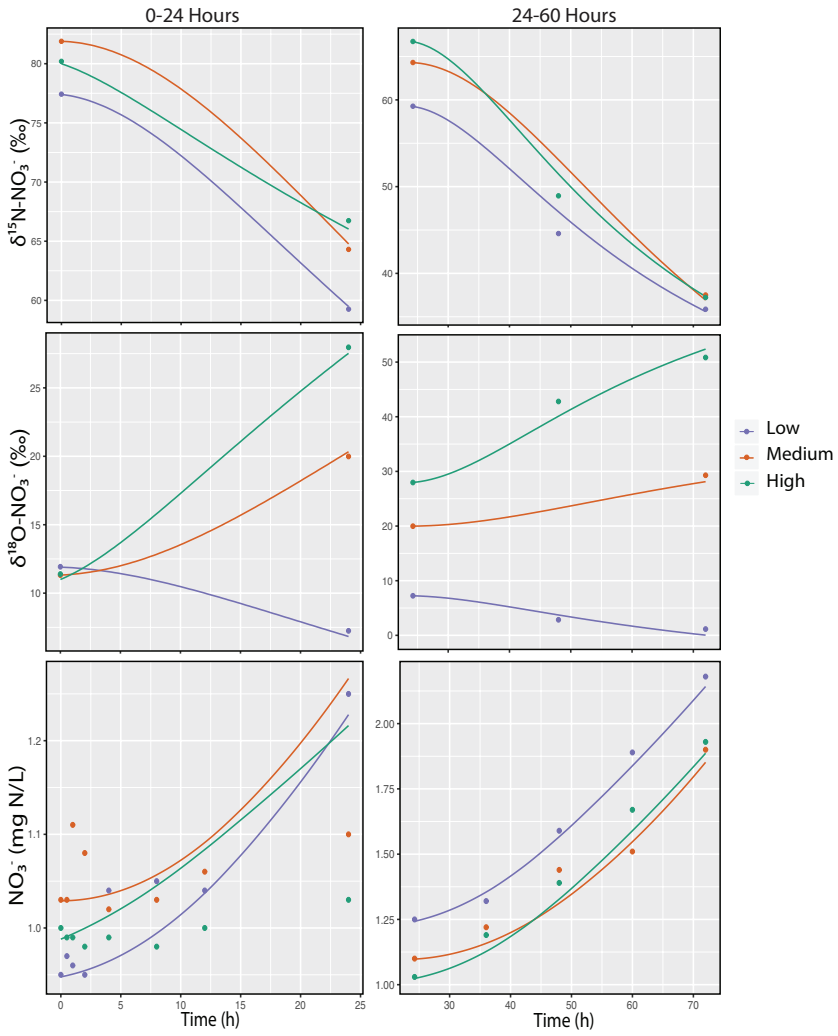

Figure 3.7: Modeled results of the incubation experiment conducted on September 2, 2015 at West Montrose. The model used an estimated fabiotic of 0.88 for 0-24 hours and a calculated (Figure 3.4) of 0.77 for 24-72 hours, fractionation factors for N cycling processes (Appendix A), and incubation data to look at the rates of N cycling processes (Figure 2.12). Incubation water that was not spiked with enriched $\delta^{18}O$-H_2O (Low) is depicted as purple lines (modeled) and dots (actual incubation values). The incubation water that was spiked with enriched $\delta^{18}O$-H_2O was shown as orange (Medium = +50‰) and green (High = +90‰) lines and dots. NO_3^- (top), $\delta^{18}O$-NO_3^-(middle) and $\delta^{15}N$-NO_3^- (bottom) were the parameters modeled.

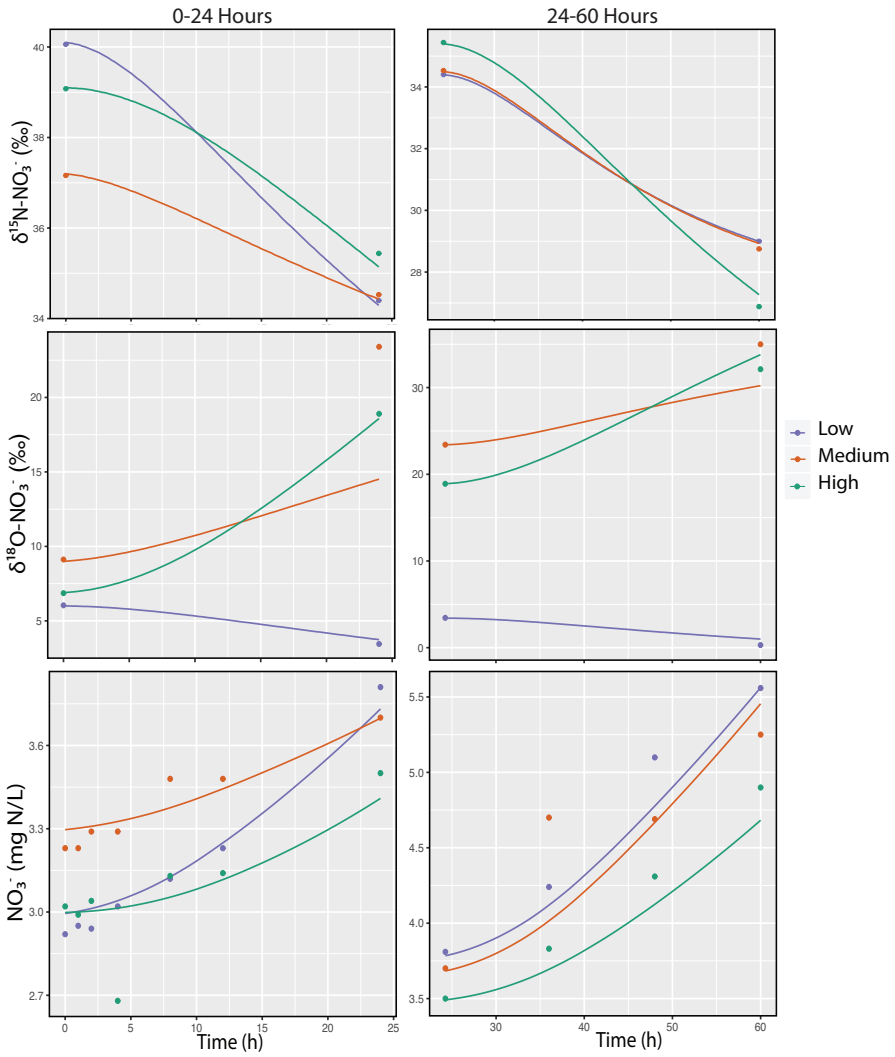

Figure 3.8: Modeled results of the Blair incubation experiment conducted on July 29, 2015. The model used calculated fabiotic values from Figure 3.4 of 1.06 and 0.43 for Time (0-24 and 24-60 hours, respectively), fractionation factors for N cycling processes (Appendix A), and incubation data to look at the rates of N cycling processes (Figure 2.13). Incubation water that was not spiked with enriched $\delta^{18}O\text{-}H_2O$ (Low) is depicted as purple lines (modeled) and dots (actual incubation values). The incubation water that was spiked with enriched $\delta^{18}O\text{-}H_2O$ was shown as orange (Medium = +50‰) and green (High = +90‰) lines and dots. NO_3^- (top), $\delta^{18}O\text{-}NO_3^-$(middle) and $\delta^{15}N\text{-}NO_3^-$ (bottom) were the parameters modeled.

Table 3.3: Root mean squared error values for $\delta^{15}N\text{-}NO_3^-$ (‰) for each modeled incubation experiment

Experiment	Low		Medium		High	
	0-24 h	*24-60 h*	*0-24 h*	*24-60 h*	*0-24 h*	*24-60 h*
West Montrose July 2015	0.11	0.28	0.58	0.38	NA	0.99
West Montrose September 2015	0.11	0.84	0.23	0.30	0.36	0.83
Blair July 2015	0.058	0.19	0.053	0.12	0.15	0.058

Table 3.4: Root mean squared error values for $\delta^{18}O\text{-}NO_3^-$ (‰) for each modeled incubation experiment

Experiment	Low		Medium		High	
	0-24 h	*24-60 h*	*0-24 h*	*24-60 h*	*0-24 h*	*24-60 h*
West Montrose July 2015	0.17	0.44	0.24	0.87	NA	3.18
West Montrose September 2015	0.21	0.47	0.18	0.60	0.29	1.04
Blair July 2015	0.14	0.37	4.45	2.62	0.16	2.58

Table 3.5: Root mean squared error values for NO_3^- (mg N/L) for each modeled incubation experiment

Experiment	Low		Medium		High	
	0-24 h	*24-60 h*	*0-24 h*	*24-60 h*	*0-24 h*	*24-60 h*
West Montrose July 2015	0.073	0.053	0.029	0.030	0.067	0.006
West Montrose September 2015	0.013	0.014	0.025	0.062	0.027	0.025
Blair July 2015	0.021	0.058	0.021	0.016	0.051	0.049

Table 3.6: Average Gross rates of N cycling processes for the West Montrose July and September 2015 incubations and the Blair July 2015 incubation. Gross rates were corrected for the West Montrose July 2015 and the Blair July 2015 incubation experiments.

Experiment	0-24 Hours ($\mu g\ N\ L^{-1}\ h^{-1}$)	0-24 Hours ($\mu g\ N\ cm^{-2}\ h^{-1}$)	24-60 Hours ($\mu g\ N\ L^{-1}\ h^{-1}$)	24-60 Hours ($\mu g\ N\ cm^{-2}\ h^{-1}$)
West Montrose July 2015				
Mineralization	52.7	0.38	60.3	0.45
Nitrification	44.7	0.30	84.4	0.65
Denitrification	4.07	0.025	2.73	0.023
Uptake	0.010	$7.43x10^{-05}$	0.010	$7.43x10^{-05}$
West Montrose September 2015				
Mineralization	30.3		37.0	
Nitrification	67.7		39.9	
Denitrification	0.47		0.10	
Uptake	0.010		0.010	
Blair July 2015				
Mineralization	46.0	0.29	71.5	0.51
Nitrification	59.0	0.33	122.3	0.57
Denitrification	0.50	0.031	0.500	0.031
Uptake	0.010	$6.23x10^{-05}$	0.010	$6.23x10^{-05}$

Table 3.7: Gross literature rates from different stream and watershed characteristics.

Rate ($\mu g\ N\ cm^{-2}\ h^{-1}$)	Source	Stream/Watershed Characteristics
0.040	(Mulholland et al., 2008)	1st order stream, forested catchment
0.080	(Ensign & Doyle, 2006)	Compilation of 404 studies with stream orders 1-5 and mixed catchments

3.4 Discussion

Productive systems allow for build-up of inorganic N and/or rapid N cycling that would allow for greater O-exchange. A mechanistic model can be used to get at the rates of NO_3^- transformation processes in the Grand River.

i. Role of O-exchange between NO_2^- and H_2O in the Grand River

The *f*abiotic calculated for each of the three incubation experiments provided valuable information for two Grand River sampling sites. All the slopes of the regression lines (Figure 3.4) were greater than 0.67 ("1:2" rule) and the calculated *f*abiotic values were greater than 0. The greatest *f*abiotic O-exchange was in the first 24 hours of each incubation experiment when NO_3^- concentrations changed the least. This clearly indicates substantial isotopic O-exchange between NO_2^- and H_2O that altered the $\delta^{18}O\text{-}NO_3^-$ value produced from nitrification so that it no longer represents the "1:2" rule. This presents further evidence that the $\delta^{18}O$ of NO_3^- is not conservative because of large amounts of biological cycling and O-exchange.

ii. Can a mechanistic model explain the variation in the observed experimental data?

The model was successful in reproducing the patterns observed in the incubation experiments (Chapter 2) and adequately described N biogeochemical cycling in the Grand River at two locations with different NO_3^- source inputs.

The $\delta^{15}N\text{-}NO_3^-$ predictably decreased by the same amount in each of the incubation experiments and thus was useful for constraining the rates of the NO_3^- transformation processes.

The *f*abiotic was useful for best-fit modeling in each of the incubations. The greater the *f*abiotic, the more $\delta^{18}O\text{-}NO_3^-$ values tended to shift toward the respective $\delta^{18}O\text{-}H_2O$ of the experimental medium, further confirming that this shift was the result of isotopic O-

exchange between NO_2^- and H_2O. The $\delta^{18}O\text{-}O_2$ signal (+24.2‰) present during the first oxidation step in nitrification is effectively eliminated in the NO_3^- isotope value after nitrification. This also means that if isotopic O-exchange were to occur between H_2O and denitrification intermediates (in addition to nitrification), the denitrification signal as well as any other potential NO_3^- source signals would be eliminated.

The y-intercept that was calculated (Figure 3.4) varied between the two time points (0-24 hours and 24-60 or 72 hours) and between each of the three experiments. The y-intercept is a function of the $\delta^{18}O\text{-}O_2$ as well the potentially large isotope effects associated with the incorporation of O during nitrification (Figure 3.1 and Equation 3.2). The unknown affect of diel shifts in $\delta^{18}O\text{-}O_2$ on the final NO_3^- isotope values as well as the variability of ^{18}O isotopic fractionation amplifies the complexity of apportioning NO_3^- sources.

iii. Can isotopes of NO_3^- be used to estimate the gross rates of NO_3^- cycling in the Grand River?

Gross rates were successfully estimated for the West Montrose and Blair incubation experiments. The Blair experiment has the highest overall rates of nitrification and mineralization that likely resulted from the effects of the upstream WWTPs. The second West Montrose experiment conducted in September 2015 had the lowest overall rates of NO_3^- transformation processes which could have been a function of seasonality if the biofilm is more active in mid summer (July) compared to early fall (September). The model was able to capture differences between sites and thus can be used as a tool for determining the variability in the river metabolism that is caused by different source inputs.

These results and the success of the mechanistic model demonstrate that in-river metabolism has considerable effect on NO_3^- isotope values. Although there are still many unknowns (diel $\delta^{18}O\text{-}O_2$, large ^{18}O isotopic effects and variable microbial communities) the isotopes still provide a useful tool to quantify consumption and release of NO_3^- in an impacted river such as the Grand River.

3.5 Conclusion

The fraction of abiotic O-exchange (*f*abiotic) between NO_2^- and H_2O was successfully calculated using a model II regression for all three incubation experiments. All the regression slopes for each incubation and two different time periods (0-24 hours and 24-60 or 72 hours) were greater than the slope dictated by the "1:2 rule" for O-incorporation during nitrification. The *f*abiotic ranged between 0.88-1.06 for two Grand River sites in the first 24 hours and ranged between 0.43 and 0.77 after 24 hours. A large amount of O-exchange was evident at both West Montrose and Bridgeport. The largest *f*abiotic was in the first 24 hours of the Blair experiment (1.06). A higher *f*abiotic meant a greater shift in $\delta^{18}O$-NO_3^- toward the $\delta^{18}O$-H_2O of the medium. O-exchange plays a substantial role in NO_3^- cycling and it was important to determine the extent to which it occurs in the Grand River.

The biofilm in the Grand River had a considerable impact on the in-river metabolism and resulting isotopic values that were observed and not conservative. It is difficult however, to determine whether the O-exchange that occurred was the results of a productive river where rapid N cycling affords a greater opportunity for exchange or a productive river with slower rates where NO_2^- persists and affords a greater opportunity for O-exchange.

The modeled data fit very well with the concentrations and NO_3^- isotope data in all three incubations and was able to explain almost all variability. Estimates of gross rates of mineralization, nitrification, denitrification and uptake were successfully obtained. These relative rates of NO_3^- transformations processes estimated from the model can be up-scaled to the river assuming that a surface area measurement of the river bottom is made. These rates in conjunction with estimations of the fraction of abiotic O-exchange provide valuable information on the fate of NO_3^- in the river. Higher rates of mineralization and nitrification mean a greater internal release of NO_3^- to the river whereas lower rates of mineralization and nitrification and greater rates of denitrification and/or uptake mean the river is more of an internal NO_3^- sink.

Overall these results confirmed the findings from Chapter 2 that $\delta^{15}N$- and $\delta^{18}O$-NO_3^- are not conservative and cannot be used to indicate denitrification or NO_3^- sources because of in-river biological cycling. The combined *f*abiotic and ^{18}O isotope effects that occurred produced results that could not be predicted by the "1:2 rule" (Equation 3.1) but were best described by Equation 3.2. Researchers that have used or continue to use the "1:2 rule" disregard large ^{18}O isotope effects and isotopic O-exchange between NO_2^- and H_2O that influence riverine NO_3^- isotopic values.

This model will offer researchers and watershed managers (that use NO_3^- isotopes for source apportionment) with a new tool that provides estimates on the relative rates of N cycling processes. Having gross rates rather than only net rates is important because they are inclusive of all microbial processing rather than having to infer NO_3^- transformation processes by only a change in concentration. Understanding the fate of NO_3^- in the river using these rates of NO_3^- transformation processes will provide better estimates of N recycling and the contribution of microbially derived NO_3^- to the mixed source pool.

Chapter 4 – Conclusions and Recommendations

4.1 Conclusions

Nitrate (NO_3^-) is the most ubiquitous contaminant in surface and groundwaters in Canada, NO_3^- is transformed in the river by two main processes: nitrification (oxidation of NH_4^+ to NO_3^-) and denitrification (reduction of NO_3^- to N_2). The catchment of the Grand River is dominated by agricultural use (~80%). The Grand River receives NO_3^- loading from point (urban WWTPs) and non-point sources (agricultural manure and fertilizer). NO_3^- loading threatens drinking water quality where water is drawn directly from the river as well as overall aquatic ecosystem health.

The use of $\delta^{18}O$- and $\delta^{15}N$-NO_3^- isotopes has been extensively used in source apportionment studies to differentiate between NO_3^- inputs and transforming processes such as nitrification and denitrification in rivers, groundwater, soils and surface water. Sources of NO_3^- in the Grand River could be estimated with isotopes *if* they work as conservative tracers. When looking at seasonal NO_3^- isotope data from the Grand River there is no clear denitrification trend or seasonal trend but the river is highly productive. A source plot of this data suggested that all NO_3^- was derived from a nitrified WWTP or manure source; however, it is unlikely that the soil-N signal is not observed, especially in agricultural headwaters where livestock populations are lower.

Three laboratory-beaker incubations with three levels of isotopically labeled river water and biofilm covered rocks demonstrated that $\delta^{15}N$- and $\delta^{18}O$-NO_3^- are not conservative. Two distinct phases that occurred in all three experiments: one where NO_3^- concentrations did not change over time (0-24 hours), and the other with a net increase in NO_3^- concentration over time (24-60 hours). In all three experiments, the $\delta^{15}N$-NO_3^- decreased consistently toward the respective $\delta^{15}N$ of biomass value for each site during both time periods. The $\delta^{18}O$-NO_3^- was altered relative to the $\delta^{18}O$-H_2O such that three distinct water labels were evident by the end of the experiment. The NO_3^- isotopes were altered even when NO_3^-

concentrations did not change. This result proved that the $\delta^{18}O\text{-}NO_3^-$ values were driven by the $\delta^{18}O\text{-}H_2O$ of the medium while the $\delta^{15}N$ of biomass, as well as the $\delta^{15}N\text{-}NH_4^+$ being nitrified and the associated isotopic fractionations controlled the $\delta^{15}N\text{-}NO_3^-$. These incubation results matched the results from the in-river chamber experiment confirming the non-conservative nature of NO_3^- isotopes.

Incubation data can be explained with a mechanistic model that allows for isotopic O-exchange between NO_2^- and H_2O and a consideration of large kinetic ^{18}O isotope effects. Recent literature has found rapid N-cycling and abiotic O-exchange between NO_2^- and H_2O during nitrification complicates the use of NO_3^- isotopes for source partitioning and the $\delta^{18}O\text{-}NO_3^-$ can be "reset" toward the $\delta^{18}O\text{-}H_2O$ of the medium. This was confirmed in this study as a substantial amount of isotopic O-exchange was found to have occurred between NO_2^- and H_2O during incubation experiments. In addition, the model permitted for an estimation of gross rates for NO_3^- transformation processes and was successful in determining the variability in nitrogen cycling at different parts of the Grand River and at different times of the year.

In summary, source apportionment is difficult because NO_3^- isotopes are not conservative and river metabolism *does* mask the isotopic signal of NO_3^-. However, N cycling in a productive river, such as the Grand River is understood enough to build a mechanistic model to describe N biogeochemical cycling. This is important for those concerned with the fate of elevated NO_3^- in impacted rivers. Researchers should be cautious when using the dual isotopes of NO_3^- for source apportionment and must first understand the complexity of NO_3^- isotopes and transformation processes especially in productive systems.

4.2 Recommendations

The results from this thesis lead to a number of interesting questions that can be pursued through further research. A map of the microbial community composition of the rock biofilm from this study should be conducted to determine if ammonia-oxidizing archaea (AOA) and comammox in addition to ammonia-oxidizing bacteria (AOB) are present. It is possible that AOA and comammox have more of an influence on the isotopic composition of $\delta^{18}O\text{-}NO_3^-$ compared to AOB (because of potentially different ammonia oxidation pathways). If all organisms are present in the biofilm this might be another potential mechanism that alters the $\delta^{18}O\text{-}NO_3^-$ from nitrification.

Large diel effects of DO and $\delta^{18}O\text{-}O_2$ should be considered in the mechanistic model because they occur both temporally and spatially in the Grand River and would alter the NO_3^- isotope value that results from nitrification. In addition, the model should also include NO_2^- and the full denitrification reaction because it would provide a more accurate representation of N biogeochemical cycling in the river, especially if abiotic O-exchange during denitrification could be calculated.

Considering the diel measurements of $\delta^{18}O\text{-}NO_3^-$ would be beneficial to decipher whether O-exchange in the river is the result of rapid biological N cycling or slower N cycling with a persistence of NO_2^-.

It would also be advised to do another incubation experiment using Blair rocks and West Montrose water because estimated rates were the greatest at Blair, and West Montrose had the lowest NO_3^- concentrations. The effect of the biofilm on the amount of O-exchange would be enhanced because there would likely be a more pronounced change in the NO_3^- isotopes due to the faster rates and low initial concentration.

References

Almasri, M. N. (2007). Nitrate contamination of groundwater: A conceptual management framework. *Environmental Impact Assessment Review*, *27*(3), 220–242. http://doi.org/10.1016/j.eiar.2006.11.002

Amberger, A., & Schmidt, H.-L. (1987). Natürliche Isotopengehalte von Nitrat als Indikatoren für dessen Herkunft. *Geochimica et Cosmochimica Acta*, *51*(10), 2699–2705. http://doi.org/10.1016/0016-7037(87)90150-5

Anderson, D. M., Glibert, P. M., & Burkholder, J. M. (2002). Harmful algal blooms and eutrophication: nutrient sources, compositions, and consequences. *Estuaries*, *25*(4), 704–726.

Andersson, K. K., & Hooper, A. B. (1983). O_2 and H_2O are each the source of one O in NO_2^- produced from NH_3 by Nitrosomonas: ^{15}N-NMR evidence. *FEBS Letters*, *164*(2), 236–240.

Andersson, K. K., Philson, S. B., & Hooper, A. B. (1982). O isotope shift in N NMR analysis of biological N-oxidations: H_2O-NO_2 exchange in the ammonia-oxidizing bacterium Nitrosomonas. *Proceedings of the National Academy of Sciences of the United States of America*, *79*(19), 5871–5875. http://doi.org/10.1073/pnas.79.19.5871

Anisfeld, S. C., Barnes, R. T., Altabet, M. A., & Wu, T. (2007). Isotopic apportionment of atmospheric and sewage nitrogen sources in two connecticut rivers. *Environmental Science and Technology*, *41*(18), 6363–6369. http://doi.org/10.1021/es070469v

Aravena, R., Evans, M. L., & Cherry, J. A. (1993). Stable isotopes of oxygen and nitrogen in source identification of nitrate from septic systems. *Groundwater*, *31*(2), 180–186.

Aravena, R., & Robertson, W. D. (1998). Use of multiple isotope tracers to evaluate denitrification in ground water: study of nitrate from a large-flux septic system plume. *Groundwater*, *36*(6), 975–982.

Bae, W., Baek, S., Chung, J., & Lee, Y. (2001). Optimal operational factors for nitrite accumulation in batch reactors. *Biodegradation*, *12*(5), 359–366.

Bartosch, S., Hartwig, C., Spieck, E., & Bock, E. (2002). Immunological Detection of Nitrospira-like Bacteria in Various Soils. *Microbial Ecology*, *43*(1), 26–33. http://doi.org/10.1007/s00248-001-0037-5

Batchelor, B., & Lawrence, A. W. (1978). Autotrophic Denitrification Using Elemental Sulfur. *Journal (Water Pollution Control Federation)*, *50*(8), 1986–2001. http://doi.org/10.2307/25040378

Battin, T. J., Besemer, K., Bengtsson, M. M., Romani, A. M., & Packmann, A. I. (2016). The ecology and biogeochemistry of stream biofilms. *Nature Reviews Microbiology*, *14*(4), 251–263. http://doi.org/10.1038/nrmicro.2016.15

Bott, T. L., Brock, J. T., Baatrup-Pedersen, A., Chambers, P. A., Dodds, W. K., Himbeault, K. T., … Wolfaardt, G. M. (1997). An evaluation of techniques for measuring periphyton metabolism in chambers. *Canadian Journal of Fisheries and Aquatic Sciences*, *54*(3), 715–725.

Böttcher, J., Strebel, O., Voerkelius, S., & Schmidt, H.-L. (1990). Using isotope fractionation of nitrate-nitrogen and nitrate-oxygen for evaluation of microbial denitrification in a sandy aquifer. *Journal of Hydrology*, *114*(3–4), 413–424. http://doi.org/10.1016/0022-1694(90)90068-9

Brown, D. M., McKay, G. A., & Chapman, L. J. (1980). *The climate of southern Ontario*. Environment Canada, Atmospheric Environment Service= Environnement Canada, Service de l'environnement atmosphérique.

Buchwald, C., & Casciotti, K. L. (2010). Oxygen isotopic fractionation and exchange during bacterial nitrite oxidation. *Limnology and Oceanography*, *55*(3), 1064–1074. http://doi.org/10.4319/lo.2010.55.3.1064

Burgin, A. J., & Hamilton, S. K. (2007). Have we overemphasized in aquatic removal of nitrate the role ecosystems ? pathways of denitrification review. *Frontiers in Ecology and the Environment*, *5*(2), 89–96. http://doi.org/10.1890/1540-9295(2007)5[89:HWOTRO]2.0.CO;2

Burns, D. A., & Kendall, C. (2002). Analysis of δ15N and δ18O to differentiate NO3− sources in runoff at two watersheds in the Catskill Mountains of New York. *Water Resources Research*, *38*(5).

Camargo, J. A., & Alonso, Á. (2006). Ecological and toxicological effects of inorganic nitrogen pollution in aquatic ecosystems: A global assessment. *Environment International*, *32*(6), 831–849. http://doi.org/10.1016/j.envint.2006.05.002

Canadian Council of Ministers of the Environment. (2012). Canadian Water Quality Guidelines for the Protection of Aquatic Life: Nitrate. *Canadian Environmental Quality Guidelines, Canadian Council of Ministers of the Environment, Winnipeg*, 1–7.

Casciotti, K. (2015). Nitrogen and Oxygen Isotopic Studies of the Nitrogen Cycle. *Annual Review of Marine Science*, *7*(1), 379–407. http://doi.org/doi:10.1146/annurev-marine-010213-135052

Casciotti, K. L., Böhlke, J. K., McIlvin, M. R., Mroczkowski, S. J., & Hannon, J. E. (2007). Oxygen isotopes in nitrite: analysis, calibration, and equilibration. *Analytical Chemistry*, *79*(6), 2427–36. http://doi.org/10.1021/ac061598h

Casciotti, K. L., McIlvin, M., & Buchwald, C. (2010). Oxygen isotopic exchange and fractionation during bacterial ammonia oxidation. *Limnology and Oceanography*, *55*(2), 753–762. http://doi.org/10.4319/lo.2009.55.2.0753

Cejudo, E. (2016). *Dissolved inorganic nitrogen cycling in a river receiving wastewater: the*

response to changes in wastewater treatment effluent. University of Waterloo, PhD Thesis.

Cejudo, E., Schiff, S. L., & Aravena, R. O. (2014). Epilithon isotope composition as an environmental archive in rivers receiving wastewater. *Revue Des Sciences de L'eau*, *27*(3), 219. http://doi.org/10.7202/1027807ar

Cey, E. E., Rudolph, D. L., & Aravena, R. (1999). Role of the riparian zone in controlling the distribution and fate of agricultural nitrogen near a small stream in southern Ontario, 45–67.

Charbonneau, R., & Kondolf, G. M. (1993). Land use change in California, USA: Nonpoint source water quality impacts. *Environmental Management*, *17*(4), 453–460. http://doi.org/10.1007/BF02394661

Cummings, T. F. (2015). *Assessment of Nitrate Export in Agricultural Sub-Catchments of the Grand River Watershed : An Isotope Approach by*. University of Waterloo, MSc Thesis.

Daims, H., Lebedeva, E. V., Pjevac, P., Han, P., Herbold, C., Albertsen, M., … Wagner, M. (2015). Complete nitrification by Nitrospira bacteria. *Nature*, *528*(7583), 504–509. http://doi.org/10.1038/nature16461

Dawson, R. N., & Murphy, K. L. (1972). The temperature dependency of biological denitrification. *Water Research*, *6*(1), 71–83. http://doi.org/http://dx.doi.org/10.1016/0043-1354(72)90174-1

De Boer, W., & Kowalchuk, G. A. (2001). Nitrification in acid soils: micro-organisms and mechanisms. *Soil Biology and Biochemistry*, *33*(7), 853–866.

De Roos, A. J., Ward, M. H., Lynch, C. F., & Cantor, K. P. (2003). Nitrate in public water supplies and the risk of colon and rectum cancers. *Epidemiology*, *14*(6), 640–9. http://doi.org/10.1097/01.ede.0000091605.01334.d3

DeSimone, L. a, & Howes, B. L. (1998). Nitrogen transport and transformations in a shallow aquifer receiving wastewater discharge: A mass balance approach. *Water Resources Research*, *34*(2), 271–285. http://doi.org/10.1029/97wr03040

DiSpirito, A. A., & Hooper, A. B. (1986). Oxygen exchange between nitrate molecules during nitrite oxidation by Nitrobacter. *Journal of Biological Chemistry*, *261*(23), 10534–10537.

Dodds, W. K., Evans-White, M. A., Gerlanc, N. M., Gray, L., Gudder, D. A., Kemp, M. J., … Wollheim, W. M. (2000). Quantification of the nitrogen cycle in a prairie stream. *Ecosystems*, *3*(6), 574–589. http://doi.org/10.1007/s100210000050

Elliott, E. M., Kendall, C., Wankel, S. D., Burns, D. A., Boyer, E. W., Harlin, K., … Butler, T. J. (2007). Nitrogen Isotopes as Indicators of NOx Source Contributions to Atmospheric Nitrate Deposition Across the Midwestern and Northeastern United States. *Environmental Science & Technology*, *41*(22), 7661–7667. http://doi.org/10.1021/es070898t

Ensign, S. H., & Doyle, M. W. (2006). Nutrient spiraling in streams and river networks.

Journal of Geophysical Research, *111*(G4), G04009. http://doi.org/10.1029/2005JG000114

EPA. (1993). Method 350.1 Determination of Ammonia Nitrogen By Semi-Automated Office of Research and Development. *EPA Methods*, (August), 1–15.

Erisman, J. W., Sutton, M. A., Galloway, J., Klimont, Z., & Winiwarter, W. (2008). How a century of ammonia synthesis changed the world. *Nature Geosci*, *1*(10), 636–639. Retrieved from http://dx.doi.org/10.1038/ngeo325

Ernst, J. W., & Massey, H. F. (1960). The effects of several factors on volatilization of ammonia formed from urea in the soil. *Soil Science Society of America Journal*, *24*(2), 87–90.

Falkowski, P. G., Fenchel, T., & Delong, E. F. (2008). The microbial engines that drive Earth's biogeochemical cycles. *Science (New York, N.Y.)*, *320*(5879), 1034–9. http://doi.org/10.1126/science.1153213

Fan, A. M., Willhite, C. C., & Book, S. A. (1987). Evaluation of the nitrate drinking water standard with reference to infant methemoglobinemia and potential reproductive toxicity. *Regulatory Toxicology and Pharmacology*, *7*(2), 135–148.

Fewtrell, L. (2004). Drinking-Water Nitrate, Methemoglobinemia, and Global Burden of Disease: A Discussion. *Environmental Health Perspectives*, *112*(14), 1371–1374. http://doi.org/10.1289/ehp.7216

Findlay, S. (2010). Stream microbial ecology. *Journal of the North American Benthological Society*, *29*(1), 170–181. http://doi.org/10.1899/09-023.1

Fogel, M. L., & Cifuentes, L. A. (1993). Isotope Fractionation during primary production. In *Organic Geochemistry* (pp. 73–98). http://doi.org/10.1007/978-1-4615-2890-6

Galloway, J. N. (1998). The global nitrogen cycle: changes and consequences. *Environmental Pollution*, *102*(1), 15–24. http://doi.org/10.1016/S0269-7491(98)80010-9

Galloway, J. N., & Cowling, E. B. (2002). Reactive Nitrogen and The World: 200 Years of Change. *AMBIO: A Journal of the Human Environment*, *31*(2), 64–71. http://doi.org/10.1579/0044-7447-31.2.64

Gao, C., Shirota, J., Kelly, R. I., Brunton, F. R., & Van Haaften, S. (2006). Bedrock topography and overburden thickness mapping, Southern Ontario. *Ontario Geological Survey*, 34. Retrieved from http://www.geologyontario.mndm.gov.on.ca/mndmfiles/pub/data/imaging/MRD207/MRD207BedrockTopMapping.pdf

Grand River Conservation Authority. (2013). *Sources of Nutrients and Sediments in the Grand River Watershed.*

Grand River Conservation Authority. (2014). *Grand River Watershed Management Plan*.

Granger, J., Sigman, D. M., Lehmann, M. F., & Tortell, P. D. (2008). Nitrogen and oxygen

isotope fractionation during dissimilatory nitrate reduction by denitrifying bacteria. *Limnology and Oceanography*, *53*(6), 2533–2545. http://doi.org/10.4319/lo.2008.53.6.2533

Granger, J., Sigman, D. M., Needoba, J. a., & Harrison, P. J. (2004). Coupled nitrogen and oxygen isotope fractionation of nitrate during assimilation by cultures of marine phytoplankton. *Limnol. Oceanogr.*, *49*(5), 1763–1773. http://doi.org/10.4319/lo.2004.49.5.1763

Granger, J., Sigman, D. M., Rohde, M. M., Maldonado, M. T., & Tortell, P. D. (2010). N and O isotope effects during nitrate assimilation by unicellular prokaryotic and eukaryotic plankton cultures. *Geochimica et Cosmochimica Acta*, *74*(3), 1030–1040. http://doi.org/10.1016/j.gca.2009.10.044

Grimm, N. B., Valett, H. M., Stanley, E. H., & Fischer, S. G. (1991). Contribution of the hyporheic zone to stability of an arid-land stream. *Internationale Vereinigung Fuer Theoretische Und Angewandte Limnologie.Verhandlungen IVTLAP*, *24*(3).

Gris, S. (2016). *Examining the isotopic and nitrogen fluctuations of epilithon in the Grand River*. University of Waterloo, BSc Thesis.

Gruber, N., & Galloway, J. N. (2008). An Earth-system perspective of the global nitrogen cycle. *Nature*, *451*(7176), 293–296. http://doi.org/10.1038/nature06592

Gu, B., & Alexander, V. (1993). Estimation of N_2 Fixation Based on Differences in the Natural- Abundance of ^{15}N among Fresh-Water N_2-Fixing and Non-N_2- Fixing Algae. *Oecologia*, *96*(1), 43–48.

Gubry-Rangin, C., Nicol, G. W., & Prosser, J. I. (2010). Archaea rather than bacteria control nitrification in two agricultural acidic soils. *FEMS Microbiology Ecology*, *74*(3), 566–574. http://doi.org/10.1111/j.1574-6941.2010.00971.x

Hill, a R. (1983). Nitrate Distribution in the groundwater of the Alliston Region of Ontario, Canada, 696–702. http://doi.org/10.1111/j.1745-6584.1982.tb01389.x

Hollocher, T. C. (1984). Source of the oxygen atoms of nitrate in the oxidation of nitrite by Nitrobacter agilis and evidence against a PON anhydride mechanism in oxidative phosphorylation. *Archives of Biochemistry and Biophysics*, *233*(2), 721–727. http://doi.org/10.1016/0003-9861(84)90499-5

Hollocher, T. C., Tate, M. E., & Nicholas, D. J. (1981). Oxidation of ammonia by Nitrosomonas europaea. Definite ^{18}O-tracer evidence that hydroxylamine formation involves a monooxygenase. *The Journal of Biological Chemistry*, *256*(21), 10834–10836.

Hood, J. L. a., Taylor, W. D., & Schiff, S. L. (2013). Examining the fate of WWTP effluent nitrogen using δ 15N–NH4 +, δ 15N–NO 3 − and δ 15N of submersed macrophytes. *Aquatic Sciences*, *76*(2), 243–258. http://doi.org/10.1007/s00027-013-0333-4

Howarth, R. W., & Marino, R. (2006). Nitrogen as the limiting nutrient for eutrophication in coastal marine ecosystems: Evolving views over three decades. *Limnology and*

Oceanography, *51*(1), 364–376. http://doi.org/10.4319/lo.2006.51.1_part_2.0364

Janzen, H. H., Beauchemin, K. A., Bruinsma, Y., Campbell, C. A., Desjardins, R. L., Ellert, B. H., & Smith, E. G. (2003). The fate of nitrogen in agroecosystems: An illustration using Canadian estimates. *Nutrient Cycling in Agroecosystems*, *67*(1), 85–102. http://doi.org/10.1023/A:1025195826663

Jia, Z., & Conrad, R. (2009). Bacteria rather than Archaea dominate microbial ammonia oxidation in an agricultural soil. *Environmental Microbiology*, *11*(7), 1658–1671. http://doi.org/10.1111/j.1462-2920.2009.01891.x

Kato, T., Kuroda, H., & Nakasone, H. (2009). Runoff characteristics of nutrients from an agricultural watershed with intensive livestock production. *Journal of Hydrology*, *368*(1–4), 79–87. http://doi.org/10.1016/j.jhydrol.2009.01.028

Kendall, C. (1998). *Fundamentals of isotope geochemistry*. *Isotope Tracers in Catchment Hydrology*. Amsterdam: Elsevier Science. http://doi.org/10.1016/B978-0-444-81546-0.50009-4

Kendall, C. (1998). Isotope tracers in catchment hydrology. Elsevier, Amsterdam.

Kendall, C., & Aravena, R. (2000). Nitrate isotopes in groundwater systems. In *Environmental tracers in subsurface hydrology* (pp. 261–297). Springer.

Kendall, C., Elliott, E. M., & Wankel, S. D. (2007a). Tracing anthropogenic inputs of nitrogen to ecosystems. *Stable Isotopes in Ecology and Environmental Science*, *2*, 375–449.

Kendall, C., Elliott, E. M., & Wankel, S. D. (2007b). *Tracing anthropogenic inputs of nitrogen to ecosystems*. *Stable isotopes in ecology and environmental science* (Vol. 2). Blackwell Publishing New York.

Knobeloch, L., Salna, B., Hogan, A., Postle, J., & Anderson, H. (2000). Blue babies and nitrate-contaminated well water. *Environmental Health Perspectives*, *108*(November 1999), 675–678. http://doi.org/10.1289/ehp.00108675

Knöller, K., Vogt, C., Haupt, M., Feisthauer, S., & Richnow, H. H. (2011). Experimental investigation of nitrogen and oxygen isotope fractionation in nitrate and nitrite during denitrification. *Biogeochemistry*, *103*(1), 371–384. http://doi.org/10.1007/s10533-010-9483-9

Knowles, R. (1982). Denitrification. *Microbiological Reviews*, *46*(1), 43–70.

Kool, D. M., Wrage, N., Oenema, O., Dolfing, J., & Van Groenigen, J. W. (2007). Oxygen exchange between (de)nitrification intermediates and H_2O and its implications for source determination of NO_3^- and N_2O: A review. *Rapid Communications in Mass Spectrometry*. http://doi.org/10.1002/rcm.3249

Kozlowski, J. A., Stieglmeier, M., Schleper, C., Klotz, M. G., & Stein, L. Y. (2016). Pathways and key intermediates required for obligate aerobic ammonia-dependent chemolithotrophy in bacteria and Thaumarchaeota. *The ISME Journal*.

Lang, M., Li, P., & Yan, X. (2013). Runoff concentration and load of nitrogen and phosphorus from a residential area in an intensive agricultural watershed. *Science of The Total Environment*, *458–460*, 238–45. http://doi.org/10.1016/j.scitotenv.2013.04.044

Lee, K. S., Bong, Y. S., Lee, D., Kim, Y., & Kim, K. (2008). Tracing the sources of nitrate in the Han River watershed in Korea, using $\delta^{15}N\text{-}NO_3^-$ and $\delta^{18}O\text{-}NO_3^-$ values. *Science of the Total Environment*, *395*(2–3), 117–124. http://doi.org/10.1016/j.scitotenv.2008.01.058

Legendre, P. (2014). lmodel2: Model II Regression. Retrieved from https://cran.r-project.org/package=lmodel2

Lehmann, M. F., Reichert, P., Bernasconi, S. M., Barbieri, A., & McKenzie, J. a. (2003). Modelling nitrogen and oxygen isotope fractionation during denitrification in a lacustrine redox-transition zone. *Geochimica et Cosmochimica Acta*, *67*(14), 2529–2542. http://doi.org/10.1016/S0016-7037(03)00085-1

Leininger, S., Urich, T., Schloter, M., Schwark, L., Qi, J., Nicol, G. W., … Schleper, C. (2006). Archaea predominate among ammonia-oxidizing prokaryotes in soils. *Nature*, *442*(7104), 806–809. http://doi.org/10.1038/nature04983

Li, S.-L., Liu, C.-Q., Li, J., Liu, X., Chetelat, B., Wang, B., & Wang, F. (2010). Assessment of the sources of nitrate in the Changjiang River, China using a nitrogen and oxygen isotopic approach. *Environmental Science & Technology*, *44*(5), 1573–1578. http://doi.org/10.1021/es902670n

Liu, A., Ming, J., & Ankumah, R. O. (2005). Nitrate contamination in private wells in rural Alabama, United States. *Science of The Total Environment*, *346*(1–3), 112–120. http://doi.org/10.1016/j.scitotenv.2004.11.019

MacQuarrie, K. T. B., Sudicky, E. a., & Robertson, W. D. (2001). Numerical simulation of a fine-grained denitrification layer for removing septic system nitrate from shallow groundwater. *Journal of Contaminant Hydrology*, *52*(1–4), 29–55. http://doi.org/10.1016/S0169-7722(01)00152-8

Martin, T. S., & Casciotti, K. L. (2016). Nitrogen and oxygen isotopic fractionation during microbial nitrite reduction. *Limnology and Oceanography*, (2), 1000. http://doi.org/10.1002/lno.10278

Mayer, B., Boyer, E. W., Goodale, C., Jaworski, N. a., Van Breemen, N., Howarth, R. W., … Paustian, K. (2002). Sources of nitrate in rivers draining sixteen watersheds in the northeastern U.S.: Isotopic constraints. *Biogeochemistry*, *57–58*, 171–197. http://doi.org/10.1023/A:1015744002496

McIlvin, M. R., & Altabet, M. a. (2005). Chemical conversion of nitrate and nitrite to nitrous oxide for nitrogen and oxygen isotopic analysis in freshwater and seawater. *Analytical Chemistry*, *77*(17), 5589–95. http://doi.org/10.1021/ac050528s

Mengis, M., Schiff, S. L., Harris, M., English, M. C., Aravena, R., Elgood, R. J., & MacLean, A.

(1999). Multiple geochemical and isotopic approaches for assessing ground water NO3-elimination in a riparian zone. *Ground Water*. http://doi.org/10.1111/j.1745-6584.1999.tb01124.x

Michalski, G., Bhattacharya, S. K., & Mase, D. F. (2012). Handbook of Environmental Isotope Geochemistry, (Miller 2002). http://doi.org/10.1007/978-3-642-10637-8

Mulholland, P. J., Valett, H. M., Webster, J. R., Thomas, S. A., Cooper, L. W., Hamilton, S. K., & Peterson, B. J. (2008). Stream denitri cation and total nitrate uptake rates measured using a eld ^{15}N tracer addition approach, *49*(3), 809–820.

Nishizawa, M., Sakai, S., Konno, U., Nakahara, N., Takaki, Y., Saito, Y., … Takai, K. (2016). Nitrogen and oxygen isotope effects of ammonia oxidation by thermophilic *Thaumarchaeota* from a geothermal water stream. *Applied and Environmental Microbiology*, *82*(15), AEM.00250-16. http://doi.org/10.1128/AEM.00250-16

Norton, J. M. (2008). Nitrification in agricultural soils. *Agronomy*, *49*, 173.

Novotny, V. (1999). Diffuse pollution from agriculture - A worldwide outlook. *Water Science and Technology*, *39*(3), 1–13. http://doi.org/10.1016/S0273-1223(99)00027-X

Pardo, L. H., Kendall, C., Pett-Ridge, J., & Chang, C. C. Y. (2004). Evaluating the source of streamwater nitrate using $\delta^{15}N$ and $\delta^{18}O$ in nitrate in two watersheds in New Hampshire, USA. *Hydrological Processes*, *18*(14), 2699–2712. http://doi.org/10.1002/hyp.5576

Peterson, B. J., & Fry, B. (1987). Stable isotopes in ecosystem studies. *Annual Review of Ecology and Systematics*, *18*(1), 293–320.

Power, J. F., & Schepers, J. S. (1989). Nitrate contamination of groundwater in North America. *Agriculture, Ecosystems & Environment*, *26*(3–4), 165–187. http://doi.org/10.1016/0167-8809(89)90012-1

Powlson, D. S., Addiscott, T. M., Benjamin, N., Cassman, K. G., de Kok, T. M., van Grinsven, H., … Van Kessel, C. (2008). When does nitrate become a risk for humans? *Journal of Environmental Quality*, *37*(2), 291–295.

Ritter, Keith Solomon, Paul Sibley, L. (2002). Sources, Pathways, and Relative Risks of Contaminants in Surface Water and Groundwater: a Perspective Prepared for the Walkerton Inquiry. *Journal of Toxicology and Environmental Health, Part A*, *65*(1), 1–142. http://doi.org/10.1080/152873902753338572

Rosamond, M. S. (2013). *Nitrous oxide and nitrate in the Grand River , Ontario : Sources , production pathways and predictability*. University of Waterloo, PhD Thesis.

Ruiz, G., Jeison, D., & Chamy, R. (2003). Nitrification with high nitrite accumulation for the treatment of wastewater with high ammonia concentration. *Water Research*, *37*(6), 1371–1377.

Ryther, J. H., & Dunstan, W. M. (1971). Nitrogen, phosphorus, and eutrophication in the coastal marine environment. *Science (New York, N.Y.)*, *171*(3975), 1008–1013.

Saad, O. L. O., & Conrad, R. (1993). Temperature dependence of nitrification, denitrification, and turnover of nitric oxide in different soils. *Biology and Fertility of Soils*, *15*(1), 21–27. http://doi.org/10.1007/BF00336283

Savard, M. M., Paradis, D., Somers, G., Liao, S., & van Bochove, E. (2007). Winter nitrification contributes to excess NO_3^- in groundwater of an agricultural region: A dual-isotope study. *Water Resources Research*, *43*(6).

Schindler, D. W. (2006). Recent advances in the understanding and management of eutrophication. *Limnol. Oceanogr.*, *51*, 356–363. http://doi.org/10.4319/lo.2006.51.1_part_2.0356

Schindler, D. W. (2012). The dilemma of controlling cultural eutrophication of lakes. *Proceedings of the Royal Society B: Biological Sciences*, *279*(1746), 4322–4333. http://doi.org/10.1098/rspb.2012.1032

Schindler, D. W., & Fee, E. J. (1974). Experimental lakes area: whole-lake experiments in eutrophication. *Journal of the Fisheries Board of Canada*, *31*(5), 937–953.

Schindler, D. W., Hecky, R. E., Findlay, D. L., Stainton, M. P., Parker, B. R., Paterson, M. J., … Kasian, S. E. M. (2008). Eutrophication of lakes cannot be controlled by reducing nitrogen input: Results of a 37-year whole-ecosystem experiment. *Proceedings of the National Academy of Sciences*, *105*(32), 11254–11258. http://doi.org/10.1073/pnas.0805108105

Schlesinger, W. H. (2009). On the fate of anthropogenic nitrogen. *Proceedings of the National Academy of Sciences*, *106*(1), 203–208. http://doi.org/10.1073/pnas.0810193105

Sebilo, M., Mayer, B., Nicolardot, B., Pinay, G., & Mariotti, A. (2013). Long-term fate of nitrate fertilizer in agricultural soils. *Proceedings of the National Academy of Sciences of the United States of America*, *110*(45), 18185–9. http://doi.org/10.1073/pnas.1305372110

Shearer, G., Jones, J. R., & Kohl, D. H. (1992). The consequences of the isotope effect on proline dehydrogenation rates estimated by the tritium loss method. *Analytical Biochemistry*, *203*(2), 191–200. http://doi.org/10.1016/0003-2697(92)90302-N

Shearer, G., & Kohl, H. (1988). Nitrogen Isotopic Fractionation and l80 Exchange in Relation to the Mechanism of Denitrification of Nitrite by. *The Journal of Biological Chemistry*, *263*(26), 13231–13245.

Sigman, D. M., Granger, J., DiFiore, P. J., Lehmann, M. M., Ho, R., Cane, G., & van Geen, A. (2005). Coupled nitrogen and oxygen isotope measurements of nitrate along the eastern North Pacific margin. *Global Biogeochemical Cycles*, *19*(4), n/a-n/a. http://doi.org/10.1029/2005GB002458

Sigman, D. M., Robinson, R., Knapp, A. N., Van Geen, A., McCorkle, D. C., Brandes, J. A., &

Thunell, R. C. (2003). Distinguishing between water column and sedimentary denitrification in the Santa Barbara Basin using the stable isotopes of nitrate. *Geochemistry, Geophysics, Geosystems*, *4*(5), 1–20. http://doi.org/10.1029/2002GC000384

Smith, V. H. (2003). Eutrophication of freshwater and coastal marine ecosystems a global problem. *Environmental Science and Pollution Research*, *10*(2), 126–139.

Smith, V. H., Joye, S. B., & Howarth, R. W. (2006). Eutrophication of freshwater and marine ecosystems. *Limnology & Oceanography*, *51*, 351–355. http://doi.org/10.4319/lo.2006.51.1_part_2.0351

Smith, V. H., & Schindler, D. W. (2009). Eutrophication science: where do we go from here? *Trends in Ecology and Evolution*, *24*(4), 201–207. http://doi.org/10.1016/j.tree.2008.11.009

Smith, V. H., Tilman, G. D., & Nekola, J. C. (1998). Eutrophication: Impacts of excess nutrient inputs on freshwater, marine, and terrestrial ecosystems. *Environmental Pollution*, *100*(1–3), 179–196. http://doi.org/10.1016/S0269-7491(99)00091-3

Snider, D. M., Schiff, S. L., & Spoelstra, J. (2009). $^{15}N/^{14}N$ and $^{18}O/^{16}O$ stable isotope ratios of nitrous oxide produced during denitrification in temperate forest soils. *Geochimica et Cosmochimica Acta*, *73*(4), 877–888. http://doi.org/10.1016/j.gca.2008.11.004

Snider, D. M., Spoelstra, J., Schiff, S. L., & Venkiteswaran, J. J. (2010). Stable oxygen isotope ratios of nitrate produced from nitrification: ^{18}O-labeled water incubations of agricultural and temperate forest soils. *Environmental Science & Technology*, *44*(14), 5358–64. http://doi.org/10.1021/es1002567

Snider, D. M., Venkiteswaran, J. J., Schiff, S. L., & Spoelstra, J. (2013). A new mechanistic model of δ18O-N2O formation by denitrification. *Geochimica et Cosmochimica Acta*, *112*(3), 102–115. http://doi.org/10.1016/j.gca.2013.03.003

Sonthiphand, P., Cejudo, E., Schiff, S. L., & Neufeld, J. D. (2013). Wastewater effluent impacts ammonia-oxidizing prokaryotes of the Grand River, Canada. *Applied and Environmental Microbiology*, *79*(23), 7454–7465. http://doi.org/10.1128/AEM.02202-13

Sorokin, D., Tourova, T., Schmid, M. C., Wagner, M., Koops, H.-P., Kuenen, G. J., & Jetten, M. (2001). Isolation and properties of obligately chemolithoautotrophic and extremely alkali-tolerant ammonia-oxidizing bacteria from Mongolian soda lakes. *Archives of Microbiology*, *176*(3), 170–177.

Spoelstra, J., Schiff, S. L., Elgood, R. J., Semkin, R. G., & Jeffries, D. S. (2001). Tracing the sources of exported nitrate in the Turkey Lakes Watershed using $^{15}N/^{14}N$ and $^{18}O/^{16}O$ isotopic ratios. *Ecosystems*, *4*(6), 536–544. http://doi.org/10.1007/s10021-001-0027-y

Stahl, D. A., & de la Torre, J. R. (2012). Physiology and diversity of ammonia-oxidizing archaea. *Annu Rev Microbiol*, *66*, 83–101. http://doi.org/10.1146/annurev-micro-092611-150128

Starry, O. S., Valett, H. M., & Schreiber, M. E. (2005). Nitrification rates in a headwater

stream: influences of seasonal variation in C and N supply. *Journal of the North American Benthological Society*, *24*(4), 753–768. http://doi.org/10.1899/05-015.1

Stein, L. Y., & Yung, Y. L. (2003). Production, isotopic composition, and atmospheric fate of biologically produced nitrous oxide. *Annual Review of Earth and Planetary Sciences*, *31*(1), 329–356.

Straub, K. L., Benz, M., Schink, B., & Widdel, F. (1996). Anaerobic, nitrate-dependent microbial oxidation of ferrous iron. *Applied and Environmental Microbiology*, *62*(4), 1458–1460.

Strauss, E. A., & Lamberti, G. A. (2000). Regulation of nitrification in aquatic sediments by organic carbon. *Limnology and Oceanography*, *45*(8), 1854–1859. http://doi.org/10.4319/lo.2000.45.8.1854

Thamdrup, B. (2012). New Pathways and Processes in the Global Nitrogen Cycle. *Annual Review of Ecology, Evolution, and Systematics*, *43*(1), 407–428. http://doi.org/10.1146/annurev-ecolsys-102710-145048

Townsend, A. R., Howarth, R. W., Bazzaz, F. a, Booth, M. S., Cory, C., Collinge, S. K., … Keeney, D. R. (2003). Nitrogen Health Cycle Effects of Changing Global. *Frontiers in Ecology and the Environment*, *1*(5), 240–246.

Treusch, A. H., Leininger, S., Kletzin, A., Schuster, S. C., Klenk, H.-P., & Schleper, C. (2005). Novel genes for nitrite reductase and Amo-related proteins indicate a role of uncultivated mesophilic crenarchaeota in nitrogen cycling. *Environmental Microbiology*, *7*(12), 1985–1995. http://doi.org/10.1111/j.1462-2920.2005.00906.x

USEPA. (1993). *Method 353.2 Determination of Nitrate-nireite nitrogen by automated colorimetry*.

Van Meter, K. J., & Basu, N. B. (2015). Catchment Legacies and Time Lags: A Parsimonious Watershed Model to Predict the Effects of Legacy Storage on Nitrogen Export. *Plos One*, *10*(5), e0125971. http://doi.org/10.1371/journal.pone.0125971

Venkiteswaran, J. J., Schiff, S. L., & Taylor, W. D. (2015). Linking aquatic metabolism, gas exchange, and hypoxia to impacts along the 300-km Grand River, Canada. *Freshwater Science*, *34*(4), 1216–1232. http://doi.org/10.1086/683241

Venkiteswaran, J. J., Schiff, S. L., & Wassenaar, L. I. (2008). Aquatic metabolism and ecosystem health assessment using dissolved O_2 stable isotope diel curves. *Ecological Applications : A Publication of the Ecological Society of America*, *18*(4), 965–982. http://doi.org/10.1890/07-0491.1

Venkiteswaran, J. J., Wassenaar, L. I., & Schiff, S. L. (2007). Dynamics of dissolved oxygen isotopic ratios: A transient model to quantify primary production, community respiration, and air-water exchange in aquatic ecosystems. *Oecologia*, *153*(2), 385–398. http://doi.org/10.1007/s00442-007-0744-9

Vitousek, P. M., Aber, J. D., Howarth, R. W., Likens, G. E., Matson, P. a., Schindler, D. W., …

Tilman, D. G. (1997). Human alteration of the global nitrogen cycle: Sources and consequences. *Ecological Applications*, *7*(3), 737–750. http://doi.org/10.1890/1051-0761(1997)007[0737:HAOTGN]2.0.CO;2

Walker, C. B., de la Torre, J. R., Klotz, M. G., Urakawa, H., Pinel, N., Arp, D. J., … Stahl, D. A. (2010). Nitrosopumilus maritimus genome reveals unique mechanisms for nitrification and autotrophy in globally distributed marine crenarchaea. *Proceedings of the National Academy of Sciences of the United States of America*, *107*(19), 8818–23. http://doi.org/10.1073/pnas.0913533107

Wassenaar, L. I. (1995). Evaluation of the origin and fate of nitrate in the Abbotsford Aquifer using the isotopes of ^{15}N and ^{18}O in NO_3^-. *Applied Geochemistry*, *10*(4), 391–405.

Wassenaar, L. I., Hendry, M. J., & Harrington, N. (2006). Decadal geochemical and isotopic trends for nitrate in a transboundary aquifer and implications for agricultural beneficial management practices. *Environmental Science & Technology*, *40*(15), 4626–4632.

Wassenaar, L. I., Venkiteswaran, J. J., Schiff, S. L., & Koehler, G. (2010). Aquatic community metabolism response to municipal effluent inputs in rivers quantified using diel $\delta^{18}O$ values of dissolved oxygen. *Canadian Journal of Fisheries and Aquatic Sciences*, *67*(8), 1232–1246.

Worrall, F., Howden, N. J. K., & Burt, T. P. (2015). Evidence for nitrogen accumulation: the total nitrogen budget of the terrestrial biosphere of a lowland agricultural catchment. *Biogeochemistry*, 411–428. http://doi.org/10.1007/s10533-015-0074-7

Wunderlich, A., Meckenstock, R. U., & Einsiedl, F. (2013). A mixture of nitrite-oxidizing and denitrifying microorganisms affects the $\delta^{18}O$ of dissolved nitrate during anaerobic microbial denitrification depending on the $\delta^{18}O$ of ambient water. *Geochimica et Cosmochimica Acta*, *119*, 31–45. http://doi.org/10.1016/j.gca.2013.05.028

Xu, S., Kang, P., & Sun, Y. (2015). A stable isotope approach and its application for identifying nitrate source and transformation process in water. *Environmental Science and Pollution Research*, (3). http://doi.org/10.1007/s11356-015-5309-6

Zhang, L.-M., Hu, H.-W., Shen, J.-P., & He, J.-Z. (2012). Ammonia-oxidizing archaea have more important role than ammonia-oxidizing bacteria in ammonia oxidation of strongly acidic soils. *The ISME Journal*, *6*(5), 1032–1045. http://doi.org/10.1038/ismej.2011.168

Appendix A

Chapter 2 - Model II Regression (Figure 2.8 - 1:2 denitrification line)

Model II regression: West Montrose (WM)

n = 29 r = 0.2813632 r-square = 0.07916524

Parametric P-values: 2-tailed = 0.1392479 1-tailed = 0.06962396

Angle between the two OLS regression lines = 58.5334 degrees

Regression results

	Method	Intercept	Slope	Angle (degrees)	P-perm (1-tailed)
1	OLS	-2.085556	0.2665449	14.92491	NA
2	**MA**	**-7.400517**	**0.8259535**	**39.55512**	**NA**
3	SMA	-8.553758	0.9473341	43.45081	NA

Confidence intervals

	Method	2.5%-Intercept	97.5%-Intercept	2.5%-Slope	97.5%-Slope
1	OLS	-5.544278	1.3731661	-0.09242133	0.6255112
2	MA	-59.202644	0.7520602	-0.03211900	6.2782154
3	SMA	-12.588811	-5.7677089	0.65409777	1.3720303

Eigenvalues: 3.245237 1.80138

H statistic used for computing C.I. of MA: 0.4372429

Model II regression: Bridgeport (BR)

n = 16 r = 0.6441039 r-square = 0.4148699

Parametric P-values: 2-tailed = 0.007083136 1-tailed = 0.003541568

Angle between the two OLS regression lines = 23.79459 degrees

Regression results

	Method	Intercept	Slope	Angle (degrees)	P-perm (1-tailed)
1	OLS	-3.901569	0.5042335	26.75877	NA
2	**MA**	**-5.860822**	**0.6872557**	**34.49902**	**NA**
3	SMA	-6.884104	0.7828449	38.05543	NA

Confidence intervals

	Method	2.5%-Intercept	97.5%-Intercept	2.5%-Slope	97.5%-Slope
1	OLS	-7.637657	-0.1654818	0.1609744	0.8474926
2	MA	-12.723623	-1.5675345	0.2862013	1.3283393
3	SMA	-11.328909	-3.9797321	0.5115350	1.1980531

Eigenvalues: 5.555598 1.098747

H statistic used for computing C.I. of MA: 0.1009747

Model II regression: Blair (BL)

n = 17 r = 0.5649005 r-square = 0.3191126

Parametric P-values: 2-tailed = 0.01813951 1-tailed = 0.009069754

Angle between the two OLS regression lines = 31.06915 degrees

Regression results

	Method	Intercept	Slope	Angle (degrees)	P-perm (1-tailed)
1	OLS	-6.213801	0.5521545	28.90548	NA
2	**MA**	**-10.512042**	**0.9604130**	**43.84317**	NA
3	SMA	-10.691273	0.9774368	44.34627	NA

Confidence intervals

	Method	2.5%-Intercept	97.5%-Intercept	2.5%-Slope	97.5%-Slope
1	OLS	-11.00506	-1.422538	0.1082845	0.9960245
2	MA	-25.84614	-4.266702	0.3672138	2.4168870
3	SMA	-16.37582	-7.029486	0.6296305	1.5173705

Eigenvalues: 9.224 2.562246

H statistic used for computing C.I. of MA: 0.1612954

Chapter 3 - Model II Regression (Figure 3.4- *f*abiotic)

West Montrose July 2015 – 24 Hours

Method Intercept Slope Angle (degrees) P-perm (1-tailed)

1 OLS 9.759117 0.9620592 43.89220 NA

2 MA 9.325465 0.9705733 44.14446 NA

3 SMA 9.312119 0.9708354 44.15219 NA

Confidence intervals

Method 2.5%-Intercept 97.5%-Intercept 2.5%-Slope 97.5%-Slope

1 OLS -103.2029 122.72114 -0.6928405 2.616959

2 MA 272.1061 72.53939 -0.2705378 -4.188733

3 SMA -123.2528 45.32637 0.2637494 3.573549

Eigenvalues: 5990.091 27.17346

H statistic used for computing C.I. of MA: 0.7390816

West Montrose July 2015 – 24-60 Hours

Method Intercept Slope Angle (degrees) P-perm (1-tailed)

1 OLS 0.3831008 0.8974486 41.90634 NA

2 MA 0.1211626 0.9028237 42.07647 NA

3 SMA 0.0914613 0.9034332 42.09571 NA

Confidence intervals

Method 2.5%-Intercept 97.5%-Intercept 2.5%-Slope 97.5%-Slope

1 OLS -85.37011 86.13631 -0.4216552 2.216552

2 MA -2909.49621 48.29595 -0.0857624 60.610553

3 SMA -98.07669 30.48580 0.2797165 2.917924

Eigenvalues: 5027.265 16.53433

H statistic used for computing C.I. of MA: 0.5345005

West Montrose September 2015 – 24-60 Hours

Method	Intercept	Slope	Angle (degrees)	P-perm (1-tailed)
1 OLS	-1.740084	0.9230605	42.70888	NA
2 MA	**-1.747013**	**0.9232269**	**42.71403**	**NA**
3 SMA	-1.747614	0.9232413	42.71448	NA

Confidence intervals

Method	2.5%-Intercept	97.5%-Intercept	2.5%-Slope	97.5%-Slope
1 OLS	-14.87264	11.392474	0.6908809	1.155240
2 MA	-12.77906	6.979922	0.7136128	1.188208
3 SMA	-12.61086	6.721959	0.7198088	1.184168

Eigenvalues: 4072.794 0.3964017

H statistic used for computing C.I. of MA: 0.01571663

Blair July 2015 – 24 Hours

Method Intercept Slope Angle (degrees) P-perm (1-tailed)

1 OLS 3.564636 1.019336 45.54861 NA

2 MA 3.530278 1.020108 45.57029 NA

3 SMA 3.530949 1.020092 45.56986 NA

Confidence intervals

Method 2.5%-Intercept 97.5%-Intercept 2.5%-Slope 97.5%-Slope

1 OLS -26.50787 33.63714 0.5202489 1.518423

2 MA -27.36451 21.77171 0.6104638 1.713905

3 SMA -23.83870 20.61000 0.6365522 1.634726

Eigenvalues: 5041.694 1.869427

H statistic used for computing C.I. of MA: 0.05990813

Blair July 2015 – 24-60 Hours

Method Intercept Slope Angle (degrees) P-perm (1-tailed)

1 OLS 3.437410 0.7939018 38.44612 NA

2 MA 2.790988 0.8087917 38.96565 NA

3 SMA 2.620515 0.8127185 39.10140 NA

Confidence intervals

Method 2.5%-Intercept 97.5%-Intercept 2.5%-Slope 97.5%-Slope

1 OLS -125.4450 132.31979 -1.4153430 3.003147

2 MA NA NA NA NA

3 SMA -160.2019 31.61942 0.1447463 4.563236

Eigenvalues: 3740.484 41.9357

H statistic used for computing C.I. of MA: 1.851317

STELLA MODEL

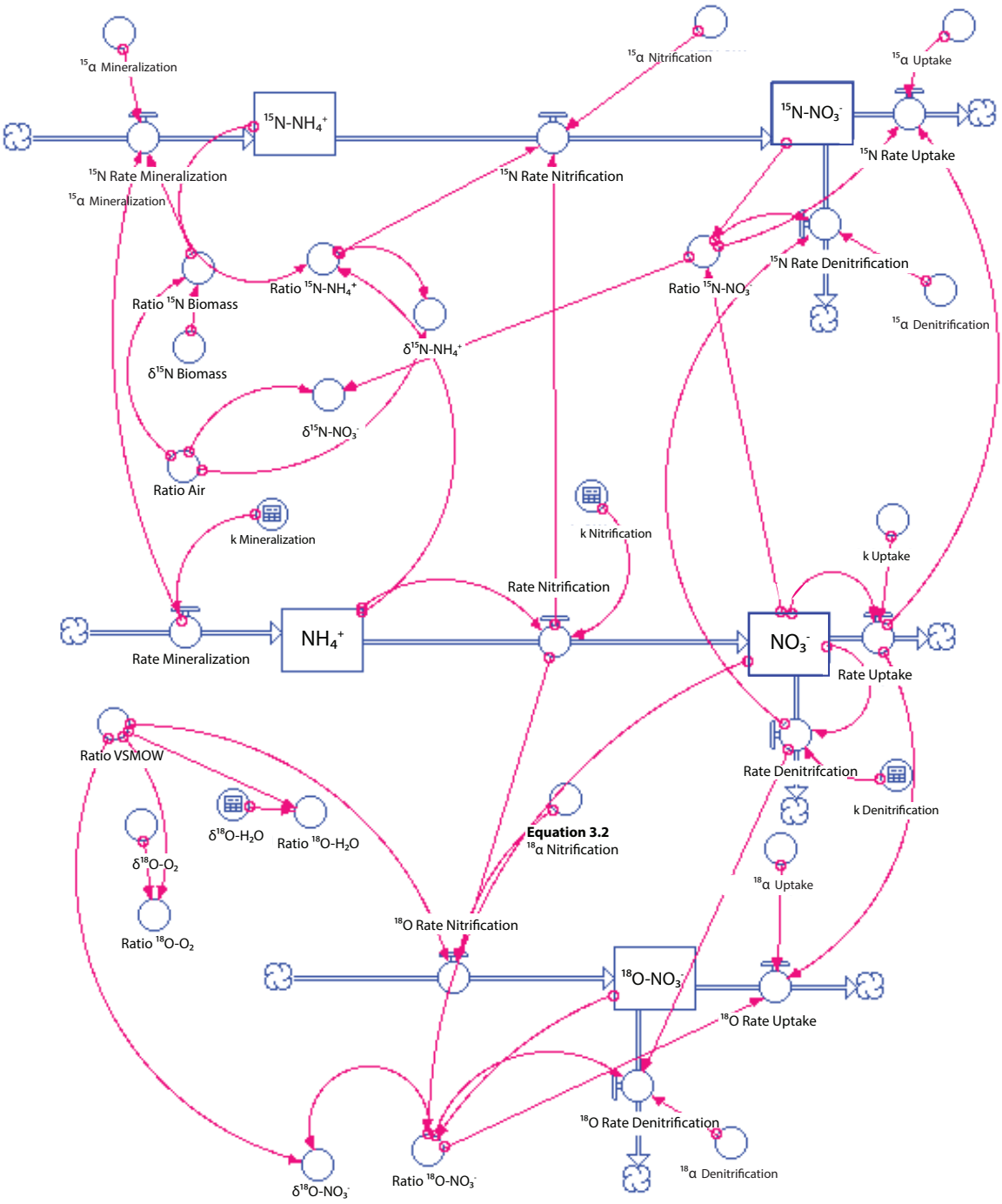

Equation 3.2: $\delta^{18}O - NO_3^- = \frac{1}{3}\left(2 + f_{ABIOTIC}\right)\delta^{18}O - H_2O + \frac{1}{3}[f_{ABIOTIC}\left(2^{18}\varepsilon_{eq} - \delta^{18}O - O_2 - {}^{18}\varepsilon_{O2} - {}^{18}\varepsilon_{H2O,1}\right) + \delta^{18}O - O_2 + {}^{18}\varepsilon_{O2} + {}^{18}\varepsilon_{H2O,1} + {}^{18}\varepsilon_{H2O,2}]$

MODEL EQUATIONS:

Model parameters that are adjusted for each incubation are indicated as *a-f* and values for these parameters are in Table A1

$^{15}N\text{-}NH_4(t) = {}^{15}N\text{-}NH_4^+(t - dt) + (^{15}N\_Rate\_Mineralization - {}^{15}N\_Rate\_Nitrification) \times dt$

INITIAL $^{15}N\text{-}NH_4 = a \times (b/1000+1) \times 0.0036764$

INFLOWS:

$^{15}N\_Rate\_Mineralization =$

$(Rate\_Mineralization) \times (^{15}\alpha\_Mineralization) \times (Ratio\_^{15}N\_Biomass)$

OUTFLOWS:

$^{15}N\_Rate\_Nitrification = (Ratio\_^{15}N\text{-}NH_4) \times (^{15}\alpha\_Nitrification) \times (Rate\_Nitrification)$

$^{15}N\text{-}NO_3(t) = {}^{15}N\text{-}NO_3^-(t - dt) + (^{15}N\_Rate\_Nitrification - {}^{15}N\_Rate\_Uptake - {}^{15}N\_Rate\_Denitrification) \times dt$

INITIAL $^{15}N\text{-}NO_3^- = d \times ((e/1000+1) \times 0.0036764)$

INFLOWS:

$^{15}N\_Rate\_Nitrification = (Ratio\_^{15}N\text{-}NH_4) \times (^{15}\alpha\_Nitrification) \times (Rate\_Nitrification)$

OUTFLOWS:

$^{15}N\_Rate\_Uptake = (^{15}\alpha\_Uptake) \times (Rate\_Uptake) \times (Ratio\_^{15}N\text{-}NO_3)$

$^{15}N\_Rate\_Denitrification = (Rate\_Denitrification) \times (^{15}\alpha\_Denitrification) \times (Ratio\_^{15}N\text{-}NO_3)$

$^{18}O\text{-}NO_3(t) = {}^{18}O\text{-}NO_3(t - dt) + (^{18}O\_Rate\_Nitrification - {}^{18}O\_Rate\_Uptake - {}^{18}O\_Rate\_Denitrification) \times dt$

INITIAL $^{18}O\text{-}NO_3 = d \times ((f/1000+1) \times 0.0020052)$

INFLOWS:

$^{18}O\_Rate\_Nitrification$ = (Rate_Nitrification) x ((Equation 3.2/1000+1) x Ratio_VSMOW)

OUTFLOWS:

$^{18}O\_Rate\_Uptake$ = (Rate_Uptake) x ($^{18}\alpha$_Uptake) x (Ratio_^{18}O-NO_3)

$^{18}O\_Rate\_Denitrification$ = (Rate_Denitrification) x ($^{18}\alpha$_Denitrification) x (Ratio_^{18}O-NO_3)

$NH_4(t) = NH_4(t - dt) + (Rate\_Mineralization - Rate\_Nitrification) \times dt$

INITIAL $NH_4 = a$

INFLOWS:

Rate_Mineralization = k_Mineralization

OUTFLOWS:

Rate_Nitrification = k_Nitrification x NH_4

$NO_3(t) = NO_3(t - dt) + (Rate\_Nitrification - Rate\_Denitrification - Rate\_Uptake) \times dt$

INITIAL $NO_3 = d$

INFLOWS:

Rate_Nitrification = k_Nitrification x NH_4

OUTFLOWS:

Rate_Denitrification = k_Denitrification x NO_3

Rate_Uptake = k_Uptake x NO_3

$^{15}\alpha$_Denitrification = -24/1000+1

$^{15}\alpha$_Nitrification = -15/1000+1

$^{15}\alpha$_Uptake = -8/1000+1

$^{18}\alpha$_Denitrification = -12/1000+1

$^{18}\alpha$_Uptake = -8/1000+1

$^{15}\alpha$_Mineralization = 1

δ^{15}N_Biomass = c

δ^{15}N-NH_4 = (Ratio_^{15}N-NH_4/Ratio_AIR-1) x 1000

δ^{15}N-NO_3 = (Ratio_^{15}N-NO_3/Ratio_AIR-1) x 1000

δ^{18}O_NO_3 = (Ratio_^{18}O-NO_3/Ratio_VSMOW-1) x 1000

Ratio_^{15}N_Biomass = (c/1000+1) x Ratio_AIR

Ratio_^{15}N-NH_4 = ^{15}N-NH_4/NH_4

Ratio_^{15}N-NO_3 = ^{15}N-NO_3/NO_3

Ratio_AIR = 0.0036764

Ratio_H_2O = (δ^{18}O-H_2O/1000+1) x (Ratio_VSMOW)

Ratio_^{18}O-NO_3 = ^{18}O-NO_3/NO_3

Ratio_O_2 = (δ^{18}O-O_2/1000+1) x (Ratio_VSMOW)

Ratio_VSMOW = 0.0020052

Equation 3.2 ($^{18}\alpha$_Nitrification) = $\frac{1}{3}(2 + f_{ABIOTIC})\delta^{18}O - H_2O \ + \ \mathrm{y} - \mathrm{int}$

δ^8O-O_2 = 24.2

Table A1: Values used in the model for each of the three incubation experiments West Montrose (WM) July 2015, WM September and Blair (BL) July, 2015.

				*a**	*b**	*c**	*d**	*e**	*f**
Experiment	**$\delta^{18}O\text{-}H_2O$ (‰)**	***f*abiotic**	**y-int**	**NH_4^+ (mgN/L)**	**$^{15}N\text{-}NH_4$ (‰)**	**^{15}N of Biomass (‰)**	**NO_3^- (mgN/L)**	**$^{15}N\text{-}NO_3^-$ (‰)**	**$^{18}O\text{-}NO_3^-$ (‰)**
M = Measured E= Estimated	**M**	**M**	**M**	**E**	**E**	**M**	**M**	**M**	**M**
WM July Low 0-24h	-9.0	0.88	9.32	0.030	+12	+8.5	2.00	+76.0	+11.2
WM July Low 24-60h	-9.0	0.70	0.12	0.030	+12	+8.5	2.16	+57.0	+10.5
WM July Medium 0-24h	+50	0.88	9.32	0.030	+12	+8.5	2.00	+78.5	+10.5
WM July Medium 24-60h	+50	0.70	0.12	0.030	+12	+8.5	2.34	+65.4	+18.3
WM July High 0-24h	+90	0.88	9.32	0.030	+12	+8.5	2.00	+83.0	+13.0
WM July High 24-60h	+90	0.70	0.12	0.030	+12	+8.5	2.45	+69.0	+27.1
WM September Low 0-24h	-9.0	0.88	-1.75	0.030	+12	+8.5	0.95	+77.4	+11.9
WM September Low 24-60h	-9.0	0.77	-1.75	0.030	+12	+8.5	1.25	+59.3	+7.24
WM September Medium 0-24h	+50	0.88	-1.75	0.030	+12	+8.5	1.00	+81.0	+11.0
WM September Medium 24-60h	+50	0.77	-1.75	0.030	+12	+8.5	1.10	+64.0	+19.0
WM September High 0-24h	+90	0.88	-1.75	0.030	+12	+8.5	1.00	+80.0	+11.0
WM September High 24-60h	+90	0.77	-1.75	0.030	+12	+8.5	1.03	+66.7	+27.9
BL Low 0-24h	-9.0	1.06	3.53	0.030	+12	+18	3.00	+40.1	+6.00
BL Low 24-60h	-9.0	0.43	2.79	0.030	+12	+18	3.80	+34.4	+3.45
BL Medium 0-24h	+50	1.06	3.53	0.030	+12	+18	3.30	+37.0	+9.00
BL Medium 24-60h	+50	0.43	2.79	0.030	+12	+18	3.70	+34.0	+23.4
BL High 0-24h	+90	1.06	3.53	0.030	+12	+18	3.00	+39.1	+6.90
BL High 24-60h	+90	0.43	2.79	0.030	+12	+18	3.50	+35.4	+18.9

*Experiment values used in the model equations